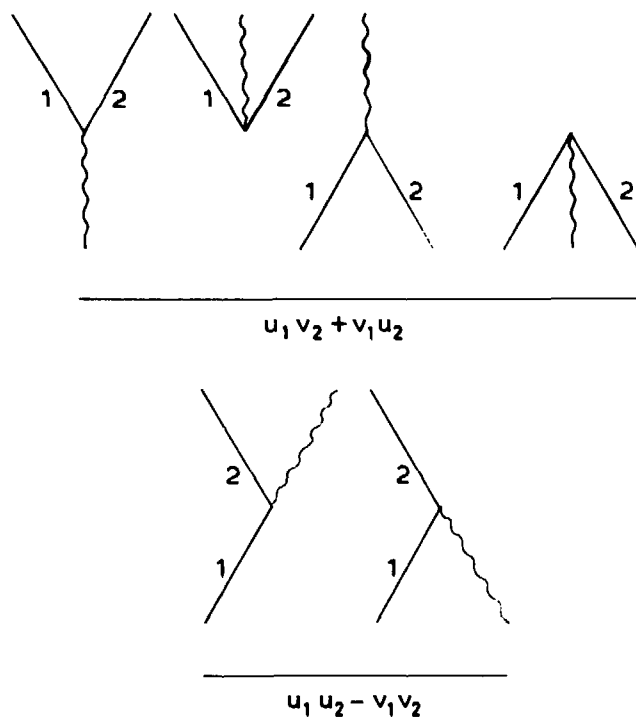


✓ NLB 30359 K
1N11-ut.-5685

THE BROKEN-PAIR MODEL FOR NUCLEI AND ITS EXTENSION WITH QUADRUPOLE VIBRATIONS



P. Hofstra

**THE BROKEN-PAIR MODEL FOR NUCLEI AND ITS EXTENSION
WITH QUADRUPOLE VIBRATIONS**

VRIJE UNIVERSITEIT TE AMSTERDAM

**THE BROKEN-PAIR MODEL FOR NUCLEI
AND ITS EXTENSION WITH
QUADRUPOLE VIBRATIONS**

a description of odd
N=50 isotones and Z=30 isotopes

ACADEMISCH PROEFSCHRIFT

ter verkrijging van de graad van
doctor in de wiskunde en natuurwetenschappen
aan de Vrije Universiteit te Amsterdam,
op gezag van de rector magnificus
dr. H. Verheul,
hoogleraar in de faculteit der wiskunde en natuurwetenschappen,
in het openbaar te verdedigen
op donderdag 8 november 1979 te 13.30 uur
in het hoofdgebouw der universiteit,
De Boelelaan 1105

door

PAULUS HOFSTRA

geboren te Amsterdam

The logo for Rodopi, featuring the word 'Rodopi' in a stylized, calligraphic script font.

AMSTERDAM 1979

Promotor: Prof. dr. E. Boeker

Copromotor: Dr. K. Allaart

This investigation was part of the research program of the "Stichting voor Fundamenteel Onderzoek der Materie (FOM)", which is financially supported by the "Nederlandse Organisatie voor Zuiver Wetenschappelijk Onderzoek (ZWO)".

Aan Cocky

VOORWOORD

Bij de voltooiing van dit proefschrift wil ik iedereen bedanken die er een bijdrage aan heeft geleverd. Enkele personen wil ik in het bijzonder vermelden.

Egbert Boeker, als mijn promotor heb je mij in de gelegenheid gesteld dit onderzoek te verrichten. Ik wil je bedanken voor de kritische wijze waarop je mijn onderzoek gevolgd hebt. Ook aan jouw suggesties voor de wijze van presentatie van de gegevens heb ik veel gehad.

Klaas Allaart, voor jouw bijdragen aan het onderzoek en de wijze waarop je mij terzijde hebt gestaan ben ik je zeer erkentelijk. Nooit heb ik tevergeefs een beroep op je gedaan. De hulp bij het opschrijven van de resultaten is zeer belangrijk voor mij geweest.

Vladimir Paar, you stimulated me to couple a number-projected quasiparticle cluster to quadrupole vibrations. I thank you for your help and suggestions to realize this line of investigations. I thank the staff of the "Ruđer Bošković" Institute for my interesting and enjoyable visit of their institute in Zagreb.

De nog niet genoemde leden van de werkgroep Kernmodellen wil ik bedanken voor de prettige sfeer, waarin ik de laatste jaren heb kunnen werken.

De Stichting F.O.M. en de direktie van het Natuurkundig Laboratorium hebben mij de gelegenheid geboden dit onderzoek in aangename omstandigheden te verrichten. Daar ben ik hen zeer erkentelijk voor.

De heren Pomper en Van Sijpveld dank ik hartelijk voor de goede verzorging van de figuren.

Cocky, jij hebt het manuscript getypt en de lay-out verzorgd. Bedankt voor de nauwgezette manier waarop je dit alles hebt gedaan.

CONTENTS

Chapter 1	SURVEY AND MAIN RESULTS	1
	1. The Broken-Pair model	2
	2. The extension of the Broken-Pair model with quadrupole vibrations	4
	3. Future prospects of the investigations	7
Chapter 2	THE NUMBER-CONSERVING QUASIPARTICLE MODEL; FORMALISM AND METHODS	10
	1. Introduction	10
	2. The low-seniority approximation	13
	3. The BCS formalism for superfluid nuclei	15
	4. Particle-number projection; the Broken-Pair model	19
	5. Relationship between odd and even spectra in the BCS model	20
Chapter 3	APPLICATION OF THE SUPERFLUIDITY MODEL TO SCS NUCLEI IN THE PF SHELL	24
	1. Introduction	24
	2. Determination of the parameters	25
	3. The Hartree-Fock-Bogolyubov ground state	28
	4. Results	32
	5. Conclusion	35
Chapter 4	A BROKEN-PAIR DESCRIPTION OF ^{89}Y , ^{91}Nb AND ^{93}Tc	37
	1. Introduction	37
	2. Model and computational procedure	38
	3. Results and discussion	38
	4. Summary and conclusion	44

Chapter 5	THE CLUSTER-VIBRATION COUPLING MODEL	48
	1. The particle-vibration model	48
	2. The cluster-vibration model	50
	3. The quasiparticle (cluster)- vibration model (Q(C)VM)	55
	1. Introduction	55
	2. Quasiparticle cluster-vibration coupling for odd nuclei (formalism)	57
	4. 1. Truncation of the model space; computational procedure	60
	2. Some properties and illustrations of the QCVM	68
Chapter 6	APPLICATION OF THE THREE-QUASIPARTICLE CLUSTER VIBRATION MODEL TO ODD Zn ISOTOPES	86
	1. Introduction and choice of the parameters	86
	2. Spectra and wave functions	89
	3. Electromagnetic properties	97
	4. Comparison of the QCV model with other models	102
	1. Comparison of the QCV model to the QV model	104
	2. Comparison of the QCV model with the shell model	105

THE BROKEN-PAIR MODEL FOR NUCLEI
AND ITS EXTENSION WITH QUADRUPOLE VIBRATIONS

a description of odd
N=50 isotones and Z=30 isotopes

Chapter 1

SURVEY AND MAIN RESULTS

In this thesis calculations are presented for low-energy properties of nuclei with an odd number of particles. So either the number of protons or the number of neutrons is odd. The kind of particles of which the number is odd will be referred to as odd particles; the other kind as even particles. In all the presented calculations the odd particles are described in the Broken-Pair approximation, which is equivalent to the number-projected quasiparticle model. It is assumed that all but three particles occur as ordered Cooper pairs; the unpaired (one or three) particles are called quasiparticles.

First it is attempted to describe nuclei of which the even particles form a closed shell in terms of three types of states:

- 1) one-quasiparticle states which take into account the simplest excitations of the odd particles.
- 2) three-quasiparticle states. These states are obtained, when in addition to the one quasiparticle one pair of the odd nucleons is broken.
- 3) one-quasiparticle states coupled to the $1p-1h$ states of the even particles. These states account for core excitations.

In the second part of the thesis a model is developed with which it is hoped to describe odd nuclei with two open shells in terms of both single-particle and collective degrees of freedom. The odd particles are again described with a (one-plus) three-quasiparticle cluster. The even particles as well as some neglected states of the odd particles are approximated by quadrupole vibrations. It is hoped that this model may be useful for nuclei in the transitional regions, *i.e.* with two, four, six even particles outside a closed shell.

1.1 THE BROKEN-PAIR MODEL

The single-particle degrees of freedom are treated with the Broken-Pair model¹⁾. In this model most particles are assumed to occur in pairs of identical nucleons. These pairs consist of two particles in orbits which are each other's time reversed state. The attractive effective interaction produces a nuclear ground state which is similar to that of a superfluid system. States of a higher energy may be generated by breaking one or more pairs in the ground state wave function. The Broken-Pair model is equivalent to the number-projected BCS model. The particles which do not occur in superfluid pairs are referred to as quasiparticles.

The BCS model was designed in the field of solid state physics to describe superfluidity²⁾; it turned out to be useful also in the nuclear spectroscopy. In the BCS model the number of particles is treated in an average way. In the solid state physics where the number of particles is of the order 10^{23} , this approximation appears to be valid. In nuclear physics, however, the number of particles is about a hundred; projection on the desired number of particles results in sizeable effects on the spectra and wave functions. The method used for the particle-number pro-

jection was developed in refs^{3,4)}. The basic notions of the BCS model are presented in chapter 2.

The parameters which occur in the Broken-Pair model are the same as in a shell model, *viz.* single-particle energies and the effective nucleon-nucleon interaction. Gillet et al.⁵⁾ have shown, that the single-particle energies and the strength of the force, to be used in the unprojected BCS model, can be extracted from the spectroscopic data of the odd single-closed-shell nuclei with a simple method and in a unique way. Allaart et al.⁶⁾ have developed a possible extension of this method to the number-projected BCS model. Since it is interesting to investigate the meaning of the parameter values which are thus obtained, chapter 3 is devoted to the question whether these parameters may be applied to more complex calculations. It appears then, that these parameters are model dependent.

In single-closed-shell nuclei one expects that the collective effects are not strong. It is interesting to check if just single-particle degrees of freedom will suffice for the description of these nuclei, when only two or three nucleons (of one kind) are allowed not to be bound in Cooper pairs. Recently number-projected two- and three-quasiparticle calculations have been performed for the even $N=50$ isotones⁷⁾ and Sn isotopes^{3,8)} and for the odd Sn isotopes^{3,9,11)}, respectively. In these calculations only one kind of particles was assumed to be excited within one major shell. Many experimental states could be described reasonably well; for states with a collective character (for example: the 2_1^+ and 3_1^- states in the even nuclei), however, the collectivity was not strong enough.

Core excitations; application to odd N=50 isotones

In chapter 4 it is attempted to improve the number-projected three-quasiparticle BCS model for odd nuclei by including core excitations, *i.e.* excitation of particles out of the closed shell into the higher empty shell. This model is applied to the odd N=50 isotones ^{89}Y , ^{91}Nb and ^{93}Tc . The protons could occupy one major shell and the neutrons two major shells in such a way that at most one proton or neutron pair was broken. Using a Gaussian residual interaction between the nucleons, the spectra as well as the electromagnetic properties can be reproduced in reasonable agreement with experiment. The results for the N=50 isotones are better than the results for the Z=50 isotopes. The inclusion of the neutron (core) excitations appears to be essential, especially for states with a collective character. Analogous calculations for even Z=50 isotopes and N=50 isotones show that the collectivity of the 2_1^+ and 3_1^- states improves considerably¹⁰⁾.

1.2 THE EXTENSION OF THE BROKEN PAIR MODEL WITH QUADRUPOLE VIBRATIONS

When we consider odd nuclei with two, four, six, particles (holes) beyond closed shells, collective effects become more dominant. If one would try to account for these effects with single-particle degrees of freedom only, too many excitations in a large model space would be needed. In chapter 5 a model is proposed to describe this type of nuclei with a model in which both the single-particle degrees of freedom and the collective degrees of freedom are explicitly taken into account.

We will illustrate this for the example of 7 neutrons outside a closed shell and 2 protons outside another shell.

As the number-projected BCS model is rather successful for odd single-closed-shell nuclei, the neutrons are represented by a three-quasiparticle cluster. This means that 4 neutrons are distributed in ordered pairs over the valence shells. The other 3 neutrons are not paired. All the other excitations such as protons excitations and neutron-core excitations are represented by quadrupole vibrations. This model is an extension of the three-particle cluster vibration model (Alaga model)¹²⁾, which is meant to describe nuclei in the transitional regions with *three* particles or holes in the valence shell. Recently many applications of this model have been published by Paar. The three-quasiparticle cluster vibration model is developed in close collaboration with Paar; it is designed to describe nuclei in the transitional regions with *three, five, seven,* particles in the valence shell.

The three-quasiparticle cluster vibration model may also be considered as an extension of the one-quasiparticle vibration coupling model of Kisslinger and Sörenson¹³⁾. These authors have indicated, that for many states three-quasiparticle components should be included in their model.

Truncation of the model space

The dimension of the configuration space for a certain spin and parity in the three-quasiparticle cluster vibration model may become about a thousand. The calculations become very time consuming then. So when one has to fit the model parameters it may be preferable to truncate the number of basis vectors for reasons of economy. In general the resulting spectra will depend on the method of selection of these vectors. In section 4 of chapter 5 the spectra, resulting from two selection methods, are compared with a spectrum, resulting from a complete diagonalization.

The first method is used frequently in the Alaga model, viz. a selection based on diagonal energies of the basis vectors, only. The second method (see section 5.4) takes also the off-diagonal matrix elements into account. This method appears to be preferable over the first one, especially, when the coupling between basis vectors with a large energy difference is large, as may be the case when the valence shell is about half filled. The second method, however, is still not a very good approximation of a complete diagonalization. The latter has to be preferred for the production of final results.

Application to odd Z=30 isotopes

A nice property of the three-quasiparticle cluster model is that it can be applied to a whole series of odd isotopes or isotones; the single-particle energies and the strength of the interaction between the particles should be considered then as constants for the whole series of nuclei. The phonon energy and the coupling strength between the single-particle and phonon degrees of freedom are the only parameters, which may be allowed to change from nucleus to nucleus. This is reasonable, since the softness of the core nucleus, which is treated as the model vibrator and which represents the nucleons which appear not explicitly in the excitations, will change when two particles are added.

In chapter 6 the three-quasiparticle cluster vibration model is applied to the isotopes ^{61}Zn , ^{63}Zn , ^{65}Zn and ^{67}Zn . The neutrons occupy the orbits $2p_{3/2}$, $1f_{5/2}$ and $2p_{1/2}$. The interaction is assumed to be a pairing force. All parameters (except the number of valence-shell neutrons) are kept constant for all Zn isotopes. The nucleus ^{67}Zn has been described before¹⁴⁾ rather successfully with the

Alaga model (three holes in a $N=40$ "closed shell"). With the same parametrization it is now tried to describe the other Zn isotopes (five, seven and nine holes in a $N=40$ "closed shell"), to which the Alaga model is not applicable. The three-quasiparticle cluster vibration model produces the same results for ^{67}Zn as the Alaga model, because the two models are equivalent for cases with three particles or holes beyond a closed shell.

The spectra and electromagnetic properties produced by the three-quasiparticle cluster vibration model agree reasonably well with experimental values; the agreement for $^{61,63,65}\text{Zn}$ is of the same quality as one obtains with the Alaga model in the case of three holes (^{67}Zn).

These Zn isotopes have been described earlier with a one-quasiparticle vibration model¹⁵⁾ and with the shell model¹⁶⁾. The three-quasiparticle cluster vibration model shows that the one-quasiparticle and three-quasiparticle states are strongly mixed, so one cannot expect that a model with only one-quasiparticle states is a good tool to describe these nuclei. In the spectra obtained by the one-quasiparticle vibration model levels are missing with an excitation energy as low as 0.5 MeV. The results of a shell model calculation, in which matrices had to be diagonalized with ten times larger dimensions are comparable with the results of the three-quasiparticle cluster vibration model. The latter model has a smaller configuration space (maximum: 124 vectors) and is therefore a more convenient tool to describe this type of nuclei.

1.3 FUTURE PROSPECTS OF THESE INVESTIGATIONS

Up to now the Broken-Pair model has been applied to the following single-closed-shell nuclei: even $N=50$ isotones⁷⁾, odd $N=50$ isotones¹⁷⁾, even and odd $Z=50$ isotopes^{3,8,11)}. The results were found to be better for the

N=50 than for the Z=50 region. It seems interesting to apply this model to other single-closed-shell nuclei, for example, the N=82 isotones, so as to obtain more conclusive results.

One can apply the Broken-Pair model also to nuclei with one open shell and one or two particles or holes in the other shell. We may think for example at ^{94}Zr with 2 protons and 4 neutrons outside a ^{88}Sr core. Both the protons and the neutrons can be handled in the Broken-Pair Approximation. Such calculations are in progress^{18,19}.

The three-quasiparticle cluster vibration model is able to describe the low-energy properties of the odd Zn isotopes. It is evident that such an agreement of experimental energies and electromagnetic properties for one series of isotopes is not a sufficient proof that the lowest states of the spectra of nuclei in transitional regions are generally described well with this model. To investigate further the applicability of the three-quasiparticle cluster vibration model, it should be applied to many other cases, such as the odd Te, Xe, Ge, Se, isotopes and the odd N=52, 54, 48, 46 isotones.

A similar model, in which a two-quasiparticle cluster is coupled to quadrupole vibrations can be applied to the even nuclei in transitional regions. Such a model has been applied recently to the even Zn and Ge isotopes²⁰. Particle-number projection was not performed in this work, however; so one has to consider the results with care. Particle-number projected two-quasiparticle cluster vibration model calculations have not been reported so far.

Another possible interesting line of investigation is: modifying the description of the vibrator. This may be done in several ways. Firstly, one can introduce an anharmonic term in the phonon Hamiltonian. Secondly, one can replace the harmonic phonon Hamiltonian by the

Truncated Quadrupole Model Hamiltonian²¹⁾ (TQM). This Hamiltonian is a realization of the Bohr Hamiltonian. The TQM is equivalent to the Interacting Boson Approximation²²⁾ With these extensions it might be possible to describe strongly deformed odd nuclei as well.

Chapter 4 will be published in Zeitschrift für Physik; it is reproduced here with kind permission of the Springer Verlag, Heidelberg.

References

- 1) Y.K. Gambhir, A. Rimini and T. Weber, Phys. Rev. 188 (1969) 1573
- 2) J. Bardeen, L.N. Cooper and R. Schrieffer, Phys. Rev. 108 (1957) 1175
- 3) P.L. Ottaviani and M. Savoia, Phys. Rev. 187 (1969) 1306; Nuovo Cim. 67 A (1970) 630
- 4) K. Allaart and W.F. van Gunsteren, Nucl. Phys. A 234 (1974) 53
- 5) V. Gillet, B. Giraud, J. Picard and M. Rho, Phys. Lett. 27 B (1968) 483
V. Gillet, B. Giraud and M. Rho, Phys. Rev. 178 (1969) 1695
- 6) K. Allaart and E. Boeker, Nucl. Phys. A 198 (1972) 33
- 7) K. Allaart, thesis, Vrije Universiteit, Amsterdam (1972)
- 8) W.F. van Gunsteren, E. Boeker and K. Allaart, Z. Phys. A 267 (1974) 87
- 9) W.F. van Gunsteren, thesis, Vrije Universiteit, Amsterdam (1976)
- 10) Unpublished calculations by K. Allaart
- 11) W.F. van Gunsteren, K. Allaart and P. Hofstra, Z. Phys. A 288 (1978) 49
- 12) V. Paar, Nucl. Phys. A 211 (1973) 29
- 13) L.S. Kisslinger and R.A. Sörenson, Rev. Mod. Phys. 35 (1963) 853
- 14) G. Vanden Berghe, Nucl. Phys. A 265 (1976) 479
- 15) M.J. Throop, Y.T. Chang and D.K. McDaniels, Nucl. Phys. A 239 (1975) 333
J.J. Dikshit and B.P. Singh, J. Phys. G: Nucl. Phys. 2 (1976) 219
- 16) J.F.A. van Hienen, W. Chung and B.M. Wildenthal, Nucl. Phys. A 269 (1976) 159
- 17) Chapter 4
- 18) J.N.L. Akkermans, private communication
- 19) Y.K. Gambhir, S. Haq and J.K. Suri, Phys. Rev. C 20 (1979) 381
- 20) H.F. de Vries, thesis, Rijksuniversiteit, Utrecht (1976)
- 21) D. Janssen, R.V. Jolos and F. Dönau, Nucl. Phys. A 224 (1974) 93
- 22) A. Arima and F. Iachello, Ann. of Phys. 99 (1976) 253

Chapter 2

THE NUMBER-CONSERVING QUASIPARTICLE MODEL;
FORMALISM AND METHODS

2.1 INTRODUCTION

In this chapter the basic notions of the quasiparticle model or BCS model are given; the BCS model may be considered as an approximation of the shell model¹⁾. In the BCS model¹⁻⁷⁾ one calculates with so-called *quasiparticles*, which can be dealt with as particles, but they also incorporate an important property in nuclei, *viz.*: the pairing correlations of nucleons.

The shell model Hamiltonian is written in second quantization in terms of particle creation and annihilation operators as:

$$H = \sum_{\alpha} \epsilon_{\alpha} a_{\alpha}^{\dagger} a_{\alpha} + \frac{1}{4} \sum_{\alpha\beta\gamma\delta} V_{\alpha\beta\gamma\delta} a_{\alpha}^{\dagger} a_{\beta}^{\dagger} a_{\delta} a_{\gamma} \quad (2.1.1)$$

where $\alpha \equiv (n_{\alpha}, l_{\alpha}, j_{\alpha}, m_{\alpha}) \equiv (a, m_a)$ are the quantumnumbers of the particle orbits; ϵ_{α} is the single-particle energy of shell a ; $V_{\alpha\beta\gamma\delta}$ is the antisymmetrized matrix element of the residual interaction V .

Without interaction V the particles would stay in the orbits with the lowest energies ϵ_{α} , obeying the Pauli principle. Due to their interactions, however, they may be scattered over all possible orbits. Therefore the wave function of the nuclear states will be superpositions of

all possible particle configurations within these orbits in general. The coefficients of these configurations in the wavefunctions are obtained by diagonalizing H within the chosen configuration space. The number of configurations rapidly increases with the number of nucleons and the number of orbits which one chooses to consider. For example: consider the orbits, shown in fig. 2.1, the $1f_{5/2}$, $2p_{3/2}$, $2p_{1/2}$ and $1g_{9/2}$ orbits (this major shell is important in the calculations on the $N=50$ isotones; see Ch.4).

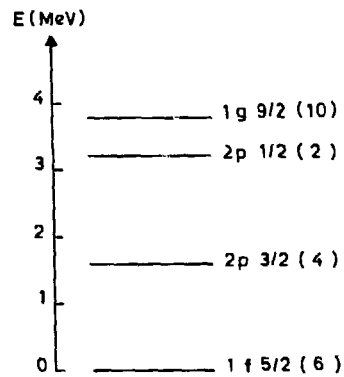


Figure 2.1 (Proton) single-particle orbits for the $N=50$ isotones with their maximum occupation number in parentheses.

If one particle moves in this single-particle space there are 3 possible ways to obtain a state with negative parity and one way to obtain a state with positive parity. If three particles are distributed in this space the number of ways to distribute them increases drastically.

Table 2.1 Number of configurations for the negative-parity states with three particles in the shells $1f_{5/2}$, $2p_{3/2}$, $2p_{1/2}$ and $1g_{9/2}$.

j^π			$1/2^-$	$3/2^-$	$5/2^-$	$7/2^-$	$9/2^-$	$11/2^-$	$13/2^-$	$15/2^-$	$17/2^-$	$19/2^-$	$21/2^-$
a	b	c											
$f_{5/2}$	$f_{5/2}$	$f_{5/2}$		1	1		1						
$f_{5/2}$	$f_{5/2}$	$p_{3/2}$	1	2	2	2	1	1					
$f_{5/2}$	$f_{5/2}$	$p_{1/2}$	1	1	1	1	1						
$p_{3/2}$	$p_{3/2}$	$p_{3/2}$		1									
$p_{3/2}$	$p_{3/2}$	$f_{5/2}$	1	1	2	1	1						
$p_{3/2}$	$p_{3/2}$	$p_{1/2}$	1	1	1								
$p_{1/2}$	$p_{1/2}$	$f_{5/2}$			1								
$p_{1/2}$	$p_{1/2}$	$p_{3/2}$		1									
$f_{5/2}$	$p_{3/2}$	$p_{1/2}$	1	2	2	2	1						
$g_{9/2}$	$g_{9/2}$	$f_{5/2}$	1	2	3	3	3	3	3	2	2	1	1
$g_{9/2}$	$g_{9/2}$	$p_{3/2}$	1	2	2	2	2	2	2	2	1	1	
$g_{9/2}$	$g_{9/2}$	$p_{1/2}$	1	1	1	1	1	1	1	1	1		
total			8	15	16	12	11	7	6	5	4	2	1 total 87

Every configuration is determined by the quantum numbers $[(ab)Jc]j^\pi$ where a, b and c are the quantum numbers of the single-particle orbits; the particles in shell a and b couple to angular momentum J; the total angular momentum is j; if the number of configurations for a certain choice of a, b, c and j is larger than one, more choices for J are possible.

In table 2.1 the number of configurations for negative parity states is shown; vertically the orbits are listed, which the particles occupy; horizontally the total angular momentum is shown; the numbers in the table are the numbers of configurations - *i.e.* possible ways to distribute the particles over the subshells, while they are coupled to a certain angular momentum - for the negative parity states. The total number of configurations is 87. Although the number in the example can be easily dealt with by computer techniques, for larger spaces reductions are required.

There are a few approximations which reduce the number of configurations. In section 2 the low-seniority approximation is introduced, which relies upon the pairing correlations of nucleons.

In section 3 the basic notions of the quasiparticle formalism are explained. It appears to be necessary to perform particle-number projection, the method of which is outlined in section 4.

A method to determine the parameters, used in the quasiparticle model is discussed in section 5.

2.2 THE LOW-SENIORITY APPROXIMATION

Nuclear binding energies depend systematically on whether the proton number Z and the neutron number N are even or odd⁸⁾

$$\delta B \approx \begin{cases} \Delta & Z \text{ even}, N \text{ even} \\ 0 & A \text{ odd} \quad (A=N+Z) \\ -\Delta & Z \text{ odd}, N \text{ odd} \end{cases}$$

where $\Delta \approx 12/A^{1/2}$ MeV.

This feature indicates, that it is preferable for

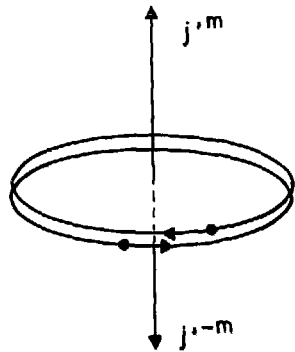


Figure 2.2 Classical picture of two nucleons with angular momentum j , which form a pair.

nucleons to move in pairs. Fig 2.2 shows a pair in a classical way. Two particles (with angular momentum j) form a pair, if their angular momenta are coupled to zero. The overlap of their orbitals is then very large. Therefore the two particles can gain more than 1 MeV energy in spite of the short range of the nucleon-nucleon interaction⁸⁾. This pairing property is the basis of the low-seniority approximation^{3, 4, 9, 10)}. In this approximation it is assumed that as many nucleons as possible move in pairs. The assumption of the occurrence of pairs yields two important simplifications of the formalism:

1) The number of pairs, that have to be distributed over the single-particle shells is only half the number of particles.

2) Angular momentum coupling of pairs is trivial.

The number of unpaired particles is called the seniority number ν ¹¹⁾. The number of configurations is rapidly increasing with seniority number. If one restricts oneself for ground states of even nuclei to $\nu=0$ basis states then the number of configurations in a shell model calculation is about a hundred for five single-particle shells. For the description of excited states at least $\nu=2$ states are necessary, the number of which is then several hundreds.

So still the number of configurations is very large. There exists a helpful formalism to simplify the description of many-body systems with pairing properties by supposing a special ordering of the pairs. This is the BCS-superfluidity theory, which will be touched upon in the next section.

2.3 THE BCS FORMALISM FOR SUPERFLUID NUCLEI

In the theory of superfluidity one assumes that fermions occur pairwise in states which are each other's time reverse and moreover that all these pairs may be described by the same pair-wave function. In terms of our formalism this means that the nuclear wave function is described as

$$\Psi(1,2,\dots,A) = N(S^\dagger)^{\frac{1}{2}A} |0\rangle \quad (2.3.1)$$

where $S^\dagger = \sum_a \phi_a S_a^\dagger$ is the creation operator of a pair which has coefficients ϕ_a for the particles to be created in the shell a . If one releases the condition that (2.3.1) should describe a system with a specific number of nucleon pairs, one may replace this expression by the exponential

$$\Psi_{\text{BCS}} = N' \exp(S^\dagger) |0\rangle \quad (2.3.2)$$

which is more convenient to perform simple calculations. The form (2.3.2) may be rewritten as

$$|\text{BCS}\rangle = \prod_{\alpha>0} (u_\alpha + v_\alpha s_\alpha a_\alpha^\dagger a_\alpha^\dagger) |0\rangle \quad (2.3.3)$$

which was (for the case of plane waves) introduced by Bardeen, Cooper and Schrieffer (BCS) in their original

treatise on superfluidity¹²⁾. In (2.3.3) α runs over all available states with $m_a > 0$; $\bar{\alpha} \equiv (a, -m_a)$; $s_\alpha = (-)^{j_a - m_a}$; u_a and v_a are the BCS parameters, which satisfy the normalization condition

$$u_a^2 + v_a^2 = 1 \quad (2.3.4)$$

The quantity v_a^2 is the occupation probability of shell a . These occupation probabilities completely determine the BCS wave function, which again illustrates the simplicity and coherence of its structure. It is therefore completely specified by a drawing like fig 2.3.

The parameters u_a and v_a are usually determined by the conditions:

$$\begin{aligned} \langle \text{BCS} | H | \text{BCS} \rangle &= \text{minimum} \\ \langle \text{BCS} | \hat{N} | \text{BCS} \rangle &= n_0 \end{aligned} \quad (2.3.5)$$

where \hat{N} denotes the particle number operator:

$$\hat{N} = \sum_{\alpha} a_{\alpha}^{\dagger} a_{\alpha} \quad (2.3.6)$$

and H is the Hamiltonian (2.1.1). The second condi-

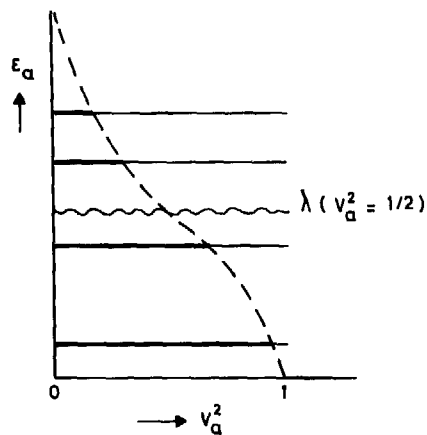


Figure 2.3 Sketch of a BCS pair distribution. The dotted line connects the occupation probabilities v_a^2 of the shells a . The level λ indicates the Fermi energy.

tion gives the BCS wave function the desired average number of particles n_0 (from definition (2.3.3) it is obvious that the BCS wave function contains components with different number of particles).

The equations (2.3.5) can be solved by introducing a Lagrange multiplier λ . One then obtains the so-called *gap equations*^{4,13}:

$$\begin{aligned} 2u_a v_a (\epsilon_a - \mu_a - \lambda) &= (u_a^2 - v_a^2) \Delta_a \\ \sum_a (2j_a + 1) v_a^2 &= n_0 \end{aligned} \quad (2.3.7)$$

$$\text{where } \Delta_a = -\frac{1}{2} \sum_{\alpha\beta} s_{\alpha\beta} V_{\alpha\alpha\beta\beta} \bar{u}_{\alpha} v_{\beta}$$

$$\mu_a = \sum_{\beta} V_{\alpha\beta\alpha\beta} v_{\beta}^2$$

The self-energy μ_a represents the binding for a particle in shell a with all other particles. The gap parameters Δ_a are related to the energy gap which occurs in superconductors. They are a measure of the diffuseness of the pair distribution; if Δ_a is large then the diffuseness is large. A typical value in nuclei is $\Delta_a \approx \Delta \approx 12/A^{1/2}$ MeV. The Lagrange multiplier λ is the energy of the Fermi level.

One easily proves that (2.3.3) is the vacuum for objects created by the operator:

$$\eta_{\alpha}^{\dagger} = u_a a_{\alpha}^{\dagger} - v_a s_{\alpha} a_{\alpha}^{-} \quad (2.3.8)$$

These operators obey the same anticommutation rules as the particle creation and annihilation operators. They are called *quasiparticle* (creation) operators. One has:

$$\eta_{\alpha} |BCS\rangle = 0 \quad (2.3.9)$$

$$\eta_{\beta}^{\dagger} |BCS\rangle = a_{\beta}^{\dagger} \prod_{\substack{\alpha > 0 \\ \alpha \neq \beta}} (u_{\alpha} + v_{\alpha} s_{\alpha} a_{\alpha}^{\dagger} a_{\alpha}^{\dagger}) |0\rangle \quad (2.3.10)$$

Equation (2.3.10) shows that η_{β}^{\dagger} destroys the pair $s_{\beta} a_{\beta}^{\dagger} a_{\beta}^{\dagger}$ and creates a particle a_{β}^{\dagger} . The state (2.3.10) is called a one-quasiparticle state (1q.p.) and has components with an odd number of particles only; this state should have its counterpart in an odd nucleus. Other states in odd nuclei may be generated by creating any odd number of quasiparticles.

The states of an even nucleus can be described by a superposition of states with an even number of quasiparticles.

As a quasiparticle operator destroys a coherent pair it will create a wave function with higher energy. The increase of energy is about 1 to 1.5 MeV for each quasiparticle, if one adopts a current nucleon-nucleon interaction. This follows from a transcription of the Hamiltonian in terms of quasiparticle operators.

The Hamiltonian (2.1.1) can be expressed in quasiparticle operators by transforming the particle operators into the quasiparticle operators by the inverse of (2.3.8):

$$a_{\alpha}^{\dagger} = u_{\alpha} \eta_{\alpha}^{\dagger} + v_{\alpha} s_{\alpha} \eta_{\alpha}^{-} \quad (2.3.11)$$

Then the Hamiltonian has the form:

$$H = H_0 + \sum_{\alpha} E_{\alpha} \eta_{\alpha}^{\dagger} \eta_{\alpha} + H_{22} + \text{other terms, which} \\ \text{change the number of quasiparticles.} \quad (2.3.12)$$

where H_{22} describes the interaction between quasiparticles. More details may be found in ref^{1,3 5,14}.

If one approximates the energy of a n-quasiparticle state by taking only the second term in (2.3.12) (the first term gives for all states the same constant $E(BCS) = H_0$), then

one has:

$$\begin{array}{llll}
 0 \text{ q.p.} & | \text{BCS} \rangle & E=0 & \\
 1 \text{ q.p.} & n_{\alpha}^{\dagger} | \text{BCS} \rangle & E=E_a & \geq \Delta \\
 2 \text{ q.p.} & \left[n_a^{\dagger} \times n_b^{\dagger} \right]_{M}^{J} | \text{BCS} \rangle & E=E_a + E_b & \geq 2\Delta \\
 3 \text{ q.p.} & \left[\left[n_a^{\dagger} \times n_b^{\dagger} \right]_{M}^{J} \times n_c^{\dagger} \right]_{m}^{j} | \text{BCS} \rangle & E=E_a + E_b + E_c & \geq 3\Delta
 \end{array}
 \tag{2.3.13}$$

$$\text{where } E_a = \left((\epsilon_a - \mu_a - \lambda)^2 + \Delta_a^2 \right)^{\frac{1}{2}} \geq \Delta_a
 \tag{2.3.14}$$

All Δ_a are roughly equal to Δ , which has a value of about 1.5 MeV in our applications.

So, if one neglects the interactions between the quasiparticles, then the energy difference between ν -quasiparticle states and $(\nu+2)$ -quasiparticle states is $2\Delta \approx 3\text{MeV}$. If one wants to calculate states of a single-closed-shell nucleus below 2 MeV one may therefore hope that it is sufficient to consider 0 q.p. and 2 q.p. for even nuclei and 1 q.p. and 3 q.p. for odd nuclei.

2.4 PARTICLE-NUMBER PROJECTION; THE BROKEN-PAIR MODEL

The BCS model presented in section 3 is simple. It has the drawback however, that the wave functions don't have a fixed number of particles. It is obvious, looking at (2.3.3), that the BCS wave function has components with 0, 2, 4, particles. This means that the BCS wave function for a nucleus with n_0 particles also contains components for nuclei with $n_0 \pm 2$, $n_0 \pm 4$, particles. One even can construct states, which do not have any component with the desired number of particles⁴⁾, the so-called *spurious states*. These spurious states describe in fact only states in neighbouring nuclei. It is necessary that these spurious components are removed from the model space by performing particle-number projection. The method of

particle-number projection, used for the calculations in this thesis is the one of refs^{4,5,14}).

The particle-number projected BCS model is equivalent to the broken-pair approximation¹⁵). The unnormalized $v=0,2$ broken-pair states are:

$$(S^\dagger)^P |\tilde{0}\rangle \quad (2.4.1)$$

$$A_{JM}^\dagger(ab) (S^\dagger)^{P-1} |\tilde{0}\rangle \quad (2.4.2)$$

where $|\tilde{0}\rangle$ denotes the closed shell state and $S^\dagger = \sum_a \frac{1}{2} \hat{a} v_a (u_a)^{-1} A_{00}^\dagger(aa)$ in the notation of ref¹⁴).

The relation of the broken-pair states (2.4.1) and (2.4.2) with the number-projected quasiparticle states of ref¹⁴) is:

$$(p!)^{-1} \left(\prod_a u_a^{\Omega_a} \right) (S^\dagger)^P |\tilde{0}\rangle = |\psi_{2p}\rangle \quad (2.4.3)$$

$$\begin{aligned} & ((p-1)!)^{-1} (1+\delta_{ab})^{-\frac{1}{2}} A_{JM}^\dagger(ab) \left(\prod_a u_a^{\Omega_a} \right) (S^\dagger)^{P-1} |\tilde{0}\rangle = \\ & u_a u_b |\psi_{2p, JM}(ab)\rangle + \frac{1}{2} \delta_{J0} \delta_{ab} \hat{a} u_a v_a |\psi_{2p}\rangle \end{aligned} \quad (2.4.4)$$

For the odd nuclei the relation of the broken-pair states with the number-projected quasiparticle states can be found in the appendix of Chapter 4.

2.5 RELATIONSHIP BETWEEN ODD AND EVEN SPECTRA IN THE BCS MODEL

In section 3 it is argued and globally indicated in (2.3.14), that a one-q.p. and two-q.p. state are about Δ and 2Δ respectively higher in energy than the BCS state. This leads to the picture, shown in fig 2.4 for the case of which the single-particle energies are shown in fig 2.1. The interaction is the pairing force with strength

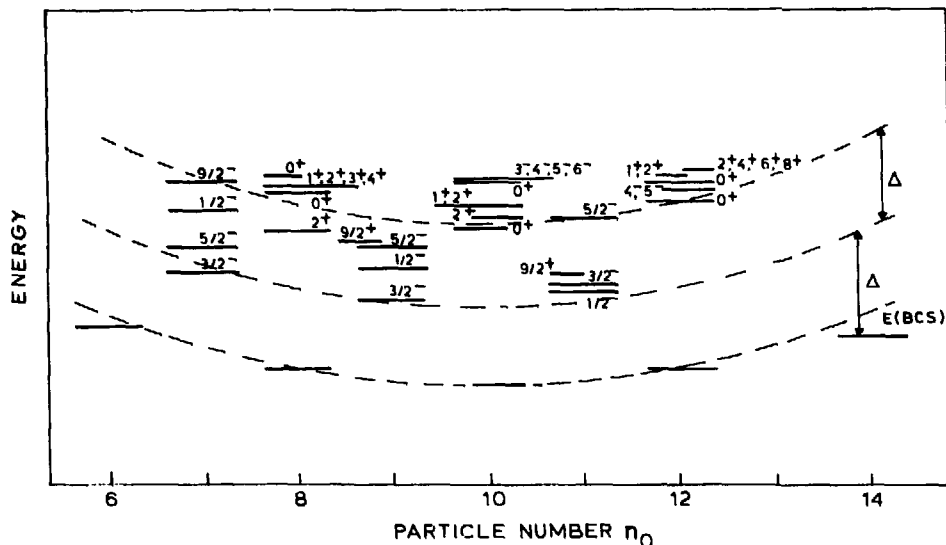


Figure 2.4 The spectra of odd and even nuclei as predicted by the BCS model. The single-particle energies of figure 2.1 and a pairing force with strength $G=0.4$ MeV are adopted. No number projection was performed, but the spurious 0^+ state was removed.

$V_0=0.4$ MeV. The ground states of the even nuclei are considered to be BCS (0 q.p.) states and the excited states the 2 q.p. states. In the odd nuclei the lowest states are considered to be 1 q.p. states. If the relative single-particle energies $\epsilon_a - \epsilon_b$ and the force strength V_0 are known the gap equations (2.3.7) can be solved; then the quasiparticle energies E_a (2.3.14) are obtained.

Gillet et al.¹⁶⁾ proved that one may reverse this procedure, *viz.*: starting from the experimental quasiparticle energies E_a one calculates the relative single-particle energies and the force strength.

The quasiparticle energies are derived from the experimental spectra of the odd nuclei in the following way. First one needs the odd-even mass difference (which mainly determines the force strength). Secondly one needs for all single-particle levels with angular momentum and parity j^π the lowest level with j^π in the odd nucleus. These levels

are considered as 1 q.p. states. If more than one level with a certain j^π have been observed then a sum of the energies, weighted with the spectroscopic factors from one-nucleon transfer data is used. The quasiparticle energies are the sum of the odd even mass difference and the excitation energy of this lowest state.

With these quantities the inverse of the gap equation (2.3.7) can be used to calculate u_a, v_a, ϵ_a and V_0 ; this method is known as the Inverse Gap Equation method (IGE)¹⁶⁾.

For even nuclei the parameters can now be obtained by interpolation of the parameters found for the odd nuclei. In this way one can perform for even nuclei calculations, which are free of further adjustable parameters. In the method IGE no particle-number projection is used. Particle-number projection may have a considerable effect on the excitation energies. Therefore one should use the Inverse Modified Gap Equations (IMGE) + $\nu=1$ fit or equivalently a IMGE + 1q.p.GCM fit. This was introduced by Allaart³⁾ and applied by Van Gunsteren⁵⁾ as the particle-number projected analogue of IGE. In Chapter 3 this procedure is used for several single-closed-shell nuclei in the pf shell. The meaning of the resulting parameters is discussed there.

The procedure IMGE + 1 q.p.GCM fit yields good results for single-closed-shell nuclei. Examples of these calculations can be found in refs^{3, 5-7)} and in Chapter 4 of this thesis.

In Chapters 5 and 6 quasiparticle degrees of freedom are coupled to harmonic vibrations. In this model it is not so easy to extract parameters from the odd nuclei as described above; phonon admixtures can play a large role in the low-lying states; in this case these states cannot be considered any more as 1 q.p. states. Therefore in such cases one normally considers the single-particle energies ϵ_a and force strength V_0 as free parameters.

References

- 1) M. Baranger, Phys. Rev. 120 (1960) 957
M. Baranger, in "1962 Cargèse lectures in theoretical physics", ed. M. Lévy, Benjamin, New York (1963)
- 2) A. Bohr, B.R. Mottelson and D. Pines, Phys. Rev. 110 (1958) 936
S.T. Belyaev, Kgl. Danske Videnskab. Selskab Mat.-Fys. Medd. 31 (1959) 11
- 3) K. Allaart and E. Boeker, Nucl. Phys. A 168 (1971) 630
- 4) K. Allaart, thesis, Vrije Universiteit, Amsterdam (1972)
- 5) W.F. van Gunsteren, thesis, Vrije Universiteit, Amsterdam (1976)
- 6) W.F. van Gunsteren, E. Boeker and K. Allaart, Z. Phys. 267 (1974) 87
- 7) W.F. van Gunsteren, K. Allaart and P. Hofstra, Z. Phys. 288 (1978) 49
- 8) A. Bohr and B.R. Mottelson, Nuclear Structure, vol.1, Benjamin, New York (1969)
- 9) M.H. Mc Farlane, Lectures in Theoretical Physics, eds. P.D. Kunz, D.A. Lind and W. Brittin, University of Colorado Press, Boulder, Colorado, (1966) 583
- 10) A.R. Edmonds, Angular momentum in quantum mechanics, Princeton University Press, Princeton, New Jersey (1960)
- 11) A. de Shalit and I. Talmi, Nuclear Shell Theory, Academic Press, New York (1963)
- 12) J. Bardeen, L.N. Cooper and R. Schrieffer, Phys. Rev. 108 (1957) 1175
- 13) J.M. Eisenberg and W. Greiner, Nuclear Theory, vol.3, North-Holland, Amsterdam (1976)
- 14) P.L. Ottaviani and M. Savoia, Phys. Rev. 187 (1969) 1306
G. Bonsignori and M. Savoia, Nuovo Cim. 3A (1971) 309
P.L. Ottaviani and M. Savoia, Nuovo Cim. 57A (1970) 630; Phys. Rev. 178 (1969) 1594
- 15) Y.K. Gambhir, A.Rimini and T. Weber, Phys. Rev. 188 (1969) 1573
- 16) V. Gillet, B. Giraud, J. Picard and M. Rho, Phys. Lett. 27B (1968) 483
V. Gillet, B. Giraud and M. Rho, Phys. Rev. 178 (1969) 1695

*Chapter 3*APPLICATION OF THE SUPERFLUIDITY MODEL TO SCS NUCLEI
IN THE PF SHELL

3.1 INTRODUCTION

In chapter 2 a brief outline has been given of the number-projected BCS model. In the Shell Model Hamiltonian it was assumed that the single-particle energies are independent of the magnetic quantum number m_a . Therefore the formulas given there apply to spherical nuclei only. Nuclei with a single closed shell are indeed expected to have a spherical shape. Examples of this type of nuclei are the Ca and Ni isotopes and the N=28 isotones.

First, single-particle energies will be determined for these nuclei with the method IMGE + 1 q.p.GCM fit, mentioned in chapter 2. The single-particle shell model space for the protons and the neutrons consists of the pf shell. As residual interactions the Kuo Brown force, the Mc Grory force and a Gaussian Serber force are used.

Next, the obtained values of the single-particle energies for ^{52}Cr will be used in a HFB calculation to see whether the intrinsic groundstate is spherical or whether it turns out to be deformed. In the former case the model would be consistent; in the latter case we conclude that one should not consider the parameters obtained by the IMGE + 1 q.p.GCM fit as suitable parameters in other model spaces.

Finally these parameters will be used in a projected

two-quasiparticle calculation for ^{50}Ti , ^{52}Cr and ^{54}Fe .

3.2 DETERMINATION OF THE PARAMETERS

In the pf shell single-particle energies were determined for protons as well as for neutrons. For protons the spectroscopic data of the odd $N=28$ isotones⁴⁾ were used. The quasiparticle energy for an orbit j^π , given in table 3.1, is the sum of the odd-even mass difference^{1,2)} plus the sum of the energies of the levels with j^π in the odd nucleus weighted with the spectroscopic factors for one-nucleon transfer. The number of levels we used to calculate a quasiparticle energy for these nuclei was mostly less than five; for a few cases it was even about ten. For higher levels the available experimental data become less clear. This introduces considerable uncertainties of the order of 0.5 MeV. The neutron single-particle energies were extracted from the nuclei $^{41,43,45,47}_{20}\text{Ca}$ and $^{57,59}_{28}\text{Ni}$. In both cases only one kind of particles is assumed to be excited. The obtained quasiparticle energies are listed in table 3.1. Three residual interactions were used.

The first is the Kuo Brown force¹⁾, which was determined, starting from the Hamada-Johnston nucleon-nucleon interaction.

The second is the Mc Grory force²⁾, which is a modification of the Kuo Brown force, to fit better the spectra of light pf shell nuclei for some shell model calculation.

The third interaction is the simple Gaussian Serber force

$$V(r_{12}) = -V_0 P_S \exp\left(\frac{-r_{12}^2}{\mu^2}\right)$$

where V_0 is the force strength,

P_S is the singlet even projection operator,

$\mu = 2.0$ fm is the range.

Table 3.1 Proton and neutron quasiparticle energies (MeV) used to determine the single-particle energies.

Protons						
	⁴⁹ Sc	⁵¹ V	⁵³ Mn	⁵⁵ Co		
1f _{7/2}	1.70	1.61	1.56	1.46		
2p _{3/2}	5.23	4.17	3.97	4.05		
1f _{5/2}	6.47	5.76	5.29	5.03		
2p _{1/2}	7.60	7.09	6.03	4.79		
Neutrons						
	⁴¹ Ca	⁴³ Ca	⁴⁵ Ca	⁴⁷ Ca	⁵⁷ Ni	⁵⁹ Ni
1f _{7/2}	1.68	1.78	1.68	1.50	5.37	5.65
2p _{3/2}	3.86	3.76	3.68	3.50	1.25	1.55
1f _{5/2}	6.57	5.72	6.18	6.50	2.03	2.05
2p _{1/2}	5.76	5.43	5.18	5.50	2.36	2.35

For these interactions first overall force strengths were adjusted so as to fit the odd-even mass differences with the IMGE method. For the Kuo Brown and Mc Grory interactions the resulting factor was within a few percent 1.0. This shows some consistency of these forces with our method to fit these parameters. For the Serber force the result was $V_0=44.0$ MeV. These values were next used in the one-quasiparticle GCM fit.

For the resulting single-particle energies for the N=28 isotones and the Ni isotopes a correction was made for the binding by 8 nucleons of the other kind in the 1f_{7/2} shell:

$$\Delta\epsilon_k = -\frac{1}{2}(2j_k+1)^{-1} \sum_{J,T} (2J+1) G(k^7/2k^7/2J^T) \quad (3.1)$$

This means that the energies for all nuclei are calculated relative to a ⁴⁰Ca core. Without the correction (3.1) the energies would be given relative to a ⁴⁸Ca core for the N=28 isotones or a ⁴⁸Ni core for the Ni isotopes. The correction amounts to a downward shift of the 2p_{3/2}, 1f_{5/2} and 2p_{1/2} single-particle levels relative to the 1f_{7/2}

level of 1.35 MeV, -1.81 MeV and 0.80 MeV respectively for the Kuo Brown force and of 4.16 MeV, 1.02 MeV and 3.63 MeV respectively for the Mc Grory force. The shifts of the Mc Grory force are 2.83 MeV larger. This is due to the fact that this force has stronger matrix elements $G (7/2 \ 7/2 \ 7/2 \ 7/2 \ JT)$; this results in a stronger binding for the $1f_{7/2}$ single-particle level if the 8 particles of the other kind are included. The energy shifts (3.1) for the Serber force are much smaller, *viz.* 0.32 MeV, -0.62 MeV and 0.21 MeV for the $2p_{3/2}$, $1f_{5/2}$ and $2p_{1/2}$ level. The single-particle energies are drawn in figure 1. Especially important for a calculation on an even $N=28$ nucleus is the gap between the $1f_{7/2}$ proton and neutron level and the other levels; therefore let us consider the relative single-particle energies $\varepsilon(p_{3/2}) - \varepsilon(f_{7/2})$.

For the protons the results for the Kuo Brown and Mc Grory matrix elements are nearly identical relative to a ^{48}Ca core. Due to the binding correction (3.1) there is a difference of 2.83 MeV relative to a ^{40}Ca core. The result for the Serber force is a little different. The main difference with the other forces is again the correction (3.1). For the neutrons the situation is almost the same as for protons; the large differences between the three forces for 9 and 11 particles are due to the correction (3.1): *i.e.* relative to a ^{48}Ni core they are almost the same.

We consider single-particle energies to be acceptable if they satisfy the following two criteria:

- i) The variation of the single-particle energies as a function of particle-number should be smooth^{1,2)};
- ii) the difference between the relative proton and neutron single-particle energies should not be too large. The only relevant difference between protons and neutrons is the Coulomb potential but the relative effect on the single-particle energies is known to be small.

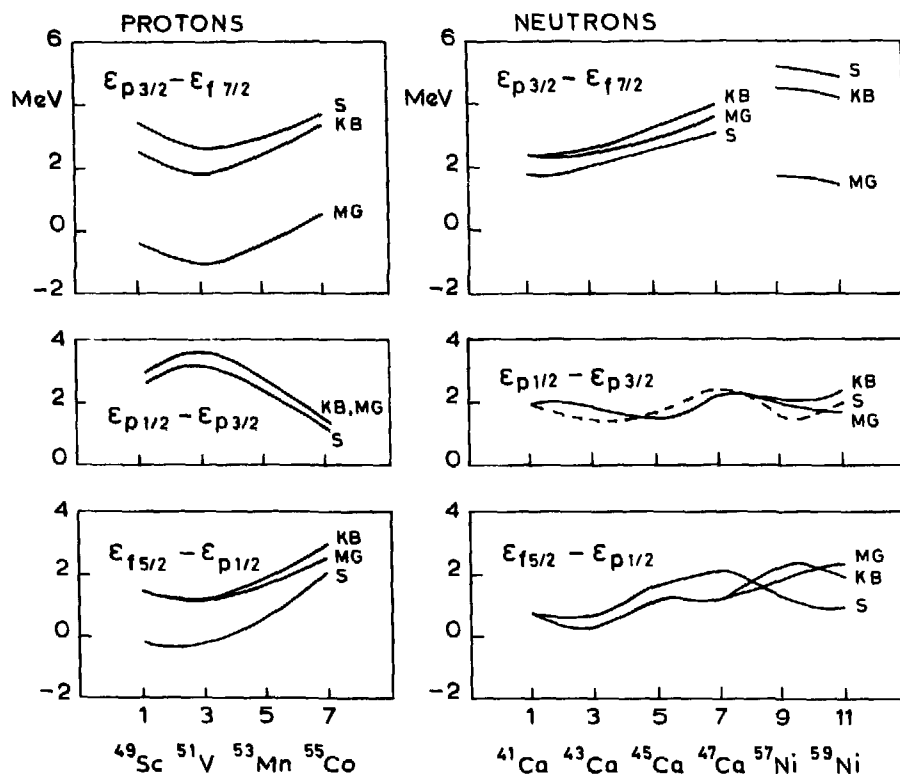


Figure 3.1 Single-particle energies for protons and neutrons in the pf shell for the Kuo Brown interaction (KB), the Mc Grory interaction (MG) and the Serber force (S). The nuclei, from which the quasiparticle energies were taken are given below in the figure.

From figure 3.1 one may notice that the Kuo Brown force satisfies the two criteria best. The Serber force and the Mc Grory force show discontinuities in the relative single-particle energies $\epsilon(p_{3/2}) - \epsilon(f_{7/2})$ for the neutrons; for the Mc Grory force the difference between the energies of the proton and neutron $p_{3/2}$ level relative to the $f_{7/2}$ level is about 3 MeV. Mc Grory's ad hoc changes of the Kuo Brown force, to fit the light pf shell nuclei better, are responsible for this effect.

3.3 THE HARTREE-FOCK-BOGOLYUBOV (HFB) GROUND STATE

The HFB theory may be considered as a generalization of the Hartree-Fock (HF) theory. Therefore, it is first indicated, how the HF ground state energy is calculated.

Thereafter the extension to the HFB case is simple.

3.3.1 The Hartree-Fock ground state⁶⁾

In second quantization the Hamiltonian \hat{H} in the HF theory is given by:

$$\hat{H} = \sum_{\alpha\beta} \langle \alpha | T | \beta \rangle a_{\alpha}^{\dagger} a_{\beta} + \frac{1}{4} \sum_{\alpha\beta\gamma\delta} \langle \alpha\beta | V | \gamma\delta \rangle a_{\alpha}^{\dagger} a_{\beta}^{\dagger} a_{\delta} a_{\gamma} \quad (3.2)$$

where T is the kinetic energy operator,

V is the nucleon-nucleon interaction.

One determines the nuclear wave function ϕ , which is a solution of the Schrödinger equation

$$\hat{H}\phi = E\phi \quad (3.3)$$

in an approximate way by assuming, that for a nucleus, consisting of A particles, ϕ can be written as a Slater determinant

$$\prod_{\mu=1}^A a_{\mu}^{\dagger} |0\rangle \quad (3.4)$$

The precise nature of the single-particle states μ are not yet specified. Only orthogonality is required. ϕ has to satisfy:

$$\delta \langle \phi | \hat{H} | \phi \rangle = 0 \quad (3.5)$$

which is equivalent to

$$\langle \delta\phi | \hat{H} | \phi \rangle = \langle \phi | \hat{H} | \delta\phi \rangle = 0 \quad (3.6)$$

where $\delta\phi$ is orthogonal to ϕ . In second quantization $\delta\phi$ is given by:

$$|\delta\phi\rangle = \eta a_{\sigma}^{\dagger} a_{\lambda} | \phi \rangle \quad (3.7)$$

with η infinitesimal; σ should refer to an empty state and λ to an occupied state.

Then equations (3.6) lead to:

$$\langle \sigma | T | \lambda \rangle + \sum_{\mu=1}^A \langle \sigma \mu | V | \lambda \mu \rangle = 0 \quad \text{and} \quad (3.8)$$

$$\langle \lambda | T | \sigma \rangle + \sum_{\mu=1}^A \langle \lambda \mu | V | \sigma \mu \rangle = 0 \quad (3.9)$$

To specify the single-particle states μ in (3.4) one diagonalizes:

$$\langle \alpha | T | \beta \rangle + \sum_{\mu=1}^A \langle \alpha \mu | V | \beta \mu \rangle = \epsilon_{\alpha} \delta_{\alpha\beta} \quad (3.10)$$

The resulting single-particle states automatically fulfill equations (3.8) and (3.9). The self consistent HF potential U is defined by:

$$\langle \alpha | U | \beta \rangle = \sum_{\mu=1}^A \langle \alpha \mu | V | \beta \mu \rangle \quad (3.11)$$

Equation (3.10) can be written as:

$$\langle \alpha | T+U | \beta \rangle = \langle \alpha | \epsilon_{\alpha} | \beta \rangle \quad (3.12)$$

Notice, that U is still dependent on the single-particle wave functions μ . The solution of equation (3.12) is obtained by starting with trial single-particle wave functions. This process has to be repeated until the solution is stable. The energy of the ground state is then given by:

$$\begin{aligned} E_0 = \langle \Phi | \hat{H} | \Phi \rangle &= \sum_{\lambda=1}^A \langle \lambda | T | \lambda \rangle + \frac{1}{2} \sum_{\mu=1}^A \langle \lambda \mu | V | \lambda \mu \rangle \\ &= \sum_{\lambda=1}^A \epsilon_{\lambda} - \frac{1}{2} \sum_{\lambda=1}^A \langle \lambda | U | \lambda \rangle \end{aligned} \quad (3.13)$$

3.3.2 The Hartree-Fock-Bogolyubov ground state⁵⁾

The essential difference between the HF theory and the HFB theory is, that the trial wave function is chosen in a different way. Here one first defines the quasiparticle operators η_k^{\dagger} by:

$$\eta_k^\dagger = \sum_{\alpha} (A_{\alpha k} a_{\alpha}^\dagger + B_{\alpha k} a_{\alpha}) \quad (3.14)$$

The quasiparticle operators should satisfy the anticommutation rules for fermions; this requirement gives a restriction for the matrices A and B. The trial wave function Φ , given by:

$$|\Phi\rangle = \prod_k \eta_k |0\rangle \quad (3.15)$$

is a vacuum for the quasiparticle operators.

The choice $A_{\alpha k} = 0$ for occupied states and

$B_{\alpha k} = 0$ for empty states

leads to the trial wave function in the HF theory. The quasiparticle wave functions are determined by the HFB equations:

$$\sum_{\beta} \left\{ (\langle \alpha | T | \beta \rangle + \sum_{\mu\nu} \langle \alpha\mu | V | \beta\nu \rangle \langle B^* B^T \rangle_{\mu\nu}) A_{\beta p}^\dagger + \frac{1}{2} \sum_{\mu\nu} \langle \alpha\mu | V | \beta\nu \rangle \langle AB^\dagger \rangle_{\mu\nu} B_{\beta p} \right\} = E_{\alpha} A_{\alpha p} \quad \text{and} \quad (3.16)$$

$$\sum_{\beta} \left\{ (\langle \beta | T | \alpha \rangle + \sum_{\mu\nu} \langle \beta\mu | V | \alpha\nu \rangle \langle B^\dagger B \rangle_{\mu\nu}) B_{\beta p} + \frac{1}{2} \sum_{\mu\nu} \langle \beta\mu | V | \alpha\nu \rangle \langle B^T A^* \rangle_{\mu\nu} A_{\beta p} \right\} = E_{\alpha} B_{\alpha p} \quad (3.17)$$

From these equations the BCS gap equations can be derived with the choice $A_{\alpha k} = u_k \delta_{\alpha k}$ and $B_{\alpha k} = v_k \delta_{\alpha k} s_k$. Then the quasiparticle operator (3.14) is the BCS quasiparticle operator. Apparently the HFB equations generalize both the HF and BCS equations. The HFB equations determine self consistently the single-particle energies. If the single-particle shell model space is too large (for example for ^{52}Cr) then an inert core is assumed and the binding for a particle in shell λ by this core is simulated by a single-particle energy $\tilde{\epsilon}_{\lambda}$, which includes also the kinetic energy term. This single-particle energy is set equal to the single-particle

energy found in section 3.2.

3.4 RESULTS

For ^{52}Cr a HFB calculation was performed with the parameters obtained with the Kuo Brown force, because this gave a smoother behaviour of the energies of the single-particle levels as a function of the particle number. Besides, the results with the Mc Grory matrix elements will not be very different, because the energies relative to a ^{48}Ca core are not very different.

First a HFB calculation was performed, while the nucleus was restricted to a spherical shape, *i.e.* essentially a BCS calculation.

Next, in another calculation the nucleus was allowed to deform to find the minimum energy for the intrinsic ground state. The results of the second calculation are the following. It shows a minimum for the ground state energy for a prolate deformation. The energy gained by deformation is about 2.5 MeV. The quadrupole moment of the intrinsic ground state is 142 fm^2 . This means, that the single-particle energies obtained by the IMGE + 1 q.p. GCM fit should not be used in a HFB calculation; the assumption that the $N=28$ nuclei are spherical is not consistent in that case. Therefore our parameters should be considered as connected with the model space in which one considers at most two particles which are not coupled to a (spherical) pair.

Next, we proceeded to perform a two-quasiparticle calculation, to see what the result would look like. The proton single-particle energies for ^{50}Ti , ^{52}Cr and ^{54}Fe are listed in table 3.2 In the figures 3.2, 3.3 and 3.4 the results are compared with the experimental spectra and other calculations.

In figure 3.2 the results are shown for ^{50}Ti . The model

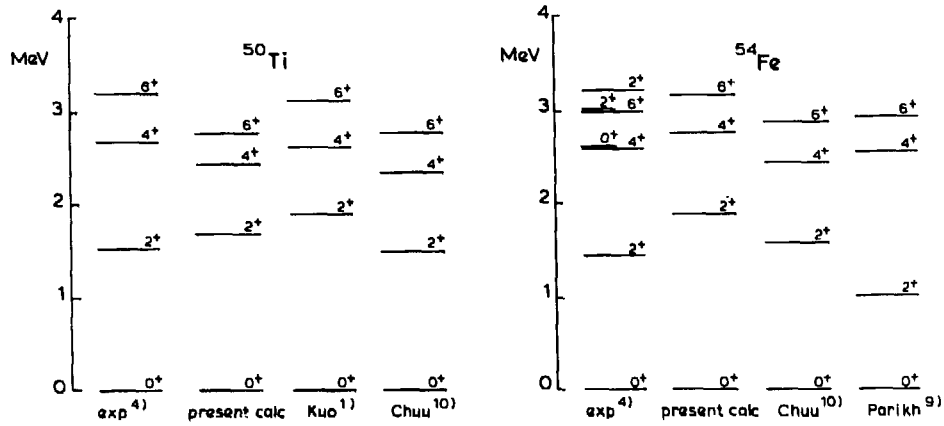


Figure 3.2 Experimental and calculated spectra of ^{50}Ti . Figure 3.3 Experimental and calculated spectra of ^{54}Fe .

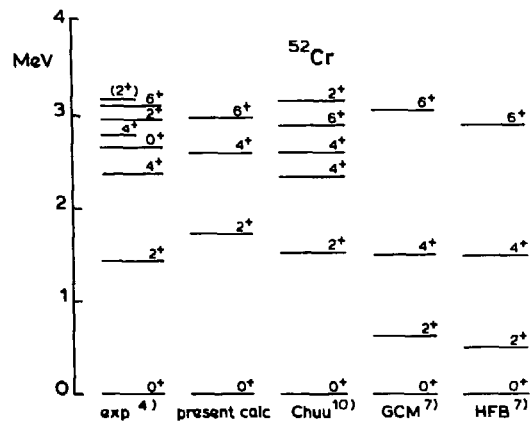


Figure 3.4 Experimental and calculated spectra of ^{52}Cr .

of Kuo and Brown is identical with ours. Only the single-particle energies are different, *viz.*: $\epsilon(f_{7/2})=0.0$, $\epsilon(p_{3/2})=4.4$, $\epsilon(f_{5/2})=5.9$ and $\epsilon(p_{1/2})=6.9$. The dominant configuration is $(f_{7/2})^2$. Therefore the result of Kuo and Brown and ours are much alike.

We also compare with the shell model calculation of Chuu et al.¹⁰⁾. In that calculation the neutron $1f_{7/2}$

Table 3.2 Proton single-particle energies in MeV for the Kuo Brown interaction, used in the 2-quasiparticle calculation.

nucleus	$\epsilon(f_{7/2})$	$\epsilon(p_{3/2})$	$\epsilon(f_{5/2})$	$\epsilon(p_{1/2})$
^{50}Ti	0.0	3.41	4.93	6.27
^{52}Cr	0.0	3.39	4.96	6.09
^{54}Fe	0.0	4.11	5.46	5.61

shell is closed; all protons but one are assumed to occupy the $f_{7/2}$ shell and the interaction of Schiffer and True¹¹⁾, the 14 parameters of which are fitted to the spectra of the N=28, N=29 and N=30 nuclei, is used. For ^{50}Ti their result is not very different from ours.

The results for ^{54}Fe are shown in figure 3.3. Like for ^{50}Ti our result does not differ much from that of Chuu et. al. The spectrum can be explained to a large extent by the configuration of two holes in the $1f_{7/2}$ shell.

In the calculation of Mrs. Parikh⁹⁾ protons and neutrons were assumed to occupy the pf shell. As an effective interaction she used the Mc Grory interaction and two bands were calculated:

- 1) a prolate HF band
- 2) a second prolate HF band

The first has the ground state with the lowest energy. The single-particle energies were varied to fit the spectrum of ^{54}Fe . The two band were mixed. The result looks more like rotational than our result and experiment.

Figure 3.4 shows the results for ^{52}Cr . Our calculation is able to reproduce the energies of the levels, which can be understood in terms of $\nu=2$ configurations. The calculation of Chuu et.al. can also describe some levels with a $\nu=4$ character. The GCM and HFB calculations of Mütter et.al. are interesting. They find using a Mc Grory interaction a HFB intrinsic ground state with a prolate minimum. This

minimum is 0.2 MeV lower than the spherical solution. The quadrupole moment was 121 fm^2 , which is near our result (142 fm^2). The calculated spectrum is too rotational. Later Mütter decreased the energy of the $1f_{7/2}$ single-particle level by 1 MeV and his results improved; the shape of ^{52}Cr was then almost spherical¹⁴⁾.

3.5 CONCLUSION

All spherical models, shown in section 4, give reasonable results for $N=28$ nuclei.

The calculations of Parikh and Mütter have a freedom for the nucleus to deform. The Kuo Brown interaction then produces a deformed solution, unless the gap between the $1f_{7/2}$ single-particle level and the other single-particle levels is increased arbitrarily, so that a spherical solution is obtained. Then this model gives reasonable results for the spectra.

It is apparent, that good results are obtained, only, if the shape of the nucleus is (almost) spherical. When the single-particle energies which are determined with the *spherical* IMGE method and the 1 q.p.GCM fit, are used in a HFB calculation, a deformed solution is obtained. This is an indication, that these parameters should not be used in a HFB calculation. Apparently parameters and model are coupled, so that one may not use parameters from an essentially spherical model 1 q.p.IMGE to perform calculation with deformed degrees of freedom.

This conclusion is not completely unexpected. A dependence of the parameters on the model space was also present in earlier calculations by Van Gunsteren for example¹³⁾. There the single-particle energies from the IMGE + 1 q.p.GCM fit did not give good results in 3 q.p. calculations for the Sn isotopes. The extension of the model space by including states with two extra quasiparticles shifted the lowest

levels by a few hundred keV. So a new determination of the parameters, which was essentially a three-quasiparticle fit for the single-particle energies, had to be performed¹³⁾. When one allows nuclear deformation, this is equivalent with including many-quasiparticle states. So the appropriate model parameters may then differ considerably from those found in our treatment.

References

- 1) T.S. Kuo and G.E. Brown, Nucl. Phys. A 114 (1968) 241
- 2) J.B. Mc Grory, Phys. Rev. C 8 (1973) 693
- 3) J. Rapaport, Nucl. Data Sheets B 3 - 5,6 (1970) 85
- 4) P.M Endt and C. van der Leun, Nucl. Phys. A 214 (1973) 1 and Nucl. Phys. A 105 (1967) 337
M.B. Lewis, Nucl. Data Sheets B 4 - 3,4 (1970) 237 and 313
S. Raman, Nucl. Data Sheets B 4 - 3,4 (1970) 397
M.N. Rao, J. Rapaport, Nucl. Data Sheets B 3 - 5,6 (1970) 37
R.L. Auble, M.N. Rao, Nucl. Data Sheets B 3 - 5,6 (1970) 127
R.L. Auble, J. Rapaport, Nucl. Data Sheets B 3 - 3,4 (1970) 1
J. Rapaport, Nucl. Data Sheets B 3 - 3,4 (1970) 103
J. Vervier, Nucl. Data Sheets B 2 - 5 (1968) 1
H. Verheul, R.L. Auble, Nucl. Data Sheets 23 (1978) 355
- 5) K. Goeke, thesis, Institut für Kernphysik, Julich, Jül 817 - KP (1971)
- 6) J.M. Eisenberg and W. Greiner, Nuclear Theory, North-Holland, Amsterdam (1972)
- 7) H. Müther, K. Allaart, K. Goeke, A. Paessler, Nucl. Phys. A 248 (1975) 451
- 8) Chapter 4
- 9) J.K. Parikh, Phys. Rev. C 10 (1974) 2568
- 10) D.S. Chuu, C.S. Han, S.T. Hsieh and H.C. Chiang, J. Phys. G.: Nucl. Phys., Vol. 4, No. 8 (1978) 1275
- 11) J.P. Schiffer and W.W. True, Rev. Mod. Phys. 48 (1976) 191
- 12) K. Allaart, thesis, Vrije Universiteit, Amsterdam (1971)
- 13) W.F. van Gunsteren, thesis, Vrije Universiteit, Amsterdam (1976)
- 14) H. Müther, K. Goeke, A. Paessler and K. Allaart, Phys. Lett. 60 B (1976) 427

Chapter 4

A Broken-Pair Description of ^{89}Y , ^{91}Nb and ^{93}Tc

The low-energy properties of ^{89}Y , ^{91}Nb and ^{93}Tc are described in a broken-pair model. The shell model space for the protons consists of one major shell and for the neutrons particle-hole states within two major shells are taken into account. The effective interaction is assumed to be a simple Gaussian Serber force, which has proved to be the most successful in adjacent even nuclei.

Energy spectra up to about 3 MeV excitation energy and one-nucleon transfer data can be described very well. Also electromagnetic properties can be reproduced rather well if reasonable effective charges are used. No indication for deformed states, as found in Sn nuclei, is observed.

1. Introduction

For many years attempts have been made to describe the $N=50$ isotones. The main reason for this has been the supposition that $^{88}\text{Sr}_{50}$ might be treated as a proper inert core, so valence protons were restricted to the $2p\ 1/2$ and $1g\ 9/2$ single-particle levels. Within this small model space relationships between the energy spectra of several nuclei as predicted by the shell model can be shown to be satisfied to a large extent [1-6].

In several investigations it has been remarked however that also excitations from the $2p\ 3/2$ level are important, especially to describe electromagnetic properties [7-12]. In the work of Vergados and Kuo [11] both proton and neutron excitations from the ^{88}Sr core were allowed for the description of the energy levels of ^{89}Y . In a recent, rather extensive study of both the even and odd $N=50$ isotones Fujita and Komoda allowed one - or two-proton excitations from the $2p\ 3/2$ level [12]. Although this is sufficient to obtain non-zero values for $M1$, $E2$ and $E3$ transitions, the comparison with experimental data points out that the results are not always satisfactory, especially for collective transitions in even nuclei. Such collective transitions have been studied extensively by Gillet et al. [13] in the framework of the BCS model. They found that the $E3$ excitations

can be reasonably well accounted for by this model, but the description of $E2$ excitations was found to be poor.

Allaart and Boeker have demonstrated however that the latter are considerably improved for $N=50$ isotones by a systematic particle-number conserving BCS treatment [14].

There are several reasons why one may prefer a number-conserving BCS quasiparticle model [15], which is equivalent with a broken-pair model [16] or the generalized seniority scheme [17], rather than a straightforward shell model treatment. One reason is that one can easily deal with more than one major shell to describe the pairing properties [18]. Also when one restricts the model to one major shell the projected quasiparticle or broken-pair model yields a good prescription how to select a few model states out of a many times larger shell model basis without losing much accuracy [19]. It also provides a transparent picture of the structure of the nuclear states, supposing that most nucleons occur as unbroken pairs (which are supposed to be the microscopic equivalent of S -bosons in [20]).

In the present paper we report the application of the projected quasiparticle [15] or broken-pair [16] model to odd $N=50$ isotones. So far this model has

been applied to odd Sn nuclei only [21, 22]. Since it is known [23] that in Sn nuclei certain deformed structures may appear at rather low excitation energy, the $N=50$ isotones might be more suitable for the application of the model. As the description of the odd nuclei can only be expected to be successful when also the lowest (collective) excited states can be described by the same method, these states are considered first, and improved by the inclusion of neutron particle-hole excitations. Therefore the basis states for the description of the odd isotones are states with one broken proton pair or a neutron particle-hole pair. In Sect. 2 the model and the computational method are outlined. Section 3 contains the resulting spectroscopic properties and a comparison with experimental data. Section 4 contains a summary and conclusions.

2. Model and Computational Procedure

2.1. The Model Space

The model space consists of states of the following three types

a) states without a broken pair:

$$a_{\pm}^{\pm} (S^{\pm})^p |\bar{d}\rangle \quad (2.1)$$

b) states with a broken proton pair:

$$a_{\pm}^{\pm} a_{\mp}^{\pm} a_{\pm}^{\pm} (S^{\pm})^{p-1} |\bar{d}\rangle. \quad (2.2)$$

c) states with a neutron particlehole pair:

$$a_{\pm}^{\pm} b_{\mp}^{\pm} b_{\pm}^{\pm} (S^{\pm})^p |\bar{d}\rangle \quad (2.3)$$

where $|\bar{d}\rangle$ denotes the closed shell ($Z=28$, $N=50$) state and $S^{\pm} = \sum_a \frac{\hat{a}}{2u_a} A_{\bar{d}0}^{\pm}(aa)$ in obvious notation

[19]. The BCS-parameters r_a, u_a are determined such that the presence of unpaired particles is accounted for in an average way [23]. The technique how to calculate matrix elements of a shell model hamiltonian in the space of states (2.1) and (2.2), coupled to proper angular momenta, is well known [15, 21]. In [15] extensive formulas have been given. The extension to include the particlehole states (2.3) is straightforward. Formulas are given in the appendix.

The shell model orbits included are the $1f5/2$, $2p3/2$, $2p1/2$ and $1g9/2$ shells for protons, the $1f5/2$, $2p3/2$, $2p1/2$ and $1g9/2$ for the neutron hole and the $2d5/2$, $1g7/2$, $2d3/2$, $3s1/2$ and $1h11/2$ shells for the neutron particle. A restriction, which was justified by some test calculations, is that the neutron particle-hole configuration should have natural parity ($J^{\pi} = 2^+, 3^-, 4^+, \dots$). The $J^{\pi} = 1^-$ configurations were ex-

Table 1. Relative single-particle energies and force strengths used in the calculation of ^{89}Y , ^{91}Nb and ^{93}Tc in MeV

	Protons			Neutrons			
	^{89}Y	^{91}Nb	^{93}Tc				
$1f5/2$	0.0	0.0	0.0	$1f5/2$	-3.0	$2d5/2$	4.0
$2p3/2$	1.59	1.19	2.04	$2p3/2$	-2.0	$1g7/2$	5.0
$2p1/2$	3.22	3.36	3.80	$2p1/2$	-1.0	$3s1/2$	5.0
$1g9/2$	3.80	3.36	3.26	$1g9/2$	0.0	$2d3/2$	6.0
						$1h11/2$	7.0
V_0	36.1	36.0	37.2				

cluded because they only produce a low-lying spurious (center of mass motion) state and high-lying states which do not contribute significantly to the lowest part of the spectra.

2.2. The Model Parameters

The shell model effective interaction is assumed to be of the form

$$V(1,2) = -V_0 R_0 \exp\left(\frac{-r^2}{\mu^2}\right) \quad (2.4)$$

where R_0 is the singlet operator. The range parameter μ is taken to be 1.9 fm. Although this force is very simple it appears to give good results in practical calculations of even single-closed-shell nuclei; better than several more complicated forces [24]. The proton single-particle energies were determined from experimental data by the number-conserving analogue of the inverse gap equations [25]. In ^{91}Nb these energies were taken slightly different from those of [25] in order to reproduce the fragmentation of the $p3/2$ and $f5/2$ single-particle strength better. For the neutron single-particle energies a reasonable guess was made. The results are not sensitive to small changes in these energies. The parameters are listed in Table 1. For the even nuclei, of which we need the ground state wave function for the calculation of one-nucleon transfer spectroscopic factors, interpolated parameters are used. Further model parameters are the effective charges $e^{\text{eff}} = 1.4e$ for protons and $0.4e$ for neutrons and the effective spin-gyromagnetic factors $g^{\text{eff}} = 3.29$ n.m. for protons and -2.50 n.m. for neutrons. With these values we reproduced the $B(E2; 2_1^+ \rightarrow \text{g.s.})$ and $B(M1; 1_1^+ \rightarrow \text{g.s.})$ in ^{88}Sr .

3. Results and Discussion

3.1. Spectroscopic Factors

Table 2 shows that the experimental values for one proton transfer reactions are reproduced reasonably well by the calculation. (The pick-up data for ^{89}Y

Table 2. Spectroscopic factors for one-proton transfer reactions

J^π	Stripping			Pick up		
	keV	calc.	exp.	calc.	exp.	
^{89}Y	$1/2^-$	0	0.77	0.92	1.41	1.91
	$9/2^+$	909	0.88	0.74	0.77	1.10
	$3/2^-$	1,507	0.11	0.10	3.55	4.25
	$5/2^-$	1,744	0.03	0.13	4.94	7.80
^{91}Nb	$7/2^+$	0	0.86	0.92	2.61	2.6
	$1/2^-$	104	0.22	0.43	1.19	1.66
	$5/2^-$	1,187	0.01	weak	0.86	0.55
	$3/2^-$	1,313	0.02	0.04	1.50	1.15
^{93}Tc	$3/2^-$	1,613	0.02	0.07	1.82	2.35
	$9/2^+$	0	0.66	0.73		
	$1/2^-$	390	0.32	0.22		
	$3/2^-$	1,193	0.07	weak		
	$5/2^-$	1,406	0.002	weak		

The experimental data are taken from [27, 29, 30]

appear to be at least 25 percent too large). Since these data have been used in the parameter fit they are only a weak test on the model. The description of the other states, which is now free of further parameters is a much more crucial test.

3.2. The Nucleus ^{89}Y

Figure 1 shows the experimental and calculated spectra. Also the positive parity states, obtained by a calculation without core-excitations, are given. Especially the energies of the two lowest $5/2^+$ and $7/2^+$ states, which can be described to a large extent as a $p_{1/2}$ quasiparticle coupled to the 3^- state in ^{88}Sr , are lowered by core-excitations. The energy of this 3^- state is calculated about 1.2 MeV too high, when neutron excitations are neglected; inclusion of these excitations makes the nucleus "softer" and gives a downward shift of the 3^- state by 1 MeV. The effect on the $5/2^+$ and $7/2^+$ states is clearly seen in the odd nucleus ^{89}Y . One notices that the calculated levels are almost in the right order; all experimentally observed levels are reproduced by the calculation. So there is little doubt about the nature of these states. A comparison with the shell model calculations [12] confirms the above statements about the $5/2^+$ and $7/2^+$ states. Within the limited (although large) shell model space these states are not predicted at the correct position, as also the 3^- states in the even nuclei cannot be described, when the $1f_{5/2}$ proton shell is omitted and, more importantly, when no neutron core-excitations are considered [13]. In their study [11] of ^{89}Y Vergados and Kuo included such excitations and consequently they find the $5/2^+$ and

$7/2^+$ states at lower energy. In [11] there seem to be too many low-lying states however. We think that this is due to the fact that much attention was paid to core excitations but relatively little to pairing correlations which increase the splitting between zero- and one-broken-pair states. Around 3.2 MeV states with a different nature seem to appear. Figure 2 shows some high spin states. The spin assignments given by [28] are tentative. It has been suggested that the state at 5.58 MeV is a $g_{9/2}$ quasiparticle coupled to the 7^- state in ^{88}Sr . The 7^- state in ^{88}Sr , however, is an almost pure configuration ($\pi g_{9/2}, \pi f_{5/2}$) in a one-broken-pair calculation. So, when a $g_{9/2}$ quasiparticle is coupled to this configuration, the Pauli principle forbids a $23/2^-$ assignment. Within our model space the first $23/2^-$ state occurs around 8 MeV, but we cannot exclude the probability of a lower state when more pairs are broken.

Table 3 shows transition rates, half-lives and mixing ratios. The $BE\lambda$ values and half-lives for most states are reproduced reasonably well. This indicates that the configuration mixing of these states is correct. The 2,873 keV state is presumably a $7/2^+$ state, for in that case the calculated $BE3$ value and the half-life are much closer to the experimental values than for the $5/2^+$ assignment, as one may notice from the table. As expected our results are much better than those obtained in shell-model calculations, e.g. [12].

3.3. The Nucleus ^{91}Nb

In ^{91}Nb some 20 states are known which have a one-broken-pair (or a more complicated) character. As one may notice from Fig. 3 the calculation can account for them reasonably well. The results are especially reasonable in view of the well known fact [23] that a careful optimization of the pair-distribution for the broken-pair states may bring them down by a few hundred keV. It cannot be excluded however that substantial admixtures of components with more than one-broken pair are important to improve these states. The calculation predicts that the second $13/2^-$ state lies only slightly above the $15/2^-$ state, so it might be observable by a weak gamma branch in the decay of the $17/2^-$ state. So up to about 3.2 MeV, like in ^{89}Y , essentially all levels can be explained as one-broken-pair states. This is also confirmed by the transition rates and half-lives, which are shown in Table 4.

The half-lives of the $9/2^+$ state at 1,637 keV and the $11/2^-$ state at 2,413 keV are quite sensitive to the effective gyromagnetic factor for the neutrons. For example, if $g_s(\text{neutron})=0$ then $T_{1/2}(11/2^-; 2,413) = 4.2$ ps.

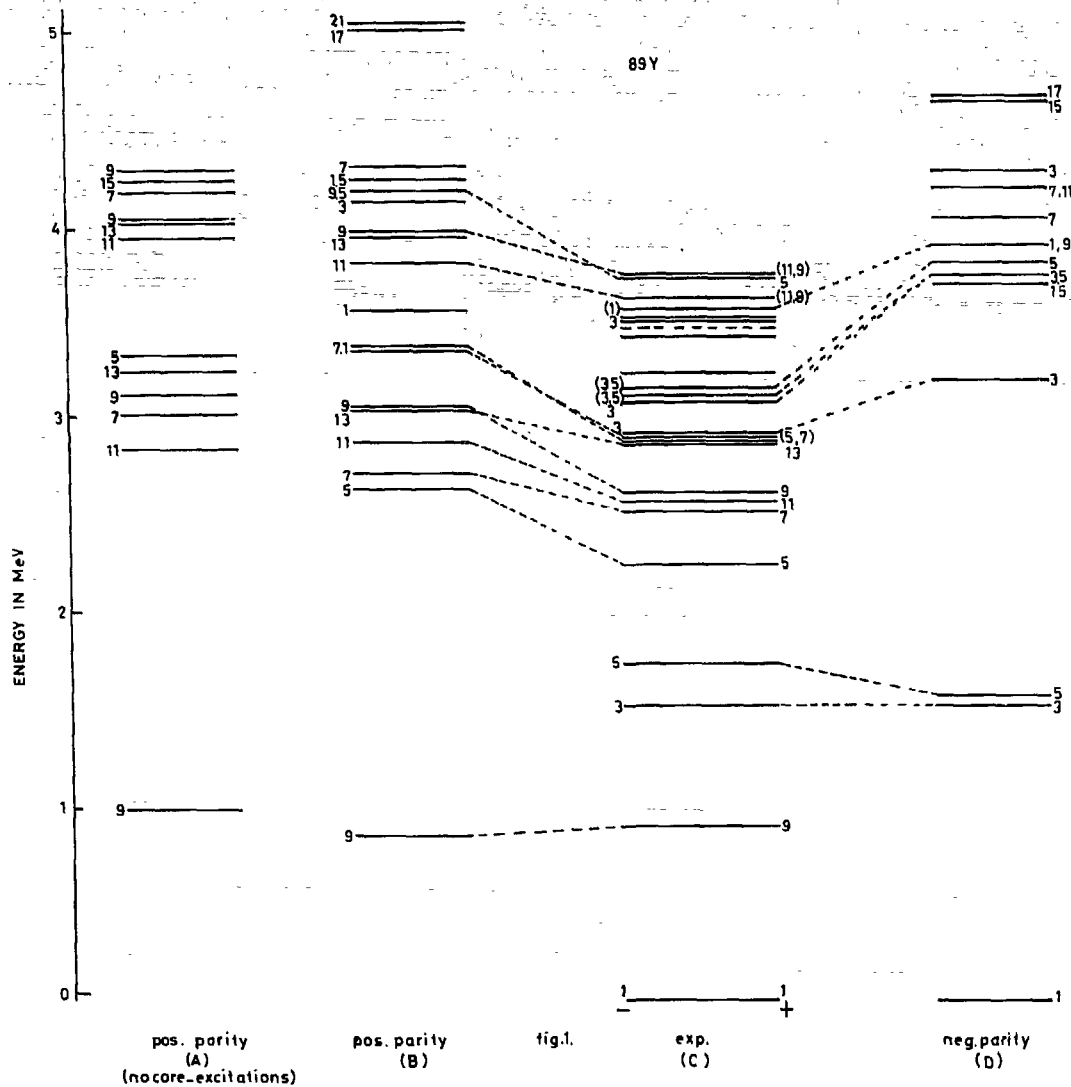


Fig. 1. Energy levels of ^{89}Y . The numbers near the levels indicate the angular momenta times two. Spectra (B) and (D) are the calculations for the positive and negative parity states respectively, with the parameters from Table I. In calculation (A) the neutron excitations were omitted. The experimental data are taken from [27]

The branching ratio for the $9/2^-$ state at 1.791 MeV is not reproduced in the calculation, probably because within our model space $E1$ transitions are not possible.

For a comparison with the most extensive shell-model calculations [12] we should mention that our

first $1/2^+$, second $3/2^+$, $5/2^+$ and third $9/2^+$ shown in Fig. 3 consist predominantly of configurations outside the $(2p_{3/2}, 2p_{1/2}, 1g_{9/2})$ proton space. The latter is found to be a kind of pairing vibration with respect to the ground state whereas the first $1/2^+$ and the second $3/2^+$ and $5/2^+$ states are mainly built of

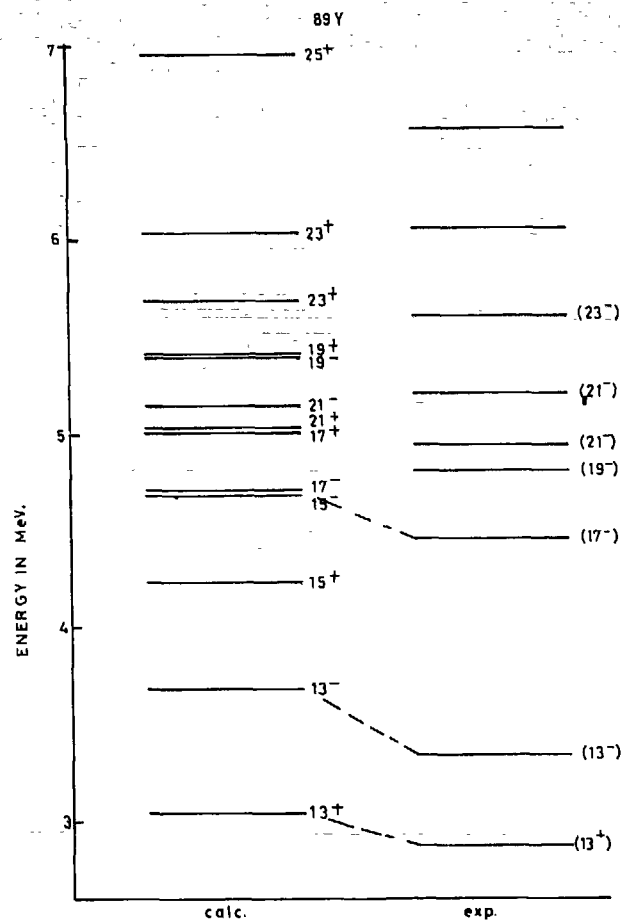


Fig. 2. High-spin energy levels of ^{89}Y . The numbers near the levels indicate the angular momenta times two. The experimental data are taken from [28]

Table 3. Transition rates, branching ratios and half-lives in ^{89}Y

Initial level		Final level		Calculated gamma transition probability in s^{-1} (Weisskopf units)		Branching ratio and half-life (ps)			
J^{π}	keV	J^{π}	keV	$E\lambda$	$M\lambda$	calc.	exp.	exp.	
9/2 ⁺	909	1/2 ⁻	0	3.1×10^{-6} (12)	6.8×10^{-2} (6.1)	10.2 s	16.06 s		
3/2 ⁻	1,507	1/2 ⁻	0	5.3×10^{11} (2.3)	1.9×10^{12} (0.18)	26 fs	24 ± 15 fs	$\delta = -0.15 \pm 0.05^*$	
5/2 ⁻	1,744	1/2 ⁻	0	1.0×10^{12} (2.2)		0.68	0.53 ± 0.04		
5/2 ⁺	2,222	1/2 ⁻	0	1.1×10^9 (16)	1.9×10^9 (0.08)	0			
		9/2 ⁺	909	5.2×10^{11} (4.6)		100	1.1	0.35 ± 0.14	$BE3 = 18 \pm 2$ W.U.
7/2 ⁺	2,530	1/2 ⁻	0	1.9×10^9 (10)		0			
		9/2 ⁺	909	1.5×10^{12} (4.5)	2.6×10^{12} (0.02)	100	169 fs	76 ± 35 fs	$BE3 = 19 \pm 2$ W.U.
11/2 ⁺	2,566	9/2 ⁺	909	3.2×10^{12} (8.9)	4.2×10^{11} (3.0×10^{-3})	0.19			
9/2 ⁺	2,622	9/2 ⁺	909	3.1×10^{12} (7.2)	8.7×10^{11} (5.5×10^{-3})	0.17	0.12		
(5/2 ⁺)	2,873	1/2 ⁻	0	1.7×10^9 (0.38)	8.8×10^9 (0.10)	0			
or		9/2 ⁺	909	4.9×10^{11} (0.58)		100	1.4	$100 \leq 0.2$	$BE3 = 36 \pm 3$ W.U.
(7/2 ⁺)	2,873	1/2 ⁻	0	2.5×10^9 (5.8)		0			
		9/2 ⁺	909	3.0×10^{12} (3.5)	5.6×10^{12} (0.02)	100	0.08	$100 \leq 0.2$	$BE2 = 27 \pm 3$ W.U.

* $\delta_{\text{calc}}(3/2^-, 1,507 \text{ keV}) = -0.16$. The experimental data are taken from [27]

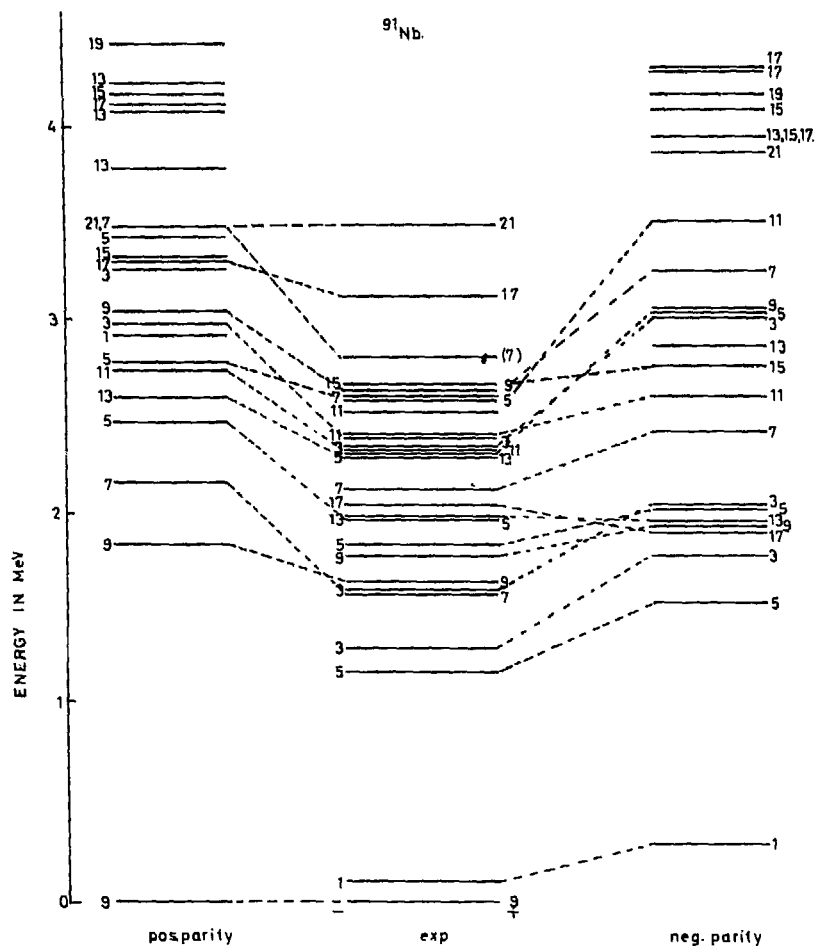


Fig. 3. Energy levels of ^{91}Nb . The numbers near the levels indicate the angular momenta times two. The experimental data are taken from [29]

neutron excitations from the $1g_{7/2}$ shell to the $3s-2d$ shell. We suggest therefore that the experimentally observed $5/2^+$ state at 2.58 MeV should be considered as a neutron excitation; our third $5/2^+$ state may be compared with the second state in [12]. In the shell model calculation [12] the high spin positive parity states $11/2^+ - 21/2^+$ have large admixtures of excitations of the ^{88}Sr core. In our wave functions these excitations are rather small, especially for the highest spins. Nevertheless we reproduce the $21/2^+ \rightarrow 17/2^+$ transition equally well as [12], so this transition does not yield conclusive evidence for the importance of the admixtures.

3.4. The Nucleus ^{93}Tc

The experimental information on ^{93}Tc is scarce; already around 2 MeV excitation energy many spin-assignments are missing. Therefore an attempt to identify the calculated levels with experimentally observed ones up to 3 MeV would be too speculative. As far as well-identified states are concerned the description seems satisfactory, with the $21/2^-$ state as a possible exception. The scarce decay data (Table 5) are of little help to clarify the picture. The mixing ratio for the $7/2^+$ state at 680 keV indicates that the M1 strength is too much hindered in the model,

Table 4. Transition rates, branching ratios and half-lives in ^{91}Nb

Initial level		Final level		Calculated gamma transition probability in s^{-1} (Weisskopf units)		Branching ratio and half-life (ps)		
J^{π}	keV	J^{π}	keV	$E\lambda$	$M\lambda$	calc.	exp.	exp.
1/2 ⁻	104	9/2 ⁺	0	3.1×10^{-6} (12)	1.1×10^{-9} (30)	41 d	62 d	
5/2 ⁻	1,187	1/2 ⁻	104	3.7×10^{11} (8.4)		1.4	$2.6^{+1.7}_{-0.8}$	
3/2 ⁻	1,313	1/2 ⁻	104	6.5×10^{11} (8.5)	5.8×10^{12} (0.10)	0.11	$0.17^{+0.05}_{-0.04}$	$-0.15 \leq \delta \leq 2.5^a$
7/2 ⁺	1,581	9/2 ⁺	0	1.9×10^{12} (6.5)	1.7×10^9 (1.3×10^{-5})	0.36	$0.33^{+0.09}_{-0.06}$	$\delta = -0.24$
3/2 ⁻	1,613	1/2 ⁻	104	1.0×10^{11} (0.44)	7.1×10^{12} (6.5×10^{-2})	96 fs	54 ± 17 fs	$\pm 0.10^a$
9/2 ⁺	1,637	9/2 ⁺	0	7.7×10^{10} (0.22)	1.8×10^9 (1.3×10^{-5})	8.8	$1.8^{+1.2}_{-0.5}$	$\delta = 0.53 \pm 0.16^a$
9/2 ⁻	1,791	9/2 ⁺	0	1.6×10^9 (0.09)*	4.9×10^7 (5.9×10^{-3})	0	93	
		5/2 ⁻	1,187	8.0×10^9 (3.3)		100	7	> 1.6
5/2 ⁻	1,845	1/2 ⁻	104	8.4×10^9 (0.01)		3	64	
		5/2 ⁻	1,187	2.4×10^8 (0.06)	3.1×10^{11} (0.03)	97	36	
5/2 ⁺	1,963	9/2 ⁺	0	3.3×10^{12} (3.8)		0.21	$0.20^{+0.07}_{-0.04}$	
13/2 ⁻	1,984	9/2 ⁺	0	7.4×10^8 (0.22)	8.7×10^{-7} (6.2×10^{-3})	80	51	
		9/2 ⁻	1,791	2.3×10^7 (2.9)		20	49	10.0 ± 0.4 ns
17/2 ⁻	2,035	13/2 ⁻	1,984	1.0×10^8 (1.0)		5.0 μ s	3.76 ± 0.12 μ s	$BE2 = 2.9$ W.U.
7/2 ⁻	2,120	9/2 ⁺	0	4.6×10^8 (0.85)*	3.6×10^6 (1.9×10^{-4})	1	10	
		5/2 ⁻	1,187	7.4×10^8 (0.35)	4.4×10^9 (1.7×10^{-4})	13	39	
		3/2 ⁻	1,313	2.2×10^{10} (2.2)		25	9	
		9/2 ⁻	1,791	4.7×10^9 (0.04)	5.5×10^{10} (4.8×10^{-2})	61	42	
13/2 ⁺	2,292	9/2 ⁺	0	7.9×10^{12} (4.2)		0.09	$0.12^{+0.04}_{-0.03}$	
11/2 ⁺	2,330	9/2 ⁺	0	7.6×10^{12} (3.7)	3.4×10^{10} (8.4×10^{-5})	0.09	0.11	$\delta = 10^{+27}_{-3}$
3/2 ⁺	2,345	1/2 ⁻	104	3.0×10^{11} (0.18)	1.6×10^{11} (4.5×10^{-4})	11	37	
		5/2 ⁻	1,187	5.5×10^{10} (0.90)	6.5×10^{11} (1.3×10^{-2})	17	18	
		3/2 ⁻	1,313	1.5×10^{11} (4.4)	1.7×10^{12} (4.9×10^{-2})	44	36	0.10 ± 0.02
		3/2 ⁻	1,613	8.3×10^9 (1.3)	1.2×10^{12} (9.6×10^{-2})	28	9	
17/2 ⁻	2,378	13/2 ⁻	1,984	2.9×10^8 (1.0)		2.4 ns	10 ns	
11/2 ⁻	2,413	9/2 ⁺	0	2.4×10^8 (1.8)*	1.8×10^{-7} (5.0×10^{-4})	0.2	67	
		9/2 ⁻	1,791	8.5×10^7 (0.03)	7.9×10^{-7} (1.0×10^{-5})	0.1	-	
		13/2 ⁻	1,984	2.4×10^8 (0.55)	1.3×10^{11} (0.05)	99.5	33	0.65 ± 0.33
		7/2 ⁻	2,120	2.1×10^8 (3.2)		0.2	-	
9/2 ⁻	2,632	9/2 ⁺	0	3.7×10^{12} (0.98)	7.5×10^{10} (1.3×10^{-4})	98	96	
		7/2 ⁺	1,581	3.2×10^{10} (0.85)	7.8×10^9 (2.1×10^{-4})	1	4	$0.12^{+0.03}_{-0.02}$
		9/2 ⁺	1,637	3.6×10^{10} (1.2)	1.4×10^9 (4.6×10^{-5})	1	0	
		5/2 ⁻	1,963	8.6×10^8 (0.21)		0	0	
21/2 ⁺	3,467	17/2 ⁻	3,110	4.5×10^8 (2.6)		1.5 ns	0.92 ± 0.10 ns	

The numbers marked with an asterisk are E3 transition probabilities. The experimental data are taken from [29].

^a $\delta_{\text{calc}}(3/2^-) = 0.33$, $\delta_{\text{calc}}(7/2^-) = 33$, $\delta_{\text{calc}}(9/2^-) = 6.5$, $\delta_{\text{calc}}(11/2^-) = 15$

possibly the inclusion of the proton $g_{7/2}$ level might improve this.

We are unable to check the statement in [12] that seniority four admixtures are large in the 5/2⁻, 9/2⁻ and 13/2⁻ states, because components with two broken pairs are omitted in the present treatment.

There is one more point we want to mention. In the odd Sn nuclei, especially for ^{117}Sn , one finds [22] in the same type of calculations that more levels (of low

spin) are observed than can be described. This could then be understood from the fact that also in even Sn nuclei collective bands have been observed [26] which do not fit into a spherical description. The spectra of the odd $N=50$ nuclei do not exhibit indications of the existence of more levels than described below 3 MeV. From this we expect, that in the even $N=50$ nuclei no collective bands, like those in Sn, will occur below 4 MeV excitation energy.

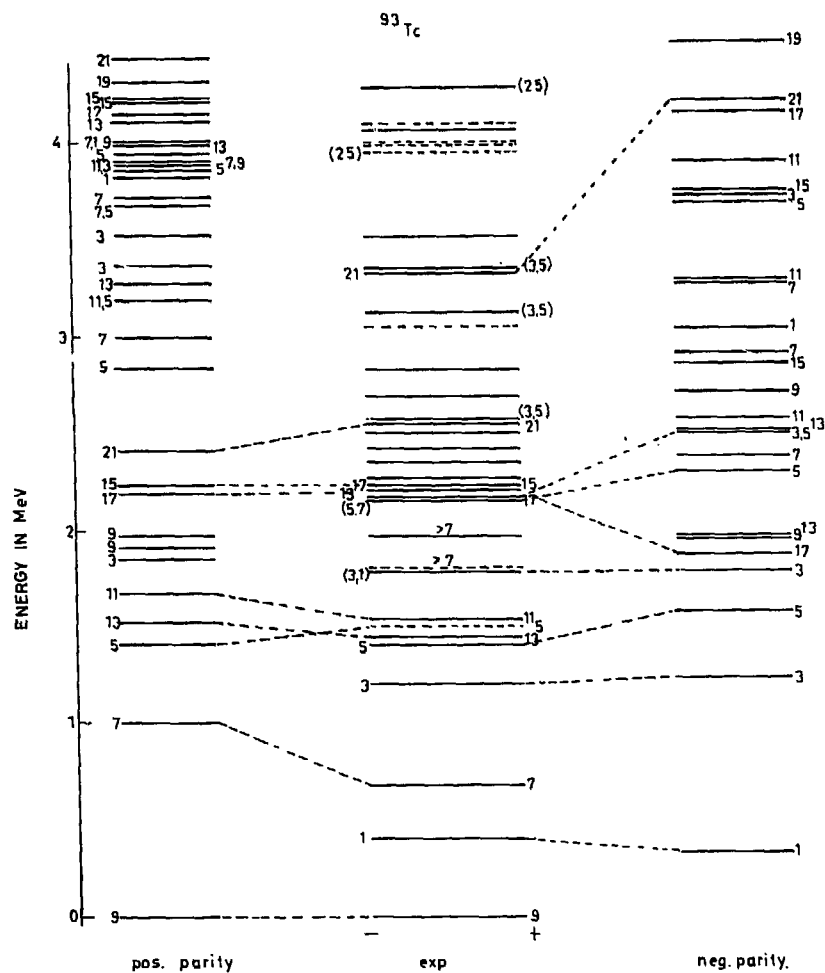


Fig. 4. Energy levels of ^{93}Tc . The numbers near the levels indicate the angular momenta times two. The experimental data are taken from [30]

4. Summary and Conclusion

We have checked whether the states, up to about 3 MeV excitation energy in odd $N=50$ isotones can be interpreted as states with at most one broken pair. For this purpose a simple Gaussian Serber force was applied which also has proved to be the most useful to describe spectra of even single-closed-shell nuclei. As the single-particle energies are derived from the lowest few states, which are assumed to have the unbroken-pair state as the main component, the description of the broken-pair states is free of further

adjustable parameters. From the nice reproduction of the energy spectra, typically the lowest twenty levels being calculated in the correct position, we conclude that such an interpretation is indeed very likely to be correct, although admixtures of more complicated configurations may not be negligible. These may also improve the calculated transition rates although the agreement with experimental data obtained here, which is mostly better than within a factor two, should be considered as quite good in microscopic model calculations.

We conclude that the results of the application of the

Table 5. Transition rates, branching ratios and half-lives in ^{93}Tc

Initial level		Final level		Calculated gamma transition probability in s^{-1} (Weisskopf units)		Branching ratio and half-life (ps)		
J^π	keV	J^π	keV	$E\lambda$	$M\lambda$	calc.	exp.	exp.
1/2 ⁻	390	9/2 ⁺	0	4.0×10^{-11} (0.14)	2.8×10^{-4} (49)	31 min	43.5 min	
7/2 ⁺	680	9/2 ⁺	0	6.5×10^{10} (15)	6.6×10^8 (6.7×10^{-5})	10.5		$\delta = 0.7 \pm 0.2^*$
3/2 ⁻	1,193	1/2 ⁻	390	1.8×10^{10} (1.7)	2.5×10^{12} (0.16)	0.26		
5/2 ⁻	1,406	1/2 ⁻	390	3.2×10^{11} (9.6)		2.2		
13/2 ⁺	1,434	9/2 ⁺	0	1.8×10^{12} (9.6)		0.43	≤ 5 ns	
11/2 ⁺	1,516	9/2 ⁺	0	1.5×10^{12} (6.0)	1.5×10^9 (1.3×10^{-5})	0.46		
13/2 ⁻	2,145	13/2 ⁺	1,434	9.9×10^3 (0.37)*	8.6×10^2 (5.2×10^{-3})	65	68	
		11/2 ⁺	1,516	4.1×10^{-1} (3.6×10^{-5})*	2.4×10^2 (5.3×10^{-3})	35	32	1.0 μs
17/2 ⁺	2,185	13/2 ⁺	1,434	1.3×10^9 (0.18)		0.52 ns	≤ 5 ns	
17/2 ⁻	2,185	13/2 ⁺	1,434	1.1×10^4 (0.28)	1.1×10^3 (1.0×10^{-3})	87	26	
		13/2 ⁻	2,145	5.3×10^2 (0.17)		13	74	$15.2 \pm 1.0 \mu\text{s}$
21/2 ⁺	2,534	17/2 ⁺	2,185	2.5×10^3 (0.16)		27 ns	≤ 5 ns	

The numbers marked with an asterisk are E3 transition probabilities. The experimental data are taken from [30]

* $\delta_{\text{calc}}(7/2^+) = 9.9$

one-broken-pair model to the odd $N=50$ isotones are considerably more convincing than earlier applications to odd Sn isotopes [21, 22]. One reason for this is that here also particle-hole excitations of the closed shell were included, which makes the nucleus sufficiently soft to lower collective excitations of the vibrational type. Another point is however that in Sn nuclei ($Z=50$) more complicated collective states have been observed in even nuclei [26] which possibly also play a role in the odd nuclei [22]. In the present investigation we do not find indications for a similar situation around the $N=50$ closed shell.

This investigation was part of the research program of the Stichting voor Fundamenteel Onderzoek der Materie (FOM), which is financially supported by the Nederlandse Organisatie voor Zuiver Wetenschappelijk Onderzoek (ZWO).

Appendix

For the formulae in the quasiparticle formalism we make use of the notation and the results of [15, 31].

A1. Matricelements of the Hamiltonian

In [15] the matricelements of the Hamiltonian \hat{H} between two number-projected 1 quasiparticle (1 q.p.) or 3 quasiparticle (3 q.p.) states and the overlaps of these states are given. In Eq. (21) of [15] a misprint has to be corrected. The term

$$-R_{13}^2 (ss' \text{tr } pJ')$$

has to be replaced by

$$-R_{13}^2 (ss' \text{tr } pJ') + R_{13}^2 p^{-2} (ss' \text{tr } pJ')$$

Using the projection method of [18] the residuum integrals $I^h(pq \dots t)$, in the expressions of [15] are replaced by the quantities $L^h(pq \dots t)$, defined in Eq. (4.3) of [18].

The relation of the broken-pair states (2.1) and (2.2) to the number-projected quasiparticle states of [15] is:

$$u_\alpha^+ |\psi_{2p}\rangle = u_\alpha |\psi_{2p+1}(\alpha)\rangle + \sum_{\substack{m_a, m_b \\ m_c, m_d}} (JM j_c m_c | j_a m_a j_b m_b | JM) a_\beta^+ a_\alpha^+ a_\gamma^+ |\psi_{p-2}\rangle \quad (\text{A.1})$$

$$= u_\alpha u_\beta u_\gamma |\psi_{2p+1}(abJc; j_a m_a)\rangle + \mathcal{H}(abJc; r) u_\alpha |\psi_{2p+1}(\rho)\rangle \quad (\text{A.2})$$

with

$$|\psi_{2p}\rangle = \prod_i u_i^{p_i} (p!)^{-1} (S^+)^p |\bar{0}\rangle, \quad (\text{A.3})$$

$$S^+ = \sum_a \frac{v_a}{u_a} \frac{d}{2} A_{00}^+(aa)$$

and

$$\mathcal{H}(abJc; r) = \delta_{J0} \delta_{ab} \delta_{cr} d u_a v_a - J p^{-1} u_c v_c \bar{P}(abJ) [\delta_{ac} \delta_{br}] \quad (\text{A.4})$$

where

$$\bar{P}(abJ) [\text{expression}] = [\text{expression}]$$

$$-(-)^{a+b+J} [\text{expression with interchanged } a \text{ and } b]$$

We define the particle-hole state related to the state (2.3) as:

$$\begin{aligned} & \sum_{\substack{m_n, m_p \\ m_c, m_r}} (JMj_c m_c | j_r m_r) (j_n m_n j_p m_p | JM) b_{p, m_p}^+ \\ & (-)^{j_n + m_n} b_{n, -m_n} u_c^+ | \psi_{2p} \rangle \\ & = u_c | \psi_{2p+1}(hpJc; j_r, m_r) \rangle \end{aligned} \quad (\text{A.5})$$

where b^+ and b are the neutron creation and annihilation operators. One finds the following expressions for the matrix elements of H :

$$\begin{aligned} & \langle \psi_{2p+1}(\rho) | \hat{H} | \psi_{2p+1}(hpJc; j_r, m_r) \rangle \\ & = -\hat{J} \hat{r}^{-1} [u_c u_r F(crhpJ) L^{2p}(rc) \\ & + (-)^{j_n + p + j} v_c v_r F(crphJ) L^{2p-2}(rc)] \end{aligned} \quad (\text{A.6})$$

$$\begin{aligned} & \langle \psi_{2p+1}(abJc; j_r, m_r) | \hat{H} | \psi_{2p+1}(hpJ'c'; j_r, m_r) \rangle \\ & = (-)^{j_n - p + j + c - c'} \bar{P}(abJ) [u_c v_b F(abphJ) \delta_{cc'} \delta_{JJ'} \\ & + \hat{J} \hat{J} \delta_{c'b} \left\{ \begin{matrix} ac'J' \\ rc'J \end{matrix} \right\} \bar{P}(ac'J) \\ & \cdot [u_c v_c F(abphJ')]] L^{2p-2}(abc) \\ & + H(abJc, r) \hat{J} \hat{r}^{-1} \\ & \cdot [u_c u_r F(c'rh p J') (L^{2p-2}(acc') - L^{2p}(acc')) \\ & + (-)^{j_n + p + j} v_c v_r F(c'rh p J') \\ & \cdot (L^{2p-4}(acc') - L^{2p-2}(acc'))] \end{aligned} \quad (\text{A.7})$$

$$\begin{aligned} & \langle \psi_{2p+1}(hpJc; j_r, m_r) | \hat{H} | \psi_{2p+1}(h'p'J'c'; j_r, m_r) \rangle \\ & = \delta_{cc'} \delta_{JJ'} \delta_{hh'} \delta_{pp'} [\langle \psi_{2p+1}(c) | \hat{H} | \psi_{2p+1}(c) \rangle \\ & + (\bar{v}_c - \bar{v}_c) L^{2p}(c) + \delta_{cc'} \delta_{JJ'} F(hp'h'p'J) L^{2p}(c) \\ & - \delta_{hh'} (-)^{j_n + r + j + h + p + j} \hat{J} \hat{J}' \sum_{j''} \hat{J}'' 2 \left\{ \begin{matrix} c'cJ'' \\ JJ'r \end{matrix} \right\} \\ & \cdot Z(cc'p'p) \left\{ \begin{matrix} J''pp' \\ h'J'J \end{matrix} \right\} - \delta_{pp'} (-)^{j_n + r + h + p} \hat{J} \hat{J}' \\ & \cdot \sum_{j''} \hat{J}'' 2 \left\{ \begin{matrix} c'cJ'' \\ JJ'r \end{matrix} \right\} (-)^{j_n + c + j''} Z(c'ch'h) \left\{ \begin{matrix} J''hh' \\ p'J'J \end{matrix} \right\} \end{aligned} \quad (\text{A.8})$$

where $\langle \psi_{2p+1}(c) | \hat{H} | \psi_{2p+1}(c) \rangle$ can be found in [15],

$$\bar{v}_j = v_j + \hat{J}^{-1} \sum_r \hat{g} v_r^2 F(jjgg_0) \quad (\text{A.9})$$

in which the summation runs over the quantum numbers (n, l, j) of the quasiparticle states, and

$$\begin{aligned} & Z(cc'nn') \\ & = (-)^{j_n - c + j''} F(cc'nn'J'') u_c u_{c'} L^{2p}(cc') \\ & - F(c'cnn'J'') v_c v_{c'} L^{2p-2}(cc') \end{aligned} \quad (\text{A.10})$$

A.2. Matricelements of Magnetic and Electric Operators

The definition of the one body (electric and magnetic) operator and the conventions used can be found in [31]; also the matricelements for this operator between two 1 q.p. and 3 q.p. states are given there. The matricelements involving particle-hole states are:

$$\begin{aligned} & \langle \psi_{2p+1}(hpJc; r) | O_\lambda | \psi_{2p+1}(r') \rangle \\ & = (-)^{j_n - r' + \lambda + x} \langle \psi_{2p+1}(r') | O_\lambda | \psi_{2p+1}(hpJc; r) \rangle \\ & = -(-)^{j_n - r' + \lambda + x} \delta_{r'c'} \delta_{\lambda J} \hat{r} \hat{r}'^{-1} \langle h | O_\lambda | p \rangle L^{2p}(r'), \end{aligned} \quad (\text{A.11})$$

where x indicates the behaviour of the operator under time reversal, $x=1$ for magnetic and $x=0$ for electric operators.

$$\begin{aligned} & \langle \psi_{2p+1}(hpJc; r) | O_\lambda | \psi_{2p+1}(h'p'J'c'; r') \rangle \\ & = (-)^{j_n + c + j} \delta_{JJ'} \delta_{hh'} \delta_{pp'} \hat{r} \hat{r}'^{-1} \langle c' | O_\lambda | c \rangle \\ & \cdot \left\{ \begin{matrix} rcJ \\ c'r'J' \end{matrix} \right\} [(-)^{j_n} u_c u_{c'} L^{2p}(cc') - c_c v_{c'} \\ & \cdot L^{2p-2}(cc')] \\ & + (-)^{j_n + j + c + r'} \delta_{cc'} \hat{r} \hat{r}'^{-1} \hat{J} \hat{J}' \left\{ \begin{matrix} rJc \\ J'r'J' \end{matrix} \right\} L^{2p}(c) \\ & + [(-)^{j_n - p - j} \langle p' | O_\lambda | p \rangle (-)^{j_n} \left\{ \begin{matrix} \lambda pp' \\ h'J'J \end{matrix} \right\} \delta_{hh'} \\ & - (-)^{j_n - p' - j'} \langle h' | O_\lambda | h \rangle \left\{ \begin{matrix} \lambda hh' \\ h'J'J \end{matrix} \right\} \delta_{pp'}] \end{aligned} \quad (\text{A.12})$$

$$\begin{aligned} & \langle \psi_{2p+1}(hpJc; r) | O_\lambda | \psi_{2p+1}(abJ'c'; r') \rangle \\ & = (-)^{j_n - r' + \lambda + x} \langle \psi_{2p+1}(abJ'c'; r') | O_\lambda | \psi_{2p+1}(hpJc; r) \rangle \\ & = \delta_{ab} \delta_{cc'} \delta_{c'r'} \delta_{\lambda J} \mathcal{H}(abJ'c'r') \hat{r} \hat{r}'^{-1} \\ & \cdot \langle h | O_\lambda | p \rangle (-)^{j_n} [L^{2p-2}(ac) - L^{2p}(ac)] \end{aligned} \quad (\text{A.13})$$

References

1. Talmi, I., Unna, I.: Nucl. Phys. **19**, 225 (1960)
2. Auerbach, N., Talmi, I.: Nucl. Phys. **64**, 458 (1965)
3. Vervier, J.: Nucl. Phys. **75**, 17 (1966)
4. Gloeckner, D.H., Macfarlane, M.H., Lawson, R.D., Serduke, F.J.D.: Phys. Lett. **40B**, 597 (1972)
5. Ball, J.B., McGroarty, J.B., Larsen, J.S.: Phys. Lett. **41B**, 581 (1972)
6. Gloeckner, D.H., Serduke, F.J.D.: Nucl. Phys. A **220**, 477 (1974)
7. Courtney, W.J., Fortune, H.T.: Phys. Lett. **41B**, 4 (1972)
8. Fujita, K., Komoda, T.: Progr. Theor. Phys. **57**, 692 (1977)
9. Dedes, C., Irvine, J.M.: J. Phys. G.: Nucl. Phys. **1**, 865 (1975)
10. Dedes, C.: J. Phys. G.: Nucl. Phys. **2**, L25 (1976)

11. Vergados, J.D., Kuo, T.T.S.: Nucl. Phys. A **168**, 225 (1971)
12. Fujita, K., Komoda, T.: Progr. Theor. Phys. **60**, 178 (1978)
13. Gillet, V., Giraud, B., Rho, M.: Phys. Lett. **27B**, 483 (1968); Phys. Rev. **178**, 1695 (1969)
14. Allaart, K., Boeker, E.: Nucl. Phys. A **194**, 33 (1972)
15. Ottaviani, P.L., Savoia, M.: Nuovo. Cim. **67A**, 630 (1970); Phys. Rev. **178**, 1594 (1969)
16. Gambhir, Y.K., Rimini, A., Weber, T.: Phys. Rev. **188**, 1573 (1969)
17. Talmi, I.: Nucl. Phys. A **172**, 1 (1971)
18. Allaart, K., van Gunsteren, W.F.: Nucl. Phys. A **234**, 53 (1974); van Gunsteren, W.F., Allaart, K.: Z. Physik A **276**, 1 (1976)
19. Allaart, K., Boeker, E.: Nucl. Phys. A **168**, 630 (1971); Haq, S., Gambhir, Y.K.: Phys. Rev. C **16**, 2455 (1977)
20. Arima, A., Iachello, F.: Ann. of Phys. **99**, 253 (1976); Otsuka, T., Arima, A., Iachello, F.: Nucl. Phys. A **309**, 1 (1978)
21. Bonsignori, G., Savoia, M.: Nuovo Cim. **3A**, 309 (1971); Ottaviani, P.L., Savoia, M.: Phys. Rev. **187**, 1306 (1969)
22. van Gunsteren, W.F., Allaart, K., Hofstra, P.: Z. Physik A **288**, 42 (1978)
23. Akkermans, J.N.L., Allaart, K., Boeker, E.: Nucl. Phys. A **282**, 291 (1977)
24. van Gunsteren, W.F., Hofstra, P., Mütber, H.: Z. Physik A **278**, 251 (1976)
25. Allaart, K., Boeker, E.: Nucl. Phys. A **198**, 33 (1972)
26. Bron, J., Hesselink, W.H.A., Peker, L.K., van Poelgeest, A., Uitzinger, J., Verheul, H., Zalmstra, J.: Proceedings of the International Conference on Nuclear Structure, Contributed papers, Tokyo, September 5-10, 1977, p. 348
27. Kocher, D.C.: Nucl. Data Sheets **16**, 445 (1975)
28. Davidson, M., Davidson, J., Behar, M., Garcia Bermudez, G., Mariscotti, M.A.J.: Proceedings of the International Conference on Nuclear Structure, Contributed Papers, Tokyo, September 5-10, 1977, p. 310
29. Verheul, H., Ewbank, W.B.: Nucl. Data Sheets **B8**, 477 (1972); Schäfer, W., Rauch, F.: Nucl. Phys. A **291**, 165 (1977); Brown, B.A., Fossin, D.B., Lesser, P.M.S., Poletti, A.R.: Phys. Rev. C **13**, 1194 (1976)
30. Kocher, D.C.: Nucl. Data Sheets **B8**, 527 (1972)
31. van Gunsteren, W.F.: Thesis Vrije Universiteit, Amsterdam, Ch. 7 (1976)

Chapter 5

THE CLUSTER-VIBRATION COUPLING MODEL

5.1 THE PARTICLE-VIBRATION MODEL

The particle-vibration model was originally suggested by Bohr and Mottelson¹⁾. One odd particle moving in the potential due to the other nucleons experiences a potential $V(r)$ when these other nucleons (the core) have a spherical distribution. A vibration of the core, described by the nuclear surface

$$R(\theta, \phi) = R_0 \left[1 + \sum_{\lambda\mu} \alpha_{\lambda\mu} Y_{\lambda\mu}(\theta, \phi) \right], \quad (5.1)$$

is assumed to change $V(r)$ into

$$V(r, \theta, \phi) = V \left[\frac{r}{1 + \sum_{\lambda\mu} \alpha_{\lambda\mu} Y_{\lambda\mu}(\theta, \phi)} \right], \quad (5.2)$$

which is approximated to first order in the deformation parameter $\alpha_{\lambda\mu}$

$$V(r, \theta, \phi) \approx V(r) - \sum_{\lambda\mu} \alpha_{\lambda\mu} Y_{\lambda\mu}(\theta, \phi) r \frac{d}{dr} V(r). \quad (5.3)$$

The Hamiltonian of the vibrating core is in lowest order that of a set of independent harmonic oscillators

$$H_{\text{VIB}} = \frac{1}{2} \sum_{\lambda\mu} (B_{\lambda} |\dot{\alpha}_{\lambda\mu}|^2 + C_{\lambda} |\alpha_{\lambda\mu}|^2) \quad (5.4)$$

where B_{λ} is a mass parameter and C_{λ} a stiffness parameter. After quantization this Hamiltonian acquires the form

$$H_{\text{VIB}} = \sum_{\lambda\mu} \hbar \omega_{\lambda} \left(\frac{1}{2} + b_{2\mu}^{\dagger} b_{2\mu} \right) \quad (5.5)$$

where

$$\omega_\lambda = \left(\frac{C_\lambda}{B_\lambda} \right)^{\frac{1}{2}} \quad (5.6)$$

and $b_{2\mu}^\dagger$ is the creation operator of a vibrational quantum (phonon). The second term of (5.3) now appears as the particle-vibration interaction or particle-phonon coupling:

$$H_{PVC} = -\sum_{\lambda\mu} (2\hbar\omega_\lambda C_\lambda)^{-\frac{1}{2}} \hbar\omega_\lambda r \frac{d}{dr} V(r) Y_{\lambda\mu}(\theta, \phi) (b_{\lambda\mu} + (-)^{\mu} b_{\lambda, -\mu}^\dagger) \quad (5.7)$$

One often introduces a parameter^{2,3)}

$$a_\lambda = \frac{1}{2} \left(\frac{\hbar\omega_\lambda}{2\pi C_\lambda} \right)^{\frac{1}{2}} r \frac{d}{dr} V(r), \quad (5.8)$$

thereby neglecting the dependence on the radial wave function of the particle. One may then write

$$H_{PVC} = -a_\lambda \sqrt{4\pi} \sum_{\lambda\mu} Y_{\lambda\mu}^*(\theta, \phi) (b_{2\mu}^\dagger + (-)^{\mu} b_{2, -\mu}) \quad (5.9)$$

which is the form which we shall also use in our numerical work, which is described in this thesis. The total Hamiltonian of the odd nucleus is now

$$H_{\text{odd}} = H_{\text{single-particle}} + H_{\text{VIB}} + H_{\text{PVC}} \quad (5.10)$$

where one may add in the Hamiltonian for the particle a spin-orbit term etc. to reproduce empirical single-particle energies.

The effect of H_{PVC} may be illustrated by the diagrams⁴⁾ in figure 5.1. Arrows pointing up (down) represent a particle (hole) with quantum numbers a or b; the wiggly line represents a phonon with angular momentum λ . The diagrams show the following physical features:

- a) a particle in orbit a is scattered to orbit b and a phonon is created.
- b) a hole in orbit a is scattered to orbit b and a phonon is created.
- c) a phonon is annihilated and a particle-hole pair is

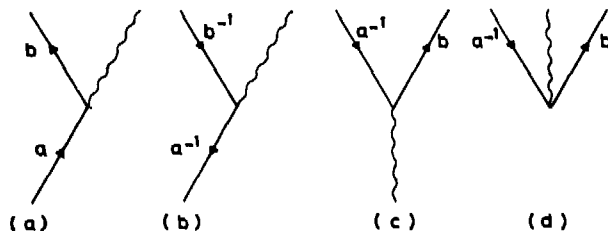


Figure 5.1 Diagrams illustrating first-order coupling between particle and vibration.

created.

d) a phonon is created and a particle-hole pair is created. In the particle (hole) vibration model only the diagrams a) and b) contribute.

5.2 THE CLUSTER-VIBRATION MODEL (CVM)

In the cluster-vibration model the nucleus is described as a system consisting of a few particles which show up in a pronounced, explicit way (the cluster) and the remaining nucleons (the core) which are accounted for by collective, vibrational degrees of freedom. In this model one usually considers quadrupole vibrations only^{2,2,5}). The Hamiltonian now reads

$$H = H_{\text{particles}} + H_{\text{VIB}} + H_{\text{CVC}} \quad (5.11)$$

where H_{CVC} is the sum of H_{PVC} (5.10) over all the cluster particles. For example one may adopt a cluster of three nucleons instead of only one in the particle-vibration model. In this manner an important part of the Pauli principle is accounted for and a broken-pair of nucleons or a promoted pair of particles appears explicitly. The importance of including cluster- and vibrational degrees of

freedom simultaneously has been demonstrated in refs^{5,11,22}). It is customary to write

$$H_{\text{particles}} = \sum_{i=1}^n H_{\text{s.p.}}(i) + \sum_{i<j}^n V(i,j) \quad (5.12)$$

where n is the number of particles in the cluster. $V(i,j)$ is the residual interaction between particle i and j . We note that the quadrupole residual interaction is already effectively included by phonon exchange as shown in figure 5.2. The most important components of the residual interaction are the quadrupole force and the pairing force. Therefore we take the pairing force with a force strength G as residual interaction in (5.12).

Then one may write

$$H_{\text{particles}} = \sum_{\alpha} \epsilon_{\alpha} a_{\alpha}^{\dagger} a_{\alpha} - \frac{1}{4} G \sum_{ab} \hat{a} \hat{b} A_{00}^{\dagger}(aa) A_{00}(bb) \quad (5.13)$$

with $\alpha \equiv (n_a, l_a, j_a, m_a)$, $a \equiv (n_a, l_a, j_a)$, $\hat{a} \equiv (2j_a + 1)^{\frac{1}{2}}$, a_{α}^{\dagger} creates a particle in a state with quantum numbers α and

$$A_{00}^{\dagger}(aa) = \sum_{m_a} (j_a m_a j_a -m_a | 00) a_{\alpha}^{\dagger} a_{\bar{\alpha}}^{\dagger}, \quad (5.14)$$

where $\bar{\alpha} \equiv (n_a, l_a, j_a, -m_a)$. The model defined by eq. (5.11) with the assumptions (5.5), (5.9) and (5.13) is the simplest version of the CVM.

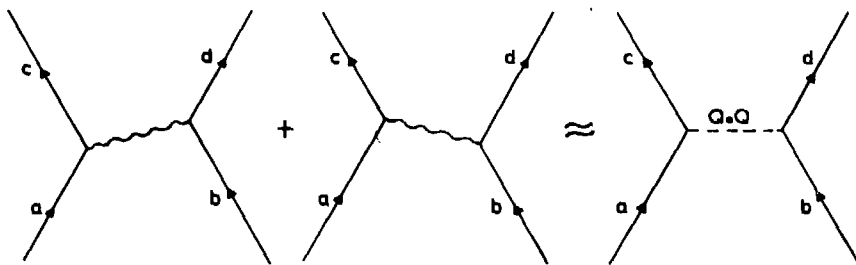


Figure 5.2 Phonon exchange causes an effective quadrupole residual interaction.

This simplest version of the CVM has some nice properties:

- 1) The leading effects of the pairing and the quadrupole-quadrupole force between nucleons are consistently taken into account.
- 2) The number of model parameters is relatively small, *viz.* the single-particle energies ϵ_a , the phonon energy $\hbar\omega_2$, the pairing force strength G and the particle-vibration coupling strength a .
- 3) The transparency of the model allows an analysis in terms of leading diagrams and thereby enables one to give simple qualitative interpretations of some pronounced features of the results.
- 4) The Pauli principle is explicitly treated in the cluster.

Point 4) leads us to mention the fact that the Pauli principle is violated to a certain extent. One can express the phonon in shell model degrees of freedom. Some of these degrees of freedom will also be described by the cluster degrees of freedom. However, since many shells are available to nucleons from the vibrational core and since we expect that the important contributions to these vibrational excitation within the valence-shell for valence-shell nucleons are of another type than those included in the cluster, it seems that the contributions to the wave function of an effective vibrator which involve excitations to the valence-shell of the cluster are not sizeable. Furthermore, the phonon might be of a very complex internal structure; for example, in TQM it is a combination of two-quasiparticle, four-quasiparticle,..... components. This might lead to an additional destructive interference.

More complex versions of the CVM may be constructed by including anharmonic vibrations and/or additional components of the particle interaction $V(i,j)$. Anharmonicities may be explicitly introduced in several ways, for example:

$$a) H_{VIB}^I = \hbar\omega_2 \sum_{\mu} \left(\frac{1}{2} + b_{2\mu}^{\dagger} b_{2\mu} \right) + A_{21} \left\{ (b_2^{\dagger} b_2^{\dagger} b_2)_0 + \text{h.c.} \right\} \quad (5.15)$$

where A_{21} is the strength of a cubic anharmonicity (h.c. is the hermitian conjugate of $(b_2^{\dagger} b_2^{\dagger} b_2)_0$);

b) the SU(6) Hamiltonian for quadrupole motion

$$H_{VIB}^n = h_1 \hat{N} + h_2 \left\{ (b_2^{\dagger} b_2^{\dagger})_0 \left\{ (N_{\max} - \hat{N}) (N_{\max} - \hat{N} - 1) \right\}^{\frac{1}{2}} + \text{h.c.} \right\} + \\ h_3 \left\{ (b_2^{\dagger} b_2^{\dagger} b_2)_0 (N_{\max} - \hat{N})^{\frac{1}{2}} + \text{h.c.} \right\} + \\ \sum_{L=0,2,4} h_{4L} \left\{ (b_2^{\dagger} b_2^{\dagger})_L (b_2 b_2)_L \right\}_0 \quad (5.16)$$

where

$$\hat{N} = \sum_{\mu} b_{2\mu}^{\dagger} b_{2\mu}$$

N_{\max} is the maximum number of phonons.

In the latter case the CVC term of the Hamiltonian is changed into

$$H_{PVC}^n = \sum_{\mu} \left\{ \kappa_1 (b_{2\mu}^{\dagger} + (-)^{\mu} b_{2,-\mu}) (N_{\max} - \hat{N})^{\frac{1}{2}} + \right. \\ \left. \kappa_2 \sum_{\nu_1 \nu_2} (2\nu_1 2\nu_2 | 2\mu) b_{2\nu_1}^{\dagger} (-)^{\nu_2} b_{2,-\nu_2} \right\} Y_{2\mu}^*(\theta, \phi) \quad (5.17)$$

The form (5.16) of the vibrational Hamiltonian may conveniently produce vibrational as well as rotational states as limiting cases, both for the axial⁶⁾ and the triaxial⁷⁾ rotor. In the rotor limit the coupling (5.17) produces states similar to those of the Nilsson model and rotational bands of odd nuclei appear⁸⁾. The model with the Hamiltonian (5.16) is also referred to as TQM; it is equivalent to the IBA model⁹⁾.

When introducing a more complex nuclear interaction between the particles one should beware of double counting. The particle-vibration coupling (5.9) already induces an effective quadrupole-quadrupole force between the particles

of the cluster, so it is not allowed to adopt an extra force of this type between the cluster particles with the same strength as one needs in models without vibrations.

Electromagnetic properties in CVM

The E2 and M1 operators contain single-particle and vibrational parts. For n particles in the cluster they read:

$$M_{sp}^{\mu}(E2) = \frac{3}{5} R_0^2 e^{sp} \sum_{i=1}^n Y_2^{\mu}(i) \quad (5.18)$$

$$M_{VIB}^{\mu}(E2) = \frac{3}{4\pi} e^{VIB} R_0^2 (b_2^{\mu+} + (-)^{\mu} b_2^{-\mu}) \quad (5.19)$$

$$\vec{M}_{sp}(M1) = \sqrt{3/4\pi} \left(g_l \vec{L} + g_s \vec{S} + g_p (Y_2 \otimes \vec{S})_1 \right) \quad (5.20)$$

$$\vec{M}_{VIB}(M1) = \sqrt{3/4\pi} g_R \vec{R} \quad (5.21)$$

Here \vec{L} , \vec{S} and \vec{R} are the orbital and spin angular momentum operators of the cluster and the angular momentum operator of the phonons, respectively. e^{sp} and e^{VIB} are the effective single-particle and vibrator charge, respectively; g_l , g_s , g_p and g_R are the gyromagnetic ratios.

Let us comment on the effective charges and gyromagnetic ratios. The single-particle charge incorporates both the bare charge and the polarization charge; in this way we simulate excitations of particles of the cluster to higher shells, which are neglected in the model. The rough estimate for this polarization charge is 0.5 for both protons and neutrons.

In the vibrational E2 operator the estimate for the vibrational charge is

$$e^{VIB} = \frac{4\pi}{3R_0^2} \{B(E2) (2_1^+ \rightarrow 0_1^+)_{VIB}\}^{\frac{1}{2}}$$

Throughout the periodic table (except deformed nuclei) it is mostly between 2 and 3.

For the gyromagnetic ratio g_R the hydrodynamic estimate is $g_R = \frac{Z}{A}$, which represents an upper limit. For the gyromagnetic ratio g_l free values are used, *i.e.* 1 for protons and 0 for neutrons. For g_s quenched values are used, as usually, in the region $0.6 - 0.8 g_s^{\text{free}}$, where $g_s^{\text{free}} = 5.59$ for protons, and -3.82 for neutrons. The tensor term, when included, has $g_p = 0.2 g_s^{\text{free}}$, in accordance with the usual estimate¹⁰⁾.

CVM calculations have been performed for a number of odd-even and even-even nuclei in the region $A=40-150$ and $A=190-220$. The overview of these calculations can be found in refs.^{11,12)}.

5.3 THE QUASIPARTICLE (CLUSTER)-VIBRATION MODEL (Q(C)VM)

5.3.1 Introduction

The particle-vibration model is especially suited for the description of a nucleus which has just one particle (or hole) beyond a magic number. Then this particle (or hole) plays a rôle which is quite distinct from the other particles; *i.e.* this particle moves in the space of valence shells while the other particles form a closed shell core. Similarly the cluster-vibration model applies to nuclei which have a small number of nucleons, two or three, beyond a closed shell core. The vast majority of nuclei however has more particles in the valence space. Especially if one wants to study nuclear systematics, *via.* the change of nuclear properties with varying number of nucleons, the treatment of nuclei with more than three particles in the valence shell is inevitable.

In chapter 2 we have already discussed a model which is hoped to be especially suitable for nuclei with many

valence nucleons. This BCS or quasiparticle model relies upon the pairing correlations of nucleons which give the nucleus the properties of a superfluid system. The essential point is that in such a superfluid system almost all particles occur in so-called Cooper pairs of time-reversed orbits and all pairs have the same pair wave functions. Therefore the description of the system may be mathematically reduced to the description of only those very few particles which do not occur in such well-arranged Cooper pairs. This is further elaborated in chapter 2, sections 3 and 4.

Extensive calculations with a quasiparticle-vibration model have been performed by Kisslinger and Sørensen¹³⁾. These authors assumed that only one particle of odd nuclei does not occur in a Cooper pair. All remaining nuclei, *i.e.* those that do occur in Cooper pairs in the valence shell as well as those which form the lower-lying closed shells, were accounted for by considering their quadrupole vibrational degrees of freedom. This model appeared to be fairly successful in several regions of the periodic table. These authors also concluded however that the assumption of only one quasiparticle is often too restrictive. Some nuclear states should obviously be interpreted as built of at least three unpaired particles.

Extensive studies of nuclear structure employing the three-quasiparticle cluster-vibration coupling model have not been reported so far. There may be several reasons for this, of which we mention three.

Firstly the number of configurations which one may build by angular momentum coupling of three nucleons in five or six valence shells to the lowest few states of a quadrupole vibrator is very large and therefore the calculations require much computational effort. This problem we shall

return to in section 4.1 of this chapter.

Secondly with three active nucleons appearing explicitly one may build states which may to some extent be considered as the microscopic analogue of one nucleon together with a quadrupole vibration. So there is some danger that certain physical states may appear in two ways. This problem is slightly diminished by using only a pairing force between the nucleons, but should perhaps be solved by partly removing certain basis states from the model space. Related with this is the problem how to choose the parameters of the vibrator as one cannot simply state that it is the nucleus with one or three particles less.

Thirdly an extension of the work of Kisslinger and Sørensen¹³⁾ to three-quasiparticle clusters is only meaningful if these are treated with sufficient care, *i.e.* by employing nuclear wave functions which properly conserve the particle number. Such number-conserving studies with three or more quasiparticles have been performed only a few times so far^{14,17)} and a coupling of such wave functions to vibrator states, which is the main subject of this thesis, has not been attempted before. The formalism of this is presented in the next section.

5.3.2 *Quasiparticle cluster-vibration coupling for odd nuclei (Formalism)*

In this section we present the formalism which we used in the calculations for odd nuclei which are reported in this and the following chapters. The assumption is that the nucleus has an odd number of nucleons, so an odd number of protons *or* an odd number of neutrons, and that this odd number of nucleons of one kind is more than three beyond a closed (magic) shell.

Then we proceed as follows:

- a) The odd number of nucleons of one kind is treated in the BCS formalism (chapter 2) and only number-projected one- or three-quasiparticle states are considered. These are of the form: (assuming a certain ordering $a=c + a=b=c$)

$$|\psi_{2p+1}(\rho)\rangle = N_p (u_r)^{-1} a_\rho^\dagger (S^\dagger)^P |\emptyset\rangle \quad (5.22)$$

and

$$\begin{aligned} |\psi_{2p+1}(abJ, c; j_r m_r)\rangle &= N_{p-1} (u_a u_b u_c)^{-1} \sum_{M m_a m_b m_c} (j_a m_a j_b m_b | JM) \\ &\times a_\beta^\dagger a_\alpha^\dagger (JM j_c m_c | j_r m_r) a_\gamma^\dagger (S^\dagger)^{P-1} |\emptyset\rangle - N_p (u_a u_b u_c)^{-1} \{ \delta_{J0} \delta_{ab} \delta_{cr} \\ &\times \hat{u}_a \hat{v}_a - \hat{J} \hat{r}^{-1} u_c v_c (\delta_{ac} \delta_{br} - (-)^{a+b+J} \delta_{ar} \delta_{bc}) \} a_\rho^\dagger (S^\dagger)^P |\emptyset\rangle, \end{aligned} \quad (5.23)$$

$$\text{where } N_p = \left(\prod_i u_i^{\Omega_i} \right) (p!)^{-1}$$

From these formulas it is obvious that this set is overcomplete:

$$\sum_a \hat{u}_a \hat{v}_a |\psi_{2p+1}(aaJ=0, c; j_c m_c)\rangle - (u_c^2 - v_c^2) |\psi_{2p+1}(\gamma)\rangle = 0 \quad (5.24)$$

Therefore we have used as basis sets in our computer codes the state (5.22) and a set of states (5.23) orthogonal to this one. This required a transformation to a new basis; in appendix 1 the transformation is given. After the transformation the number of states is the same as for the case of three particles. They read:

$$|(\tilde{j}_1 \tilde{j}_2) J \tilde{j}_3; j_r m_r\rangle \quad (5.25)$$

- b) The assumption is made that excitations of the other kind of nucleons as well as excitations of the same kind of nucleons which do not play an active rôle in formulas (5.22) and (5.23), that is the particles in closed major shells as well as the unbroken $p-1$ pairs,

may be simulated by a (harmonic) quadrupole vibrator. These oscillator states are denoted as

$$|NR\rangle \quad (5.26)$$

where N is the number of oscillator quanta (phonons) and R the total angular momentum of these phonons. As we never consider states with more than three phonons these two quantum numbers are sufficient to specify the states completely.

- c) The model space of nuclear wave functions for a certain spin and parity J^π is now built of all possible products of states (5.25) and states (5.26) coupled to $\vec{j}_R + \vec{R} = \vec{J}$ and $\pi = \text{parity of the cluster states (5.25)}$, since (5.26) has $\pi = +$. So we have states

$$|(\vec{j}_1 \vec{j}_2) J_{12} \vec{j}_3; j_R\rangle \otimes |NR\rangle |J^\pi \quad (5.27)$$

- d) The Hamiltonian is assumed to be of the form:

$$H = H_{\text{valence particles}} + H_{\text{VIB}} + \sum_{\substack{i=\text{valence} \\ \text{particles}}} H_{\text{PVC}}(i) \quad (5.28)$$

where $H_{\text{valence particles}}$ is of the form (5.13), H_{VIB} the harmonic vibrator (5.5) for $\lambda=2$ and $H_{\text{PVC}}(i)$ is the expression (5.9) for the i^{th} particle and $\lambda=2$, so

$$H = \sum_{\alpha} \epsilon_{\alpha} a_{\alpha}^{\dagger} a_{\alpha} - \frac{1}{2} G \sum_{ab} \hat{a} \hat{b} A_{00}^{\dagger} (aa) A_{00} (bb) + \sum_{\mu} \hbar \omega_2 (\frac{1}{2} + b_{2\mu}^{\dagger} b_{2\mu}) - a_2 \sqrt{4\pi} \sum_{\mu} (b_{2\mu}^{\dagger} + (-)^{\mu} b_{2,-\mu}) \sum_{\alpha\beta} \langle \alpha | Y_{2\mu}^*(\theta, \phi) | \beta \rangle a_{\alpha}^{\dagger} a_{\beta}. \quad (5.29)$$

The matrix elements of this Hamiltonian in the space of states (5.22) and (5.23) may be written as follows:

$$\begin{aligned} & \langle \psi_{2p+1}(\rho) | \otimes \langle NR | H | N'R' \rangle \otimes | \psi_{2p+1}(\rho') \rangle = \\ & = \delta_{NN'} \delta_{RR'} \langle \psi_{2p+1}(\rho) | H_{\text{valence particles}} | \psi_{2p+1}(\rho') \rangle \langle NR | NR \rangle \end{aligned}$$

$$\begin{aligned}
& + \delta_{\rho\rho'} \delta_{NN'} \delta_{RR'} \hbar\omega_2 (\frac{1}{2}+N) \langle \psi_{2p+1}(\rho) | \psi_{2p+1}(\rho) \rangle \langle NR | NR \rangle \\
& - a_2 \sqrt{4\pi} \sum_{\mu} \langle NR | b_{2\mu}^{\dagger} + (-)^{\mu} b_{2,-\mu} | N'R' \rangle \\
& \times \langle \psi_{2p+1}(\rho) | \sum_i Y_{2\mu}^*(\theta_i, \phi_i) | \psi_{2p+1}(\rho') \rangle \quad (5.30)
\end{aligned}$$

and similar expressions with $|\psi_{2p+1}(\rho)\rangle$ and/or $|\psi_{2p+1}(\rho')\rangle$ replaced by projected three-quasiparticle states. The last term of (5.30) may be rewritten by introducing reduced matrix elements²⁵⁾ as

$$-a_2 \sqrt{4\pi} \left\{ \begin{matrix} R & R & J \\ R' & R' & 2 \end{matrix} \right\} \langle NR || b_2^{\dagger} + b_2 || N'R' \rangle \langle \psi_{2p+1}(r) || Y_2^* || \psi_{2p+1}(r') \rangle \quad (5.31)$$

The explicit form of the matrix elements occurring in (5.30) and (5.31) will be given in appendix 2.

5.4.1 TRUNCATION OF THE MODEL SPACE; COMPUTATIONAL PROCEDURE

In the CVM with a space built of four or five valence shells for the cluster and up to three quanta of the vibrator one has typically a thousand or more states for each value of spin and parity. This means that one has to construct and diagonalize a matrix of the Hamiltonian (5.11) of dimension one thousand or more for each J^{π} value and each nucleus. Moreover if one does not know the model parameters (the single-particle energies ϵ_a , the phonon energy $\hbar\omega_2$, the strength parameters G and a_2) from the beginning, one will perform the computations with several parameter sets.

Another reason why one would like to choose a smaller model space is that in a complete calculation several hundreds of the thousand basis vectors will appear with uninterestingly small components in the lowest few eigenvectors which may be compared with experimental data.

The problem one faces is now that much computational labour could be saved if one knew from the beginning which basis vectors contribute very little to the lowest states and therefore may be discarded. We shall consider here two criteria:

- I: The basis vectors with smallest expectation value of H are the most important ones.
- II: One should include the basis vectors which are connected to the (few) most important vectors according to the criterion I by large off-diagonal matrix elements of H .

We shall now illustrate how these criteria work for an example.

A number of 7 particles are supposed to be in the $2d_{5/2}$, $1g_{7/2}$, $2d_{3/2}$, $3s_{1/2}$ shells with single-particle energies 0.42, 0.00, 1.60 and 1.85 MeV respectively. The other model parameters are $\hbar\omega_2=1.0$ MeV, $a=0.6$, $G=0.2$. At most three phonons were considered. Then one has for the $7/2^+$ state 973 basis vectors and for the $5/2^+$ state 894 basis vectors. For each J^π value these vectors are now first ordered in a sequence with increasing diagonal energy (criterion I). Then according to this criterion we choose the first (lowest) 150 vectors and diagonalize H within this subspace. The number 150 is the same as usual^{20, 5)} in calculations with the CVM.

Figure 5.3 shows the results of this procedure when one adopts 147 vectors for the $7/2^+$ and 152 vectors for the $5/2^+$ states as well as the results when 140 vectors are adopted for both $7/2^+$ and $5/2^+$. One may notice that the lowest $5/2^+$ state is strongly depressed (by about 500 keV) when a few more basis vectors are adopted. From a closer inspection we learned that this is due to the basis vector $|(g_{7/2}, d_{5/2})6d_{3/2}; 9/2; 12\rangle$ which is connected by a large off-diagonal matrix element to lower vectors. This illu-

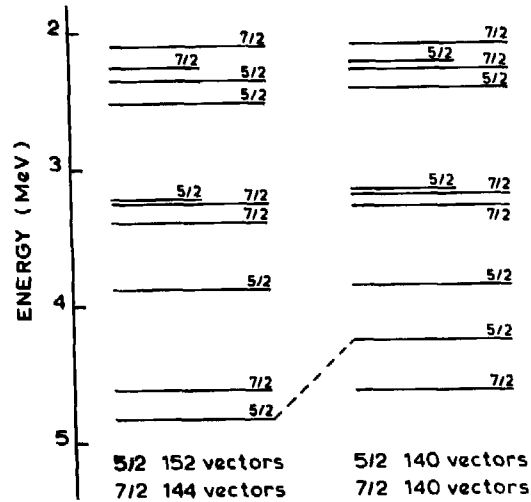


Figure 5.3 Energies of the $5/2^+$ and $7/2^+$ states calculated with selection criterion I.

states that the use of criterion I only is not a very safe procedure and therefore also the second criterion should play a role. Before we discuss our adopted procedure in more detail we comment on the applicability of criterion I only in CVM calculations which have been performed until recently^{2,3,5,20,22}). For there is a reason why this truncation method may work better in the CVM

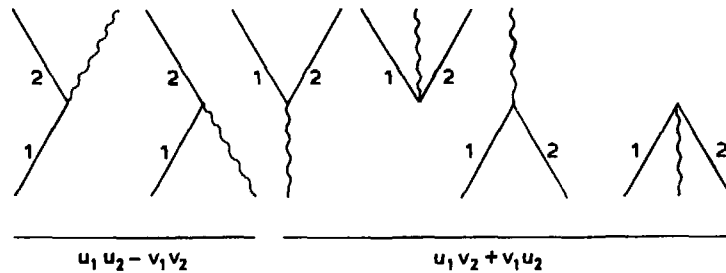


Figure 5.4 Diagrams illustrating first-order coupling between quasiparticle and vibration. The strength of the vertices are dependent on the pairing factors, which are presented below the diagrams.

than in the QCVM. This may be seen from the diagrams, presented in figure 5.4, which represent the matrix elements of H_{CVC} . The pairing factors, with which the matrix elements are multiplied due to the superfluidity correlations, are $u_1 u_2 - v_1 v_2$ for the first two diagrams and $u_1 v_2 + v_1 u_2$ for the other four diagrams. In the CVM one has $u_1 = u_2 = 1$ (particle cluster) or $u_1 = u_2 = 0$ (hole cluster) then only the first two diagrams contribute. In the QCVM the other diagrams become increasingly more important as one approaches the middle of a shell; $u_1 = u_2 = v_1 = v_2 = \frac{1}{2}\sqrt{2}$. One may notice that among these diagrams there are two which increase (or decrease) the number of phonons (by one) and the number of quasiparticles (by two), so they connect basis vectors of which the diagonal energies differ by as much as $\hbar\omega_2 + E_1 + E_2 > \hbar\omega_2 + 2\Delta$. (Δ is gap parameter, $\Delta \approx 1$ to 1.5 MeV). Therefore the mixing of basis vectors with quite different diagonal energies becomes much more important in the QCVM than in the CVM.

The procedure which we have adopted in our computations is as follows (for each J^π value):

- i) First all basis vectors with certain spin J are ordered according to the criterion I, so the one with the lowest expectation value of H is given the first position etc. Then we adopt a certain boundary energy E_B^J such that all basis vectors $|i\rangle$ with $\langle i | H_{VIB} + H_{particles} | i \rangle$ larger than E_B^J are rejected. This energy E_B^J is chosen in such a way that the number of remaining vectors is large (about one thousand) but small enough to be handled in the subsequent procedure. This large number of selected vectors spans the "total" space $\{N_t^J(E_B^J)\}$.
- ii) From the "total" space $\{N_t^J(E_B^J)\}$ a small number N_1^J with lowest diagonal energies is taken (say 30 vectors).

iii) In this small basis $\{N_1^J\}$ the (total) Hamiltonian H_{QCVM} is diagonalized. This results in N_1 eigenvectors $|J_N\rangle = \sum_{i=\{N_1\}} a_i^N |i\rangle$, $N=1,2,\dots,N_1$, with energies E_N^J .

Assuming that for a comparison with experimental data only the five lowest states of each J^π value are interesting, we choose the five lowest states which have resulted from this diagonalization and now wish to improve these by including more basis vectors $|k\rangle$ which do not belong to the space $\{N_1^J\}$ but do belong to the preselected "total" space $\{N_t^J(E_B^J)\}$. In order to have a selection criterion which of these vectors $|k\rangle$ should preferentially be included we now calculate for each vector $|k\rangle$ the quantity

$$S_k = \sum_{N=1}^5 \frac{\sum_{i=\{N_1\}} (a_i^N)^2 |\langle i | H_{QCVM} | k \rangle|^2}{E_k - E_N^J} \quad (5.32)$$

which is a measure for the contribution of the vector $|k\rangle$ to the energies of the lowest five states suggested by first order perturbation theory.

Next the N_2^J vectors with the largest sum (5.32) are added to the basis $\{N_1^J\}$, so one obtains the new basis $\{N_1^J + N_2^J\}$. In practice we chose $N_2^J \approx 40$.

iv) The procedure iii) is repeated but now starting with the basis space $\{N_1^J + N_2^J\}$ instead of $\{N_1^J\}$. Again a new set of basis states $\{N_3^J\}$ which do not belong to $\{N_1^J + N_2^J\}$ but do belong to $\{N_t^J(E_B^J)\}$ is selected by the criterion (5.32) and added. So our final selected basis space is $\{N_1^J + N_2^J + N_3^J\}$. In practice we take $N_1^J + N_2^J + N_3^J \leq 150$ for all spins. An argument to accept this total number spin-dependent is that also the total number of basis vectors of the complete space depends on J^π . So we take $N_1^J + N_2^J + N_3^J$ a constant fraction of this

dimension of the complete spaces. In this way we hope to have treated different spins on equal footing and thereby to have obtained a result which is the best to be compared with experimental data. The reason why the criterion (5.32) is used twice to select another set of vectors is that H connects vectors which differ by one phonon. So in two steps one may connect states which differ by two phonons and in large model calculations we mostly find that vectors with three phonons contribute very little.

This procedure was checked by comparing its results with those of a diagonalization in the complete model space using the Lanczos diagonalization method²³⁾.

An example is given in table 5.1. It concerns the $\frac{1}{2}^+$ state of a system of 7 valence shell particles in the orbits $1g_{7/2}$, $2d_{5/2}$, $2d_{3/2}$ and $3s_{1/2}$ with single-particle energies 0, 0.42, 1.60, 1.85 MeV respectively. The other parameters are $\hbar\omega_2=0.6$ MeV, $a=0.8$ MeV, $G=0.2$ MeV. The dimensions in the different steps were $N_t^{\frac{1}{2}}=180$, $N_1^{\frac{1}{2}}=20$, $N_2^{\frac{1}{2}}=20$, $N_3^{\frac{1}{2}}=15$. The table lists the sum of the percentage

Table 5.1 "Overlaps" ($\sum_{N=1}^5 (a_i^N)^2$) in percentages of the basic vectors and for the wave functions of the $J=\frac{1}{2}^+$ states. For parametrization see the text.

	1	2	3	4	5	6	7	8	9	10	11	12	13	14	15	16	17	18	19	20	
1	61	45	5	4	45	42	30	5	2	0	8	1	1	4	9	0	0	1	4	2	20
21	<u>5</u>	2	<u>3</u>	4	<u>15</u>	<u>7</u>	<u>11</u>	3				<u>5</u>									40
41		<u>3</u>													4	1			1	<u>1</u>	60
61	<u>3</u>	1	1	<u>4</u>	<u>5</u>	2	<u>3</u>	3	<u>1</u>	2	2	<u>3</u>		<u>3</u>	1	<u>4</u>	<u>5</u>	5	5	<u>1</u>	80
81				<u>4</u>						1	1									<u>5</u>	100
101						3							<u>2</u>		1			<u>1</u>	3	1	120
121											<u>7</u>	<u>3</u>		1							140
141	2	2	<u>2</u>	<u>2</u>			<u>3</u>		<u>1</u>												160
161					<u>2</u>						1	1	1	2							180

Each position of the 20×9 matrix corresponds to one of the 180 basis vectors. For every basis vector $|i\rangle$ the "overlap" is given. Only "overlaps" >1 per cent are presented. The 20 vectors of the preliminary basis are presented in the first row. In the rest once underlined "overlaps" correspond to the step (iii) and those which are twice underlined correspond to (iv). The total number of selected basis vectors is 55.

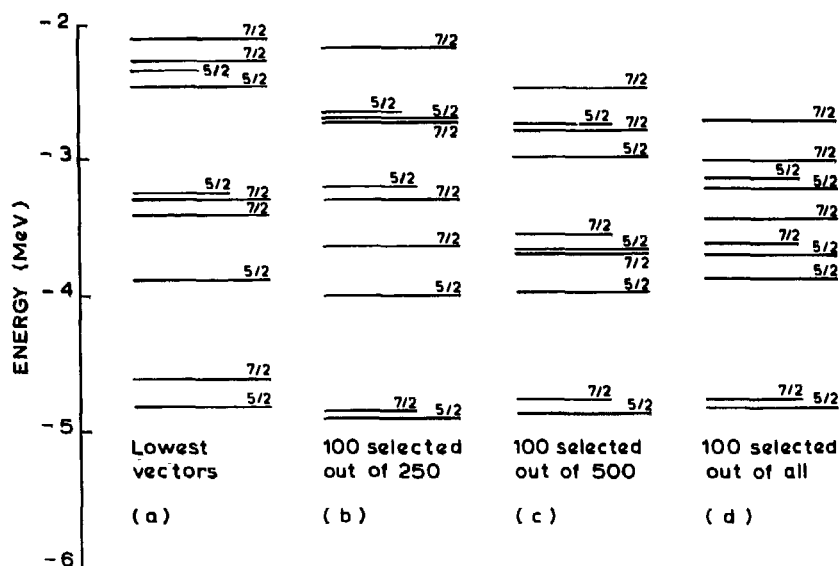


Figure 5.5 Energies of the $5/2^+$ and $7/2^+$ states. The spectrum (a) is calculated with selection criterion I. The other spectra are calculated using 100 vectors selected by criterion II; the number of vectors used in the selection is given below.

of the 180 basis vectors in the lowest five states after the complete diagonalization (the numbers should add up to five, but numbers smaller than 0.01 have been omitted). The first 20 vectors belong to the set $\{N_1^{\frac{1}{2}}\}$, the underlined ones belong to the set $\{N_2^{\frac{1}{2}}\}$ and those of the set $\{N_3^{\frac{1}{2}}\}$ have been underlined twice. One may notice from the table that our procedure has indeed selected practically all the important vectors. This selection was obviously much better than a straightforward selection of the first 55 vectors based upon the diagonal energies only. An important point is that no relatively large component, which could cause a large energy shift, has been missed.

Another illustration is shown in figure 5.5. Displayed are the results for the $7/2^+$ and $5/2^+$ states calculated with 147 and 152 vectors respectively, which were selected with

the diagonal energy as the only criterion. These are the same as in figure 5.3. Next the results of our selection procedure are shown for several cases, *viz.* the vectors $N_1^J=15$, $N_2^J=15$, $N_3^J=70$ were chosen out of $N_t^J=250, 500$ and all possible 973 vectors. As expected the higher states are the most sensitive to the number N_t^J . One may notice the 100 vectors selected by our stepwise procedure yield lower energies than 150 vectors selected by the diagonal energies only. We mention here that the same calculations as presented here for particle number 7 were also performed for particle number 3 (the CVM). Then our procedure also yields an improvement over straightforward energy-truncation. The effect is smaller then, because, as we discussed in the beginning of this section, the coupling between vectors which differ much in energy is not so strong.

Finally we present a comparison of our procedure with a complete diagonalization for a case with very strong mixing of basis states. For this purpose $\hbar\omega_2$ was lowered to 0.6 MeV and all other parameters were kept the same as before. The maximum number of phonons was now two, however. In figure 5.6 the results of a stepwise selection procedure ($N_1+N_2+N_3 \leq 150$) and those of a complete diagonalization ($N \leq 436$) are displayed as well as those of a truncation based on diagonal energies only ($N \leq 150$). One may notice that although in this case of very strong mixing of basis vectors our procedure is not quite satisfactory, especially for the $3/2^+$ states, it does yield a large improvement over the old energy-truncation procedure.

From these illustrations one may conclude that our truncation procedure is a useful improvement over straightforward truncation by considering the diagonal elements of H only. It is certainly to be recommended when many calculations with different model parameter sets have to be performed. In cases of strong configuration mixing a straightforward diagonalization by the Lanczos method

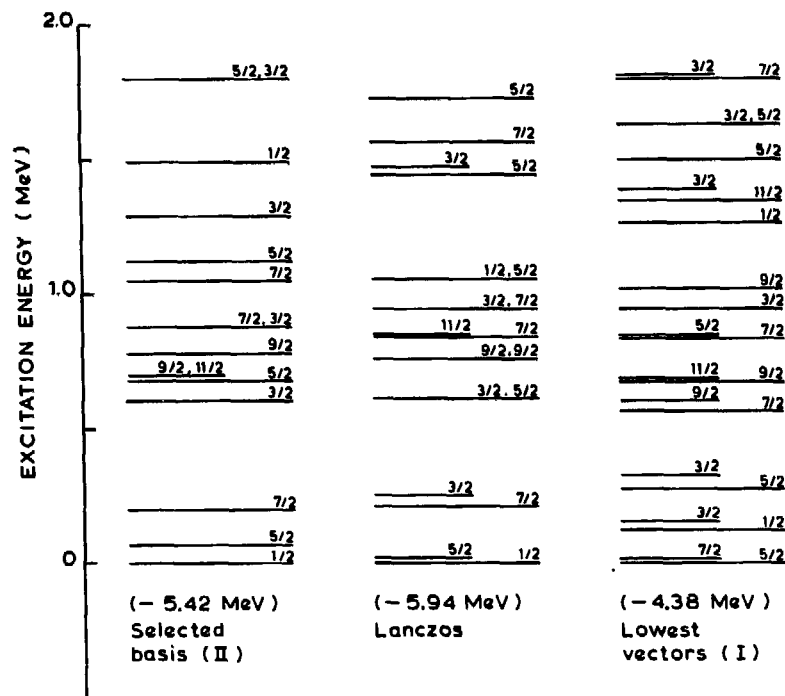


Figure 5.6 Spectra calculated with selection criterion II, the Lanczos method (diagonalization with all basis vectors), with selection criterion I. The numbers below the spectra are the energies of the ground states. In the Lanczos method the number of vectors used are: 180(1/2⁺), 328(3/2⁺), 413(5/2⁺), 436(7/2⁺), 395(9/2⁺), 323(11/2⁺). For the other calculation these numbers are 58, 105, 133, 144, 135 and 117 respectively.

(which is for a thousand basis vectors at least ten times more time consuming than our procedure selecting 150 vectors) may be required to obtain more precise final spectra.

5.4.2 Some properties and illustrations of the QCVM

In order to demonstrate the main QCVM features, we compare here the results of models with a different composition of the cluster, viz.:

- 1QP : one-quasiparticle cluster, no particle-number projection
- 1QP+NP: one-quasiparticle cluster, with particle-number projection
- 3QP : one- or three-quasiparticle cluster, no particle-number projection
- 3QP+NP: one- or three-quasiparticle cluster, with particle-number projection (QCVM)

The model 1QP coincides with the familiar quasiparticle-vibration model for odd-A nuclei¹³⁾. Models 1QP+NP and 3QP are developed as transitional models between 1QP and 3QP+NP in order to illustrate the physical correlations of QCVM. We are now able to investigate:

- a) the effect of particle-number projection (NP) on the spectra,
- b) the effect of including a three-quasiparticle cluster in addition to a one-quasiparticle cluster,
- c) the dependence of the excitation energies on the (odd) number of particles.

Before presenting results we comment on these points.

- a) The effect of NP has been investigated earlier in (number-projected) two-quasiparticle²¹⁾, three-quasiparticle¹⁴⁾ and four-quasiparticle¹⁵⁾ calculations. In these calculations the effect of NP on the energies calculated for the Hamiltonian of the valence-particles is important. If one couples a quasiparticle cluster to phonons then also the coupling matrix elements of H_{pvc} become important; in general the effect on the coupling dominates. Therefore, when discussing NP, we shall now only mention the effect on the coupling.
- b) The type of states one allows for by admitting three-quasiparticle clusters in addition to a one-quasi-

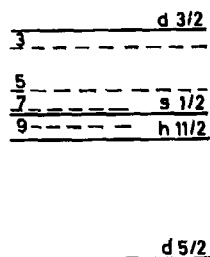


Figure 5.7 The single-particle levels, used to calculate figs. 5.9-5.11. The broken lines correspond to the position of the Fermi levels for 3, 5, 7 and 9 holes.

particle cluster is in principle the same as in the case of particles. This subject has been discussed in ref.²²⁾.

- c) The QCVN enables us to calculate the spectra (and other spectroscopic properties) of a series of odd nuclei with the same parameters. So systematic changes of nuclear properties with particle-number should be accounted for by this model, where in principle the same parameters should be suitable for a whole sequence of nuclei.

We shall now present results of calculations with the parameters of ref.²⁰⁾ for ^{133}Xe :

$$\begin{aligned} \epsilon(d_{3/2}) &= 0.0 \text{ MeV} & \epsilon(s_{1/2}) &= -0.6 \text{ MeV} & \epsilon(h_{11/2}) &= -0.8 \text{ MeV} \\ \epsilon(d_{5/2}) &= -1.7 \text{ MeV} & G &= 0.1 \text{ MeV} & \hbar\omega &= 1.0 \text{ MeV} \\ a &= 0.4 \text{ (in ref. }^{20}) & a &= 0.3 \end{aligned}$$

In figures 5.9-5.11 the excitation energies of the negative parity states are given for $n=3, 5$ and 7 holes in the single-particle space. Figure 5.7 shows the single-particle space with the energy of the Fermi level for these situations.

First we comment on the most important configurations and coupling matrix elements in these calculations, in

Table 5.2 Some important coupling matrix elements

	n=3		n=5		n=7		n=9	
	3QP	3QP+NP	3QP	3QP+NP	3QP	3QP+NP	3QP	3QP+NP
$ (3^2) 2 \overset{1}{1}; 7/2\rangle$ $2u_3v_3$	1.66	2.50	0.96	0.81	1.00	0.92	0.95	0.88
	0.93	(0.87)	0.55	(0)	0.56	(0)	0.53	(0)
$ (1\overset{1}{1}^2) 2 \overset{1}{1}; 7/2\rangle$ $2u_{11}v_{11}$	-0.81	-0.39	-1.73	-0.75	-2.61	-2.43	-3.07	-3.21
	0.25	(0)	0.53	(0)	0.80	(0.55)	0.94	(0.87)
$ \overset{1}{1}\rangle$ $ u_{11}^2 - v_{11}^2 $	3.71	3.80	3.25	3.73	2.30	2.72	1.31	1.58
	0.97	(1.0)	0.84	(1.0)	0.60	(0.83)	0.34	(0.5)

Coupling matrix elements in the models 3QP and 3QP+NP are given between the configurations $|\overset{1}{1}\rangle$ and the configurations listed in the first column. Also the corresponding pairing factors are presented. Between brackets the pairing factors for a normal distribution (without pairing correlations) are given. The symbol n denotes the number of holes in the 50-82 shell.

order to clarify the effect on NP. The most important configurations are

$$\left. \begin{array}{l}
 |\overset{1}{1}; I=1^1/2\rangle \\
 |\overset{1}{1}, 12; I\rangle \\
 |(3^2) 2 \overset{1}{1}; I\rangle \\
 |(3\overset{1}{1}) 2 \overset{1}{1}; I\rangle \\
 |(\overset{1}{1}\overset{1}{1}^2) 2 \overset{1}{1}; I\rangle \\
 |\overset{1}{1}, 22; I\rangle
 \end{array} \right\} I = 7/2 \dots \dots \dots 1^5/2 \quad (5.33)$$

We have adopted the notation $\overset{1}{1} \equiv 1^1/2$ etc.

The most important coupling matrix elements are the matrix elements which connect the states (5.33). In table 5.2 a few of these matrix elements are shown for $u=3,5,7$ and 9, both with and without NP, together with the pairing factors $2uv$ or u^2-v^2 . The numbers in parenthesis in the columns "NP" are the values of the "pairing factors" calculated with a distribution without pairing, *i.e.* the particles are placed in the orbits with lowest energy. The main effect of NP is that the pair-distribution becomes less diffuse; as should be expected because states with wrong particle number are removed. This changes effectively the factors $2uv$ and u^2-v^2 .

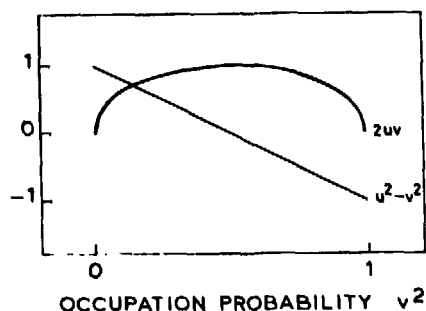


Figure 5.8 $2uv$ and $u^2 - v^2$ as functions of v^2 . The function $2uv$ has steep slopes at $v^2=0$ and $v^2=1$.

In figure 5.8 the factors $2uv$ and $u^2 - v^2$ are given as functions of the occupation probability v^2 . The steepest slopes in this figure occur in the curve for $2uv$ near $v^2=0$ and $v^2=1$. These values of v^2 correspond to the factors for the coupling matrix elements, which connect states containing a one-quasiparticle cluster with states containing a three-quasiparticle cluster; the two additional quasiparticles should be both almost particles ($v^2 \approx 0$) or both almost holes ($v^2 \approx 1$). The NP changes effectively the occupation probability v^2 ; the effect of this change on the coupling matrix element will be strongest in the above mentioned cases.

In table 5.2 the factors for a distribution without pairing correlations are indicated in brackets. In general one sees from table 5.2 that if the pairing factors in brackets are larger (smaller) also the corresponding matrix element become larger (smaller). There are two exceptions *viz.*:

$$\langle 1\uparrow || Y_2 || (\frac{3}{2})^2 1\uparrow; 7/2 \rangle \quad \text{for } n=3 \text{ and}$$

$$\langle 1\uparrow || Y_2 || (1\uparrow)^2 1\uparrow; 7/2 \rangle \quad \text{for } n=9.$$

For $n=3$ the $3/2^+$ level is near the Fermi level and for $n=5$ the $11/2^-$ level is near the Fermi level. In such a case it is difficult to predict what effect NP will have on the matrix elements. The matrix elements $\langle 1\bar{1} || Y_2 || (3^2) 2 \bar{1}\bar{1}; I \rangle$ are important for $n=3$, $\langle 1\bar{1} || Y_2 || (1\bar{1}^2) 2 \bar{1}\bar{1}; I \rangle$ for $n=7$ and 9 and $\langle 1\bar{1} || Y_2 || 1\bar{1} \rangle$ for $n=3, 5$ and 7 , because they are large in these cases and connect the dominant configurations of the lowest states.

Let us now turn to the calculated spectra, which are shown in figure 5.9. For $n=3$ the models 1QP and 1QP+NP show a quintuplet $7/2^- \dots \dots 15/2^-$ with configuration $|1\bar{1}; 12\rangle$ at about 1 MeV. The NP has hardly an effect on the spectra. The important configurations for the quintuplet are $|1\bar{1}, 12\rangle$ and $|1\bar{1}, 2R\rangle$ ($R=0, 2, 4$); quasiparticle states are coupled by the matrix element $\langle 1\bar{1} || Y_2 || 1\bar{1} \rangle$, and this does not change much by NP.

The spectrum calculated by 3QP shows an additional quintuplet based on the cluster configuration $|(3^2) 2 \bar{1}\bar{1}; I\rangle$. As we have seen before the coupling of this configuration to the configuration $|1\bar{1}; 12\rangle$ increases considerably by NP. This is reflected in the large downward shift of the $7/2^-$, $15/2^-$, $13/2^-$ and $9/2^-$ states, if NP is performed.

The spectrum of 3QP+NP resembles the spectrum shown in figure 2 of ref.²⁰⁾, which was calculated with the CVM, but with $a=0.3$. The model 3QP+NP (QCVM) for $n=3$ is equivalent with the CVM. In figure 5.10 the negative-parity spectra are shown for $n=5$. The Fermi level is now closer to the $5_{1/2}$ level. Therefore the $|(1\bar{1}^2) 2 \bar{1}\bar{1}; I = 7/2^- \dots \dots 15/2^- \rangle$ configurations become more dominant instead of the configurations $|(3^2) 2 \bar{1}\bar{1}; I = 7/2^- \dots \dots 15/2^- \rangle$. The coupling matrix elements (which are not shown in table 5.2) are not influenced

much by the NP.

In figure 5.11 the negative parity spectra are shown for $n=7$. As the Fermi level is now closer to the $h_{11/2}$ level the configurations $|(1\bar{1}^2)2\ 1\bar{1}; I = 7/2^- \dots 15/2^- \rangle$ become important. The coupling of these configurations to $|1\bar{1}, 12; I = 7/2^- \dots 15/2^- \rangle$ is also much stronger than for $n=5$. Kisslinger²⁴⁾ pointed out the importance of the inclusion of configurations $|(j^3)I = j-1 \rangle$ for the lowering of the lowest state with spin $I = j-1$. This state is indeed the lowest of the quintuplet now. For stronger coupling this state even may become the ground state.

Summarizing we conclude that NP is important for the coupling matrix elements and therefore for the excitation energies. With the QCVN one is able to calculate the properties of a series of nuclei in the same parametrization. In the next chapter we shall apply the model to the odd Zn isotopes.

Appendix 1

The transformation of the overcomplete three-quasiparticle basis to an orthogonal and normalized basis is done as follows.

The overcomplete unnormalized basis reads:

$$\left. \begin{aligned} |\psi_{2p+1}(\rho)\rangle &= \psi_0 \\ |\psi_{2p+1}(j_1 j_1^0, r; \rho)\rangle &= \psi_1 \\ |\psi_{2p+1}(j_2 j_2^0, r; \rho)\rangle &= \psi_2 \\ \vdots & \\ |\psi_{2p+1}(j_n j_n^0, r; \rho)\rangle &= \psi_n \end{aligned} \right\} \quad (\text{A1.1})$$

From the space, spanned by $\psi_1 \dots \psi_n$ one vector is removed; then a basis $\phi_2 \dots \phi_n$ is formed by Schmid-orthogonalization, where $\phi_2 \dots \phi_n$ are orthogonal to ψ_0 and to each other.

The new normalized basis reads:

$$\left. \begin{aligned} |(\overset{y}{j}_1 \overset{y}{j}_1) 0 \overset{y}{j}_r\rangle &(\equiv |\overset{y}{j}_r\rangle) = \psi_0 \\ |(\overset{y}{j}_2 \overset{y}{j}_2) 0 \overset{y}{j}_r\rangle \\ \vdots \\ |(\overset{y}{j}_n \overset{y}{j}_n) 0 \overset{y}{j}_r\rangle \end{aligned} \right\} \quad (\text{A1.2})$$

The transformation matrix A_{ik} , which is printed in the computercode TQD, gives the relation between the overcomplete normalized basis and the new normalized basis:

$$|(\overset{y}{j}_i \overset{y}{j}_i) 0 \overset{y}{j}_r\rangle = \sum_{k=0}^n A_{ik} \frac{\psi_k}{\langle \psi_k | \psi_k \rangle^{1/2}} \quad (i=1 \dots n) \quad (\text{A1.3})$$

Another orthogonalization problem may also occur.

If $j_{r-} > 9/2$ and $j_{s-} > 9/2$ then $|(\overset{y}{j}_s \overset{y}{j}_s) 2 \overset{y}{j}_s; j_r\rangle$ is not orthogonal to the basis (A1.2). In this case the vector

$|\psi_{2p+1}(j_s j_s 2 j_s; \rho)\rangle$ is added to the basis (A1.1) before the removal of the spurious state and the orthonormalization.

Appendix 2

THE MATRIX ELEMENTS OF H_{QCVM}

The matrix elements of H_{QCVM} between two states reads:

$$\begin{aligned}
 & \langle \psi_{2p+1}(1) | \langle NR | H | N'R' \rangle | \psi_{2p+1}(2) \rangle = \\
 & = \delta_{NN'} \delta_{RR'} \langle \psi_{2p+1}(1) | H_{\text{valence particles}} | \psi_{2p+1}(2) \rangle \langle NR | NR \rangle \\
 & + \delta_{NN'} \delta_{RR'} h\omega_2 \left(\frac{1}{2} + N\right) \langle \psi_{2p+1}(1) | \psi_{2p+1}(2) \rangle \langle NR | NR \rangle \\
 & - a_2 \sqrt{4\pi} \left\{ \begin{matrix} r & R & J \\ R & r & 2 \end{matrix} \right\} \langle NR | |b_2^\dagger + b_2| | N'R' \rangle \langle \psi_{2p+1}(1) | |Y_2^*| | \psi_{2p+1}(2) \rangle
 \end{aligned} \tag{A2.1}$$

where $|\psi_{2p+1}(i)\rangle (i=1,2)$ are one-quasiparticle or three-quasiparticle wave functions with angular momenta r and r' . First we evaluate the matrix elements with the phonon wave functions $|NR\rangle$.

$$\langle NR | N'R' \rangle = \delta_{NN'} \delta_{RR'} \quad \text{for } N \leq 3 \tag{A2.2}$$

$$\langle NR | |b_2^\dagger + b_2| | N'R' \rangle = \langle NR | |b_2^\dagger| | N'R' \rangle \delta_{N, N'+1}$$

$$(-)^{R-R'} \langle N'R' | |b_2^\dagger| | NR \rangle \delta_{N', N+1} \tag{A2.3}$$

where

$$\langle NR | |b_2^\dagger| | N'R' \rangle = (-)^{R+R'} \{N(2R+1)\}^{\frac{1}{2}} \langle NR | |N-1R' \rangle \tag{A2.4}$$

The boson fractional parentage coefficients $\langle NR | |N-1R' \rangle$ are given in table A2.1 (from ref.¹⁸).

Next the matrix elements

$\langle \psi_{2p+1}(1) | H_{\text{valence particles}} | \psi_{2p+1}(2) \rangle$ are given; they are taken from ref.¹⁴.

Table A2.1

N=3	R	N'=2		
		R'	0	2
	0	0	1	0
	2	$\sqrt{7/15}$	$\sqrt{4/21}$	$\sqrt{12/35}$
	3	0	$\sqrt{5/7}$	$-\sqrt{2/7}$
	4	0	$\sqrt{11/21}$	$\sqrt{10/21}$
	6	0	0	1

$$\langle \psi_{2p+1}(\rho) | H_{\text{valence particles}} | \psi_{2p+1}(\rho) \rangle = R_0^{2p}(r) + R_{11}^{2p}(rr), \quad (\text{A2.5})$$

$$\begin{aligned} \langle \psi_{2p+1}(\rho) | H_{\text{valence particles}} | \psi_{2p+1}(pqJ't; \rho) \rangle = \\ = \hat{p}_p \hat{v}_p \delta_{J'0} \delta_{tr} \{ R_0^{2p}(pr) - R_0^{2p-2}(pr) + R_{11}^{2p}(rrp) - R_{11}^{2p-2}(rrp) \} - \\ - \frac{\hat{J}'}{F} \hat{u}_t \hat{v}_t \{ R_0^{2p}(tr) - R_0^{2p-2}(tr) + R_{11}^{2p}(rrt) - R_{11}^{2p-2}(rrt) \} * \\ \bar{P}(pqJ') \delta_{pt} \delta_{qr} + \delta_{J'0} \delta_{tr} R_{20}^{2p}(ppt) - \\ \frac{\hat{J}'}{\hat{p}\hat{q}} R_{20}^{2p}(ttr) \bar{P}(pqJ') \delta_{pt} \delta_{qr} + R_{13}^{2p}(pqtrJ'), \quad (\text{A2.6}) \end{aligned}$$

$$\begin{aligned} \langle \psi_{2p+1}(abJc; \rho) | H_{\text{valence particles}} | \psi_{2p+1}(pqJ't; \rho) \rangle = \\ = \{ -(\delta_{J'0} \delta_{tr} (R_{20}^{2p-2}(papr) - R_{20}^{2p}(papr)) - \\ - (R_{20}^{2p-2}(tatr) - R_{20}^{2p}(tatr)) \frac{\hat{J}'}{\hat{p}\hat{q}} \bar{P}(pqJ') \delta_{pt} \delta_{qr} - \\ R_{13}^{2p}(pqtraJ') + R_{13}^{2p-2}(pqtraJ') \} \hat{a}_a \hat{v}_a \delta_{J0} \delta_{cr} + \\ + \left[a \leftrightarrow c \right] \frac{\hat{J}}{F} \hat{u}_c \hat{v}_c \bar{P}(abJ) \delta_{ac} \delta_{br} \} + \\ + \{ p \leftrightarrow a, q \leftrightarrow b, c \leftrightarrow t, J \leftrightarrow J' \} + \end{aligned}$$

$$\begin{aligned}
& + \hat{p}_p v_p \hat{a}_a v_a \delta_{J0} \delta_{J'0} \delta_{tr} \delta_{cr} \left(R_0^{2p-4}(\text{apr}) - 2R_0^{2p-2}(\text{apr}) + \right. \\
& + R_0^{2p}(\text{apr}) + R_{11}^{2p-4}(\text{rrap}) - 2R_{11}^{2p-2}(\text{rrap}) + \\
& \left. + R_{11}^{2p}(\text{rrap}) \right) - \hat{p}_p v_p \delta_{J'0} \delta_{tr} \frac{\hat{J}}{F} u_c v_c \bar{P}(\text{abJ}) \delta_{ac} \delta_{br}^* \\
& (a \leftrightarrow c) - \hat{a}_a v_a \delta_{J0} \delta_{cr} \frac{\hat{J}'}{F} u_t v_t \bar{P}(\text{pqJ}') \delta_{pt} \delta_{qr}^* \\
& (p \leftrightarrow t) + \frac{\hat{J} \hat{J}'}{F^2} \bar{P}(\text{pqJ}') \delta_{pt} \delta_{qr} \bar{P}(\text{abJ}) \delta_{ac} \delta_{br} u_c v_c u_t v_t^* \\
& (p \leftrightarrow q; s \leftrightarrow t) + R_{JrJ'}(\text{abc; pqt}) \left(R_0^{2p-2}(\text{abc}) + \right. \\
& \left. + R_{11}^{2p-2}(\text{aabc}) + R_{11}^{2p-2}(\text{babc}) + R_{11}^{2p-2}(\text{cabc}) \right) + \\
& + \delta_{ct} \delta_{JJ'} R_{22}^{2p}(\text{abpqJt}) - \bar{P}(\text{pqJ}') \{ \delta_{cq} (-)^{J+J'+q+t} \hat{J} \hat{J}' \} \\
& \times \left\{ \begin{matrix} q & p & J' \\ t & r & J \end{matrix} \right\} R_{22}^{2p}(\text{abptJc}) - \bar{P}(\text{abJ}) \{ a \leftrightarrow p, b \leftrightarrow q; c \leftrightarrow t; \\
& J' \leftrightarrow J \} + \sum_{J''} \bar{P}(\text{abJ}) \bar{P}(\text{pqJ}') \left(\delta_{ap} \hat{J} \hat{J}' \hat{J}''^2 (-)^{a+b+r+c} \right. \\
& \left. \left\{ \begin{matrix} a & b & J \\ c & r & J'' \end{matrix} \right\} (-)^{p+q+r+t} \left\{ \begin{matrix} p & q & J' \\ t & r & J'' \end{matrix} \right\} R_{22}^{2p}(\text{bcqtJ''a}) \right) \quad (\text{A2.6a})
\end{aligned}$$

The overlaps between the basis states are:

$$\langle \psi_{2p+1}(\rho) | \psi_{2p+1}(\rho) \rangle = L^{2p}(r) \quad (\text{A2.7})$$

$$\begin{aligned}
& \langle \psi_{2p+1}(\rho) | \psi_{2p+1}(\text{abJc}; \rho) \rangle = \\
& - \left\{ \hat{a}_a v_a \delta_{J0} \left[L^{2p-2}(\text{ac}) - L^{2p}(\text{ac}) \right] - \frac{\hat{J}}{F} u_c v_c \right. \\
& \left. \times \bar{P}(\text{abJ}) \delta_{ac} \delta_{br} \left[L^{2p-2}(\text{ab}) - L^{2p}(\text{ab}) \right] \right\} \quad (\text{A2.8})
\end{aligned}$$

$$\langle \psi_{2p+1}(\text{abJc}; \rho) | \psi_{2p+1}(\text{pqJ}'t; \rho) \rangle =$$

$$\begin{aligned}
& L^{2p-2}(abc)R_{JrJ'}(abc,pqt) + \hat{a}u_a v_a \hat{p}u_p v_p \\
& \times \delta_{J0} \delta_{J'0} \left[L^{2p-4}(apc) - 2L^{2p-2}(apc) \right] \\
& - \left\{ \hat{a}u_a v_a \frac{\hat{J}'}{F} u_t v_t \delta_{J0} \bar{F}(pqJ') \delta_{pt} \delta_{qr} \right. \\
& \times \left[L^{2p-4}(apq) - 2L^{2p-2}(abq) + L^{2p}(abq) \right] \left. - \right. \\
& - \{a \leftrightarrow p, b \leftrightarrow q, c \leftrightarrow t, J \leftrightarrow J'\} \\
& \left. + \frac{\hat{J}\hat{J}'}{F^2} u_c v_c u_t v_t \bar{F}(abJ) \delta_{ac} \delta_{br} \bar{F}(pqJ') \delta_{pt} \delta_{qr} \left[L^{2p-4}(ctr) - \right. \right. \\
& \left. \left. - 2L^{2p-2}(ctr) + L^{2p}(ctr) \right] \right\} \quad (A2.9)
\end{aligned}$$

The quantities R are defined as:

$$\begin{aligned}
R_{J'rJ}(abc; a'b'c') &= \bar{F}(abJ') \left(\delta_{aa'} \delta_{bb'} \delta_{cc'} \delta_{J'J} + \right. \\
& \left. + \hat{J}' \hat{J} \bar{F}(a'b'J) \delta_{ac'} \delta_{a'c} \delta_{bb'} \left\{ \begin{matrix} a'b'J \\ c'r'J' \end{matrix} \right\} \right), \quad (A2.10)
\end{aligned}$$

$$\begin{aligned}
R_{13}^K(abcd \dots tJ) &= \frac{1}{2} \frac{\hat{J}}{d} \left\{ G(abcdJ) \left(u_a u_b u_d v_c \right. \right. \\
& \times L^{k-2}(p \dots t) - v_a v_b v_d u_c L^{k-4}(a \dots t) \left. \right\} + \\
& + (-)^{J+c+d} F(abdcJ) \left(u_a u_b u_d v_c L^{k-2}(a \dots t) - \right. \\
& \left. - v_a v_b v_d u_c L^{k-4}(a \dots t) \right) - F(abcdJ) \\
& \times \left\{ u_b u_c u_d v_a L^{k-2}(a \dots t) - v_b v_c v_d u_a L^{k-4}(a \dots t) \right\}, \quad (A2.11)
\end{aligned}$$

$$\begin{aligned}
R_0^k(p \dots t) &= \sum_a \hat{a}^2 v_a^2 \epsilon_a L^{k-2}(ap \dots t) + \\
& + \frac{1}{2} \sum_{ab} \hat{a} \hat{b} \left(2v_a^2 v_b^2 F(aabb0) L^{k-4}(abp \dots t) + \right.
\end{aligned}$$

$$+u_a v_a u_b v_b G(aabb0) L^{k-2}(abp\dots t) \Big\}, \quad (A2.12)$$

$$R_{20}^k(pq\dots t) = -2\hat{p}u_p v_p \epsilon_p L^{k-2}(pq\dots t) \\ -\frac{1}{2} \sum_a \hat{a} \{ 4u_p v_p v_a^2 F(aapp0) L^{k-4}(apq\dots t) - \\ -u_a v_a G(aapp0) \left[v_p^2 L^{k-4}(apq\dots t) - u_p^2 L^{k-2}(apq\dots t) \right] \}, \quad (A2.13)$$

$$R_{11}^k(pq\dots t) = \epsilon_p \left(u_p^2 L^k(pq\dots t) - v_p^2 L^{k-2}(pq\dots t) \right) \\ + \sum_a \hat{a} \hat{p}^{-1} \left\{ v_a^2 F(aapp0) \left[u_p^2 L^{k-2}(apq\dots t) - \right. \right. \\ \left. \left. -v_p^2 L^{k-4}(apq\dots t) \right] - u_a v_a u_p v_p G(aapp0) L^{k-2}(apq\dots t) \right\}, \quad (A2.14)$$

$$R_{22}^k(abcdeJ) = \frac{1}{2} \bar{P}(abJ) \bar{P}(cdJ) \left\{ u_a u_b u_c u_d \right. \\ \times L^{k-2}(abcde) + v_a v_b v_c v_d L^{k-6}(abcde) \Big\} G(abcdJ) \\ + 4v_a u_b v_c u_d L^{k-4}(abcde) F(abcdJ) \Big\}$$

where $G(abcdJ)$ and $F(abcdJ)$ are the particle-particle and particle-hole matrix elements of $H_{\text{valence particles}}$.

For the pairing interaction with force strength G they read

$$G(abcdJ) = -G \delta_{ab} \delta_{cd} \delta_{J0} \hat{a} \hat{c} (-)^{l_a - l_b} \\ F(abcdJ) = (-)^{J+j_a - j_b} G \delta_{ad} \delta_{bc} \quad (A2.15)$$

For the single-particle states the coupling order $\vec{l} + \vec{s} = \vec{j}$ is adopted. The angular part of the single-particle wave function is the (θ, ϕ) of Condon and

Shortley (1935).

$$\bar{P}(pqJ)(\text{expression}) = (\text{expression}) + (-)^{J+p-q}(\text{expression} \\ \text{with } p \text{ and } q \text{ interchanged}), \quad (\text{A2.16})$$

$$\{p \leftrightarrow q\} \quad \text{means: the last expression between the brackets} \\ \{ \quad \} \text{with } p \text{ and } q \text{ interchanged.} \quad (\text{A2.17})$$

The formulas above were taken from ref. ¹⁴⁾; however, the residual integrals $I^k(pq \dots t)$ were replaced by the finite sums $L^k(pq \dots t)$. The advantage of the latter sums is elaborated in ref. ¹⁹⁾.

The sums $L^k(pq \dots t)$ are defined by

$$L^k(pq \dots t) = \frac{1}{M} \sum_{m=1}^M (z_m)^{-k} (\rho_p \rho_q \dots \rho_t)^{-2} \prod_{\alpha > 0} \rho_a^2 \quad (\text{A2.18})$$

$$\text{where } \rho_a = (u_a^2 + z_m^2 v_a^2)^{\frac{1}{2}}$$

$$z_m = \exp(i\pi m/M)$$

M should be odd. In ref. ¹⁹⁾ it is shown that the application of the sums $L^k(pq \dots t)$ remove all contributions from the wave function with a particle number different from $2p + 1 \pm 2rM$ (r integer). So for sufficiently large M only components with particle number $2p + 1$ are taken into account.

Lastly we give the reduced matrix elements of a tensor of rank λ ($\lambda \neq 0$)

$$\langle \psi_{2p+1}(abJc;r) || Q_\lambda || \psi_{2p+1}(pqJ't;r') \rangle = \\ = -\hat{f} \hat{f}' \hat{J} \hat{J}' \bar{P}(abJ) \bar{P}(pqJ') \langle p || Q_\lambda || a \rangle \\ \times \left[(-)^{\lambda} u_a u_p L^{2p-2}(apqt) - v_a v_p L^{2p-4}(apqt) \right]$$

$$\begin{aligned}
& \times \left(\delta_{ct} \delta_{bq} (-)^{r'-c+p+q+\lambda+J+J'} \left\{ \begin{matrix} \lambda & J & J' \\ c & r' & r \end{matrix} \right\} \left\{ \begin{matrix} \lambda & J & J' \\ b & p & a \end{matrix} \right\} + \right. \\
& + \left. \delta_{cq} \delta_{bt} (-)^{a+r+c+b} \left\{ \begin{matrix} a & b & J \\ p & J' & c \end{matrix} \right\} \right\} \\
& - \hat{f} \hat{f}' \hat{J} \hat{J}' \{ \bar{P}(abJ) \langle t || Q_\lambda || a \rangle \left[(-)^{\lambda} u_a u_t L^{2p-2}(abct) \right. \\
& - \left. v_a v_t L^{2p-4}(abct) \right] (-)^{a-r+J'} \left\{ \begin{matrix} r' & t & J' \\ a & r & \lambda \end{matrix} \right\} \left\{ \begin{matrix} a & b & J \\ c & r & J' \end{matrix} \right\} \bar{P}(pqJ') \delta_{cp} \delta_{bq} \\
& - \hat{f} \hat{f}' \hat{J} \hat{J}' (-)^{r-r'+\lambda+\lambda} \{ a \leftrightarrow p, b \leftrightarrow q, c \leftrightarrow t, J \leftrightarrow J', r \leftrightarrow r' \} \\
& - \hat{f} \hat{f}' \delta_{JJ'} (-)^{c-r+J'} \langle t || Q_\lambda || c \rangle \left[(-)^{\lambda} u_c u_t L^{2p-2}(abct) \right. \\
& - \left. v_c v_t L^{2p-4}(abct) \right] \left\{ \begin{matrix} r' & t & J' \\ c & r & \lambda \end{matrix} \right\} \bar{P}(pqJ') \delta_{ap} \delta_{bq} \\
& - \left\{ \hat{f}' (-)^{\lambda} \left[\delta_{\lambda J} \delta_{tr} \hat{\lambda}^{-1} \langle p || Q_\lambda || q \rangle (u_p v_q + (-)^{\lambda} v_p u_q) \right. \right. \\
& + \left. \left. \hat{J}' \bar{P}(pqJ') \delta_{pr} \left\{ \begin{matrix} s & s' & J' \\ t & r' & \lambda \end{matrix} \right\} \langle t || Q_\lambda || q \rangle (u_t v_q + (-)^{\lambda} v_t u_q) \right] \right\} \\
& \times \left\{ \delta_{J0} \delta_{ab} \delta_{cr} \hat{a} u_a v_a (L^{2p-2}(pqat) - L^{2p-4}(pqat)) + \right. \\
& - \left. \hat{J} \hat{r}^{-1} u_c v_c (L^{2p-2}(pqct) - L^{2p-4}(pqct)) \bar{P}(abJ) \delta_{ac} \delta_{br} \right\} \\
& - (-)^{r-r'+\lambda+\lambda} \{ a \leftrightarrow p, b \leftrightarrow q, c \leftrightarrow t, J \leftrightarrow J', r \leftrightarrow r' \} \\
& + (-)^{r-r'+\lambda} \langle r' || Q_\lambda || r \rangle * \\
& \cdot \left\{ \delta_{J0} \delta_{J'0} \delta_{ab} \delta_{pq} \delta_{cr} \delta_{tr} \hat{a} u_a v_a \hat{p} u_p v_p N(ap) \right. \\
& - \delta_{J0} \delta_{ab} \delta_{cr} \hat{a} u_a v_a \hat{J}' \hat{f}'^{-1} u_t v_t \bar{P}(pqJ') \delta_{pt} \delta_{qr} N(pt) \\
& - \delta_{J'0} \delta_{pq} \delta_{tr} \hat{p} u_p v_p \hat{J} \hat{f}^{-1} u_c v_c \bar{P}(abJ) \delta_{ac} \delta_{br} N(cp) \\
& + \left. \hat{J} \hat{J}' \hat{f}'^{-1} \hat{f}^{-1} u_c v_c u_t v_t \bar{P}(abJ) \delta_{ac} \delta_{br} \bar{P}(pqJ) \delta_{pt} \delta_{qr} N(qt) \right\} \quad (A2.19)
\end{aligned}$$

where

$$\begin{aligned}
 N(ps) &= (-)^{\lambda} u_r u_{r'} \left\{ L^{2p} (psrr') - 2L^{2p-2} (psrr') + \right. \\
 &+ L^{2p-4} (psrr') \left. \right\} - v_r v_{r'} \left\{ L^{2p-2} (psrr') - 2L^{2p-4} (psrr') + \right. \\
 &+ L^{2p-6} (psrr') \left. \right\}, \\
 \langle \psi_{2p+1}(r) || Q_{\lambda} || \psi_{2p+1}(pqJ't; r') \rangle &= \\
 &- \hat{r}' (-)^{\lambda} \left\{ \delta_{\lambda J'} \delta_{tr} \hat{\lambda}^{-1} \langle p || Q_{\lambda} || q \rangle (u_p v_q + (-)^{\lambda} v_p u_q) \right. \\
 &+ \hat{J}' \bar{P}(pqJ') \delta_{pr} \left\{ \begin{matrix} p & q & J' \\ t & r & \lambda \end{matrix} \right\} \langle t || Q_{\lambda} || q \rangle (u_t v_q + (-)^{\lambda} v_t u_q) \left. \right\} \\
 &\times L^{2p-2} (pqt) + (-)^{\lambda} \langle r || Q_{\lambda} || r' \rangle \\
 &\times \left\{ \delta_{J'0} \delta_{pq} \delta_{tr} \hat{p} u_p v_p \left\{ (-)^{\lambda} u_r u_{r'} \left[L^{2p} (prr') - L^{2p-2} (prr') \right] \right. \right. \\
 &- v_r v_{r'} \left[L^{2p-2} (prr') - L^{2p-4} (prr') \right] \left. \right\} \\
 &- \hat{J}' \hat{r}'^{-1} u_t v_t \{ p \leftrightarrow t \} \bar{P}(pqJ') \delta_{pt} \delta_{qr} \quad (A2.20)
 \end{aligned}$$

$$\begin{aligned}
 \langle \psi_{2p+1}(r) || Q_{\lambda} || \psi_{2p+1}(r') \rangle &= \\
 &= \langle r || Q_{\lambda} || r' \rangle \left\{ u_r u_{r'} L^{2p} (rr') - (-)^{\lambda} v_r v_{r'} L^{2p-2} (rr') \right\} \quad (A2.21)
 \end{aligned}$$

The reduced single-particle matrixelement of the $Y_{2\mu}$ operator between harmonic oscillator wave functions is defined as:

$$\begin{aligned}
 \langle a || Y_2 || b \rangle &= (-)^{a-b} \langle b || Y_2 || a \rangle = \\
 &= (-)^{n_a + n_b} (-)^{b - \frac{1}{2} \sqrt{5/4\pi} \hat{a} \hat{b}} \begin{pmatrix} a & b & 2 \\ \frac{1}{2} - \frac{1}{2} & 0 & \end{pmatrix} \quad (A2.22)
 \end{aligned}$$

References

- 1) A. Bohr and B.R. Mottelson, Mat. Fys. Medd. Dan. Vid. Selsk. 27 no. 16 (1953)
- 2) V. Lopac, Nucl. Phys. A 138 (1969) 19
- 3) V. Paar, Nucl. Phys. A 164 (1971) 576, 593
- 4) A. Bohr and B.R. Mottelson, Nuclear Structure, vol. 2, Benjamin, London (1975) Ch. 6
- 5) G. Alaga and G. Ialongo, Phys. Lett. 22 (1966) 619
V. Paar, Phys. Lett. 39 B (1972) 587
G. Van den Berghe, Nucl. Phys. A 265 (1976) 479
V. Paar, E. Coffou, U. Eberth and J. Ebert, J. Phys. G: Nucl. Phys. 2 (1976) 917
- 6) A. Arima and F. Tachello, Ann. of Phys. (N.Y.) 111 (1978) 201
- 7) A. Arima and F. Tachello, Phys. Rev. Lett. 40 (1978) 385
- 8) V. Paar, private communication
- 9) V. Paar, in Proceedings of Seminar on Boson models, Erice 1978, Plenum Press (1979)
- 10) V. Paar and S. Brant, Nucl. Phys. A 303 (1978) 96
- 11) V. Paar, in Problems of Vibrational Nuclei, eds.: G. Alaga, V. Paar and L. Sips, North-Holland, Amsterdam (1975) 15
- 12) V. Paar, in Proceedings of Int. Conf. on medium-heavy nuclei, Rhodes 1979, The Institute of Physics, to be published
- 13) L.S. Kisslinger and R.A. Sorensen, Rev. Mod. Phys. 35 (1963) 853
- 14) P.L. Ottaviani and M. Savoia, Nuovo Cim. 67 A (1970) 630;
Phys. Rev. 178 (1969) 1594
- 15) G. Bonsignori and M. Savoia, Nuovo Cim. 44 A (1978) 121
- 16) W.F. van Gunsteren, K. Allaart and P. Hofstra, Z. Phys. A 288 (1978) 49
- 17) P. Hofstra and K. Allaart, to be published, and Ch. 4
- 18) H.A. Jahn, Proc. Roy. Soc. A 205 (1951) 192
- 19) K. Allaart and W.F. van Gunsteren, Nucl. Phys. A 234 (1974) 53
- 20) V. Paar and B.K.S. Koene, Z. Phys. A 279 (1976) 203
- 21) K. Allaart, thesis, Vrije Universiteit, Amsterdam, 1971
- 22) V. Paar, Nucl. Phys. A 211 (1973) 29
- 23) P.J. Brussaard and P.W.M. Glaudemans, Shell-model applications in nuclear spectroscopy, North-Holland, Amsterdam (1977) page 371
- 24) L.S. Kisslinger, Nucl. Phys. 78 (1966) 341
- 25) A.R. Edmonds, Angular momentum in quantum mechanics, Princeton University Press, Princeton, New Jersey (1960)

Chapter 6

APPLICATION OF THE THREE-QUASIPARTICLE CLUSTER
VIBRATION MODEL TO ODD Zn ISOTOPES

Abstract: The three-quasiparticle cluster vibration (QCV) model is applied to the odd Zn isotopes. It is concluded that the inclusion of a three-quasiparticle cluster is essential for the properties of the low-lying states in the Zn isotopes. A comparison with other model calculations is made; the QCV model yields spectra and electromagnetic properties, which agree with experimental values as good as a much larger shell model calculation.

6.1 INTRODUCTION AND CHOICE OF THE PARAMETERS

In chapter 5 the QCV model was introduced. The model contains collective and single-particle degrees of freedom, *viz.*: vibrational (harmonic) phonons (with a phonon energy $\hbar\omega$) and a *number-projected* three-quasiparticle cluster, respectively. In chapter 5, section 4.2 the importance of particle-number projection is shown. The quasiparticles occupy certain shell model single-particle orbits with energy ϵ ; the residual interaction is a pairing force with strength G . The coupling between the phonons and the cluster is a quadrupole coupling (5.9) with strength a . The model is an extension of the Alaga model or (three-particle) cluster vibration (CV) model.

As an illustration we have applied the QCV model to the sequence of isotopes ${}^{61}\text{Zn}_{31}$, ${}^{63}\text{Zn}_{33}$, ${}^{65}\text{Zn}_{35}$ and

${}_{30}^{67}\text{Zn}_{37}$, with $n=3,5,7$ and 9 particles in the $N=28-50$ neutron valence shell, respectively. Of these nuclei ${}^{67}\text{Zn}$ has been treated previously in the CV model, by assuming a $N=40$ subshell closure, i.e. a three-neutron-hole cluster in the $N=28-40$ subshell^{1,2)}. So, the neutron can occupy the $2p_{3/2}$, $1f_{5/2}$ and $2p_{1/2}$ orbits. Here we adopt the parametrization from ref¹⁾ and perform the calculation for the whole sequence of Zn nuclei, by changing only the number of valence-shell neutrons.

The parameters are¹⁾:

$$\begin{aligned} \epsilon(f_{5/2}) - \epsilon(p_{3/2}) &= 0.76 \text{ MeV} & \hbar\omega &= 1.2 \text{ MeV} \\ \epsilon(p_{1/2}) - \epsilon(p_{3/2}) &= 1.08 \text{ MeV} & a &= 0.81 \text{ MeV} \\ & & G &= 0.4 \text{ MeV} \end{aligned}$$

The single-neutron energies are taken from the experimental data for ${}^{57}\text{Ni}$. The phonon energy $\hbar\omega$ is about the energy of the 2_1^+ states in the Ni-isotopes. The pairing strength G is a little higher than the estimate $23/A$ to account for the omission of the $g_{7/2}$ orbit; besides, the results are rather insensitive to the value of G . The value of the coupling strength a is fitted to the spectrum of ${}^{67}\text{Zn}$. The value of $a=0.81$ MeV is in good agreement with the estimate for the particle-vibration coupling strength¹⁸

$$a = \sqrt{4\pi/3} (ZR_0^2)^{-1} \langle k \rangle \{ B(E2) (2_1^+ \rightarrow 0_1^+)_{\text{VIB}} \}^{1/2} \quad (6.1)$$

If we use for the radial coupling matrix elements $\langle k \rangle$ the value 40 MeV, then we obtain for ${}^{62}\text{Ni}$ $a=0.9$ MeV and for ${}^{64}\text{Ni}$ $a=0.8$ MeV.

The parameters are taken constant for all Zn isotopes. In a more detailed calculation, the dependence of the phonon energy $\hbar\omega$ on the particle number A should be taken into account. However, in even Ni isotopes these changes are rather small, so we take the same $\hbar\omega$, in order to demonstrate clearly the effect of the particle number in the valence shell. An analogous argument applies to the

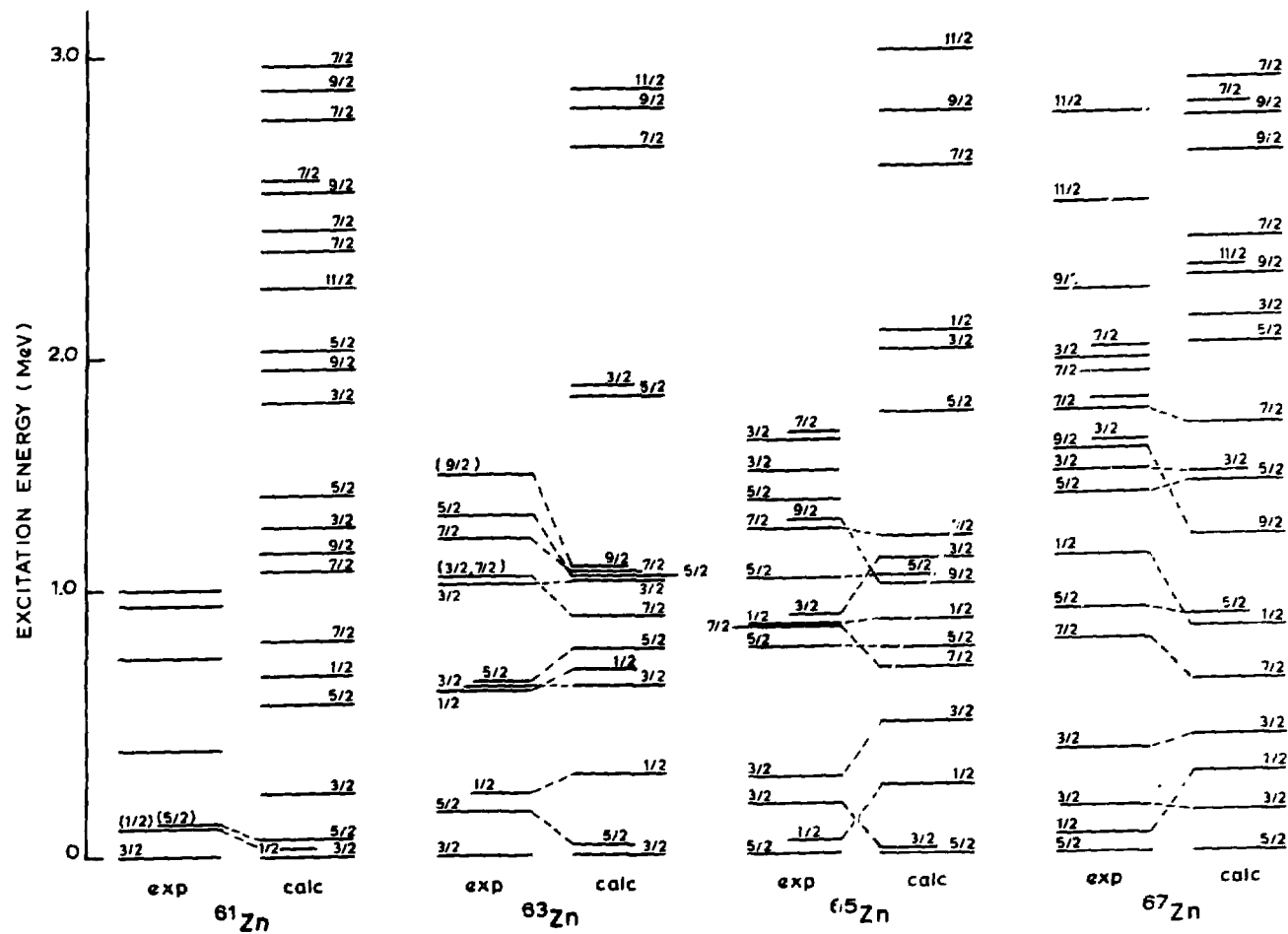


Figure 6.1 The QCV model and experimental^(6,7,8,14) negative-parity spectra of $^{61,63,65,67}\text{Zn}$. No free parameters are contained in the calculation. The parametrization is taken from a CV model calculation for $^{67}\text{Zn}^{11}$ and for the other isotopes only the number of valence-shell neutrons is changed.

strength a . It should be stressed that we take here a parametrization of the CV model for ^{67}Zn , without readjusting any of the parameters for $^{61}, ^{63}, ^{65}\text{Zn}$.

6.2 SPECTRA AND WAVE FUNCTIONS

First the BCS gap equations are solved; the resulting values for u, v, Δ and E are listed in table 6.1. Without the particle-vibration coupling the values of the quasi-particle energies E_j determine the states below 0.5 MeV. For ^{67}Zn the ground state has spin $1/2^-$ then, but the structure of the low-lying states are already roughly reproduced by the one-quasiparticle configurations only.

The spectra, calculated by the QCV model for this parametrization are compared with the experimental spectra in figure 6.1. In the calculation phonon states with only up to two phonons are included. One may notice from the figure that the spectra of the lighter isotopes are reproduced equally well as the spectrum of ^{67}Zn . This gives some confidence, that the model may indeed describe the states of these nuclei equally well as the CV model does for nuclei with only three particles beyond a closed shell. So we believe that the QCV model wave functions can tell something about the properties of the nuclear levels. These wave function are presented in tables 6.2 - 6.5 for the low-lying states of $^{61}\text{Zn} - ^{67}\text{Zn}$, respectively.

Table 6.1 The BCS solutions for $^{61}, ^{63}, ^{65}, ^{67}\text{Zn}$.

j	c_j	v_j^2				E_j (MeV)			
		3	5	7	9	3	5	7	9
3/2	0	0.48	0.69	0.82	0.90	0.95	1.17	1.42	1.63
5/2	0.76	0.15	0.30	0.51	0.72	1.33	1.17	1.10	1.09
1/2	1.08	0.10	0.20	0.34	0.54	1.59	1.36	1.16	0.98
Δ (MeV)		0.95	1.08	1.10	0.98				

Table 6.2 Wave functions for ^{61}Zn .

$(1/2)_1$		$(1/2)_2$		$(3/2)_1$	
\bar{Y}	.37	\bar{Y}	.54	\bar{Y}	-.62
$\bar{S}, 12$.47	$\bar{S}, 12$.50	$(\bar{Y}^2)0\bar{S}; 3/2$	-.24
$(\bar{Y}^2)2\bar{S}; 1/2$.20	$(\bar{Y}\bar{Y})2\bar{S}; 5/2, 12$.22	$(\bar{S}^2)2\bar{Y}; 5/2, 12$.25
$(\bar{Y}^2)0\bar{S}; 3/2, 12$	-.22	$(\bar{S}, 12)$.15	$(\bar{Y}^2)3\bar{S}; 3/2, 12$.21
$(\bar{Y}\bar{Y})2\bar{S}; 1/2$.27				
$(\bar{S}^2)2\bar{Y}; 5/2, 12$.21				
$(\bar{Y}\bar{Y})2\bar{S}; 3/2, 12$	-.21				
$(3/2)_2$		$(3/2)_3$		$(5/2)_1$	
$\bar{S}, 12$.39	\bar{S}	-.26	\bar{S}	.61
$(\bar{Y}^2)0\bar{S}$	-.21	$\bar{S}, 12$	-.24	$\bar{S}, 12$	-.36
$\bar{S}, 12$.31	$\bar{S}, 12$.33	$(\bar{Y}^2)0\bar{S}; 5/2$.20
$(\bar{Y}\bar{Y})2\bar{S}; 3/2$	-.31	$\bar{Y}, 12$.44		
$(\bar{S}^2)2\bar{S}; 7/2, 12$.20	$(\bar{S}^2)2\bar{Y}; 3/2, 12$	-.22		
		$(\bar{S}^2)2\bar{Y}; 3/2$	-.24		
$(5/2)_2$		$(5/2)_3$		$(7/2)_1$	
$\bar{S}, 12$.54	\bar{S}	.25	$\bar{S}, 12$	-.50
$(\bar{S}^2)2\bar{Y}; 5/2$.35	$\bar{S}, 12$.37	$(\bar{S}^2)2\bar{S}; 7/2$.29
$(\bar{S}^2)2\bar{S}; 5/2$	-.21	$(\bar{S}^2)2\bar{S}; 5/2$.24	$(\bar{S}^2)2\bar{S}; 7/2$	-.21
$(\bar{S}^2)2\bar{S}; 9/2, 12$.23	$\bar{Y}, 12$.40	$\bar{S}, 24$.20
		$\bar{S}, 24$.20	$(\bar{S}^2)4\bar{S}; 7/2, 12$.20
		$(\bar{Y}\bar{Y})2\bar{S}; 5/2$.25	$(\bar{S}^2)4\bar{S}; 11/2, 12$.24
				$(\bar{Y}\bar{Y})2\bar{S}; 3/2, 12$	-.22
$(7/2)_2$		$(9/2)_1$		$(11/2)_1$	
$\bar{S}, 12$.60	$\bar{S}, 12$.62	$(\bar{S}^2)4\bar{S}; 11/2$.49
$(\bar{S}^2)2\bar{S}$.26	$(\bar{S}^2)2\bar{S}$.32	$\bar{S}, 24$	-.31
$(\bar{Y}^2)0\bar{S}; 3/2, 12$.24	$(\bar{Y}\bar{Y})2\bar{S}$.27	$(\bar{S}^2)2\bar{S}; 7/2, 12$.30
$(\bar{Y}\bar{Y})2\bar{S}$.26	$(\bar{S}^2)2\bar{S}; 9/2, 12$	-.20	$(\bar{S}^2)2\bar{S}; 7/2, 12$	-.27
$(\bar{Y}\bar{Y})1\bar{S}; 7/2, 12$	-.21	$(\bar{Y}\bar{Y})2\bar{S}; 7/2, 12$	-.24	$(\bar{S}^2)4\bar{S}; 11/2, 12$	-.24
				$(\bar{S}^2)4\bar{S}; 7/2, 12$	-.20
				$(\bar{Y}\bar{Y})2\bar{S}; 7/2, 12$.27
				$(\bar{Y}\bar{Y})2\bar{S}; 9/2, 12$	-.25
				$(\bar{S}^2)4\bar{S}; 7/2, 22$.21

The following simplifying labelling is used for the quasiparticle states: $\bar{Y} \equiv \bar{p}_{1/2}$, $\bar{S} \equiv \bar{p}_{3/2}$, $\bar{S} \equiv \bar{f}_{5/2}$. The three-quasiparticle cluster is written as $(\bar{a}\bar{b})J_{12}\bar{c}; j$ where the angular momenta of quasiparticles a and b couple to J_{12} ; j is the total angular momentum of the cluster. The phonon quantum numbers N (number of phonons) and R (angular momentum of the phonon state) are added if $N \neq 0$. Only components with amplitudes larger than 0.2 are presented.

The number of valence-shell particles is $n=3$.

$(\bar{Y}^2)0\bar{S}$ stands for: $0.25|\bar{S}\rangle + 0.51|(\bar{S}^2)0\bar{S}\rangle - 0.11|(\bar{Y}^2)0\bar{S}\rangle - 0.53|(\bar{S}^2)0\bar{S}\rangle$

$(\bar{Y}^2)0\bar{S}$ stands for: $0.05|\bar{S}\rangle + 0.54|(\bar{S}^2)0\bar{S}\rangle - 0.26|(\bar{Y}^2)0\bar{S}\rangle - 0.49|(\bar{S}^2)0\bar{S}\rangle$

Table 6.3 Wave functions for ^{63}Zn .

$(1/2)_1$		$(1/2)_2$		$(3/2)_1$	
$\bar{1}$.58	$\bar{1}$	-.39	$\bar{3}$.69
$\bar{3},12$.34	$\bar{3},12$	-.59	$\bar{3},12$.32
$\bar{3},12$	-.21	$(\bar{3}^2)0\bar{1};1/2$	-.26	$\bar{3},20$.22
$(3/2)_2$		$(3/2)_3$		$(5/2)_1$	
$\bar{3}$.23	$\bar{3},12$.21	$\bar{5}$.71
$\bar{3},12$	-.63	$\bar{3},12$	-.52	$\bar{3},12$	-.26
$\bar{3},12$	-.22	$\bar{1},12$.46	$\bar{3},20$.23
$(\bar{3}^2)2\bar{5};3/2$.21	$\bar{3},24$.21		
$(\bar{3}\bar{1})2\bar{5};3/2$.22				
$(\bar{3}^2)2\bar{1};3/2$.22				
$(5/2)_2$		$(5/2)_3$		$(7/2)_1$	
$\bar{3},12$.21	$\bar{3},12$.59	$\bar{3},12$.68
$\bar{3},12$	-.72	$\bar{1},12$.43	$\bar{3},12$.32
$(\bar{3}^2)2\bar{1};5/2$	-.20	$(\bar{3}^2)2\bar{1};5/2$.20	$(\bar{3}\bar{1})2\bar{3};7/2$	-.22
$(\bar{3}\bar{1})2\bar{3};5/2$.22			$(\bar{3}^2)4\bar{1};7/2$	-.24
$(7/2)_2$		$(9/2)_1$		$(11/2)_1$	
$\bar{3},12$.30	$\bar{3},12$.78	$(\bar{3}^2)4\bar{3};11/2$	-.38
$\bar{3},12$	-.71	$(\bar{3}\bar{1})2\bar{5};9/2$.20	$\bar{3},24$.50
				$\bar{3},24$.35
				$(\bar{3}^2)2\bar{3};7/2,12$.30
				$(\bar{3}\bar{1})2\bar{3};7/2,12$	-.37
				$(\bar{3}\bar{1})2\bar{5};9/2,12$.21
				$(\bar{3}^2)4\bar{1};7/2,12$	-.30

See for the description the caption of table 6.2.

The number of valence-shell particles is $n=5$.

$(\bar{3}^2)0\bar{1}$ stands for: $0.22|\bar{1}\rangle + 0.58|(\bar{3}^2)0\bar{1}\rangle - 0.47|(\bar{3}^2)0\bar{1}\rangle$

$(\bar{a}\bar{b})J_{12}^{\nu};j$ stands for the cluster state with three quasi-particles in orbit with angular momenta $j_1=a/2$, $j_2=b/2$ and $j_3=c/2$; j_1 and j_2 are coupled to J_{12} and the angular momentum of the cluster state is j . One-quasiparticle states with angular momentum $j/2$ are written as \bar{j} . Phonon quantum-number N (number of phonons) and R (angular momentum of the N -phonon state) are added if $N \neq 0$. Note, that the configurations of the type $|(\bar{j}^2)0\bar{r}\rangle$ are in fact linear combinations of seniority $v=1$ states for spin j_r ; the latter states are linearly dependent (see chapter 5, appendix 1). The linear

Table 6.4 Wave functions for ^{65}Zn .

$(1/2)_1$		$(1/2)_2$		$(3/2)_1$	
$5,12$.35	1	.42	3	.67
$3,12$	-.32	$5,12$	-.33	$5,12$	-.22
$(5^2)21;5/2,12$.23	$3,12$.51	$3,12$.34
1	.63	$(31)25;1/2$	-.21	$3,20$.23
		$(5^2)01;1/2$			
$(3/2)_2$		$(3/2)_3$		$(5/2)_1$	
$5,12$.70	3	.20	5	.74
$3,12$.24	$1,12$.59	$3,20$.24
$(5^2)25;3/2$	-.24	$3,12$	-.46	$(5^2)41;7/2,12$.25
$(5^2)21;3/2$	-.26	$(31)25;3/2$.20		
$(5/2)_2$		$(5/2)_3$		$(7/2)_1$	
$5,12$	-.61	$5,12$.22	$5,12$.75
$1,12$	-.32	$1,12$.31	$3,12$.22
$3,12$.35	$3,12$.65	$(5^2)41;7/2$	-.29
$(5^2)21;5/2$.21	$(3^2)21;5/2$.20		
$(31)25;5/2$.25				
$(7/2)_2$		$(9/2)_1$		$(11/2)_1$	
$5,12$	-.24	$5,12$.80	$5,24$	-.69
$3,12$.76			$(5^2)41;7/2,12$.46
				$(31)25;7/2,12$.29

See for the description the caption of table 6.2.

The number of valence-shell particles is $n=7$.

$(5^2)01$ stands for: $0.18|1\rangle + 0.63|(3^2)01\rangle + 0.40|(5^2)01\rangle$

combinations may be different for different particle numbers.

From tables 6.2 - 6.5 one sees, that the dominant configurations of the low-lying states are one-quasi-particle configurations and one-quasiparticle-coupled-to-one-phonon configurations. The admixture of the three-quasiparticle cluster states are considerable, however. In $^{65,67}\text{Zn}$ the seniority three cluster state $|(5^2)25;3/2\rangle$ is responsible for pushing down a $3/2^-$ state with main configuration $|5,12\rangle$ to low energy. This low-lying $3/2^-$ state has a large $B(E2)$ value to the ground state $5/2^-$

Table 6.5 Wave functions for ^{67}Zn .

$(1/2)_1$		$(1/2)_2$		$(3/2)_1$	
Ψ	.56	Ψ	-.46	Ψ	-.21
$\Psi, 12$	-.36	$\Psi, 12$.40	$\Psi, 12$.54
$(\Psi^2) 2\Psi; 1/2$.22	$\Psi, 12$.21	$(\Psi^2) 2\Psi; 3/2$	-.35
$\Psi, 12$.28	$(\Psi^2) 2\Psi; 1/2$.31	$(\Psi^2) 2\Psi; 3/2$	-.22
$(\Psi^2) 2\Psi; 3/2, 12$.24	$(\Psi^2) 2\Psi; 3/2, 12$.25	$(\Psi^2) 2\Psi; 3/2$	-.22
$(\Psi^2) 2\Psi; 5/2, 12$.27			$(\Psi^2) 2\Psi; 3/2, 12$.21
				$(\Psi^2) 4\Psi; 7/2, 12$	-.21
$(3/2)_2$		$(3/2)_3$		$(5/2)_1$	
Ψ	.58	$\Psi, 12$.65	Ψ	.64
$\Psi, 12$.36	$\Psi, 12$	-.22	$\Psi, 12$.26
$\Psi, 20$.20	$\Psi, 12$.26	$\Psi, 20$.22
$(\Psi^2) 2\Psi; 1/2, 12$.21	$(\Psi^2) 0\Psi; 3/2$	-.21	$(\Psi^2) 2\Psi; 3/2, 12$.22
$(\Psi^2) 1\Psi; 7/2, 12$.20	$(\Psi^2) 2\Psi; 3/2$.24	$(\Psi^2) 4\Psi; 7/2, 12$.30
$(5/2)_2$		$(5/2)_3$		$(7/2)_1$	
$\Psi, 12$.37	$\Psi, 12$	-.46	$\Psi, 12$.60
Ψ	.39	$(\Psi^2) 2\Psi; 5/2$	-.23	$(\Psi^2) 4\Psi; 7/2$	-.40
$(\Psi^2) 0\Psi; 5/2$.23	$\Psi, 12$	-.42		
$(\Psi^2) 2\Psi; 5/2$.25	$\Psi, 24$.20		
$\Psi, 12$	-.30	$(\Psi^2) 1\Psi; 5/2, 12$	-.21		
$(\Psi^2) 2\Psi; 5/2$.26				
$(7/2)_2$		$(9/2)_1$		$(11/2)_1$	
$\Psi, 12$	-.59	$\Psi, 12$.65	$\Psi, 24$	-.43
$(\Psi^2) 1\Psi; 7/2$	-.33	$(\Psi^2) 4\Psi; 9/2$.23	$(\Psi^2) 4\Psi; 11/2$	-.40
$(\Psi^2) 2\Psi; 7/2$.20	$(\Psi^2) 2\Psi; 9/2$.30	$(\Psi^2) 4\Psi; 7/2, 12$.46
$(\Psi^2) 1\Psi; 7/2, 12$	-.25	$(\Psi^2) 2\Psi; 9/2, 12$.22	$(\Psi^2) 2\Psi; 7/2, 12$.27
				$(\Psi^2) 2\Psi; 9/2, 12$	-.24

See for the description the caption of table 6.2.

The number of valence-shell particles is $n=9$.

$(\Psi^2) 0\Psi$ stands for: $-0.13|\Psi\rangle + 0.07|(\Psi^2) 0\Psi\rangle + 0.64|(\Psi^2) 0\Psi\rangle - 0.35|(\Psi^2) 0\Psi\rangle$

$(\Psi^2) 0\Psi$ stands for: $-0.11|\Psi\rangle + 0.02|(\Psi^2) 0\Psi\rangle + 0.65|(\Psi^2) 0\Psi\rangle - 0.42|(\Psi^2) 0\Psi\rangle$

with main configuration $|\Psi\rangle$.

Another representation of the wave functions is given in tables 6.6 - 6.9, where is shown how the wave functions are decomposed into four types of configurations, viz.:

- 1) one-quasiparticle states (1QP)
- 2) one-quasiparticle plus phonon(s) states (1QP + ph)
- 3) three-quasiparticle states (3QP)
- 4) three-quasiparticle plus phonon(s) states (3QP + ph)

From these tables the importance of the 3QP cluster states is clearly seen; the average percentage of the 3QP (+ph) states is 50.

Let us discuss the $(3/2)_1^-$ states. In $^{61,63}\text{Zn}$ the $(3/2)_1^-$ is the ground state and in $^{65,67}\text{Zn}$ it is (in the QCV model) the first excited state. From tables 6.2 - 6.5 it is seen, that the $(3/2)_1^-$ state in $^{61,63,65}\text{Zn}$ has the 1QP state $|3\rangle$ as the largest component (amplitude ≈ 0.7). The $(3/2)_1^-$ state in ^{67}Zn , however, is of a different character: the largest component is the one-phonon multiplet state $|5,12;3/2\rangle$. In fact, the $(3/2)_2^-$ state in ^{67}Zn is analogous to the $(3/2)_1^-$ states in the lighter Zn isotopes. Going from ^{65}Zn to ^{67}Zn the $(3/2)_1^-$ and $(3/2)_2^-$ states seem to have exchanged their character. This situation is clearly reflected in the quasicluster-type composition of the $(3/2)_1^-$ states. The 1QP components are sizeably larger than the 3QP ones for $^{61,63,65}\text{Zn}$, as seen from tables 6.6 - 6.8. For the $(3/2)_1^-$ state in ^{67}Zn the 1QP components are small and the 1QP + ph and 3QP components are large. In the quasicluster composition of the $(3/2)_2^-$ state the situation is reversed.

In all four Zn isotopes considered, there appears a low-lying triplet $(1/2)_1^-$, $(3/2)_1^-$, $(5/2)_1^-$. For the $(1/2)_1^-$ states the largest individual components are of 1QP and 1QP + ph type. However, the total contribution to the norm from the 3QP and 3QP + ph states is comparable to that of the 1QP and 1QP + ph states. A similar situation appears for the $(5/2)_1^-$ states with clearly the largest component being $|5\rangle$.

The pronounced feature of the QCV model for odd Zn

Table 6.6 The quasicluster-type composition of the states in ^{61}Zn . In second to fifth column the squares of the amplitudes in percentages are given with which components of the types: one-quasiparticle, one-quasiparticle plus phonons, three-quasiparticle and three-quasiparticle plus phonons, respectively, appear in the wave functions of the ^{61}Zn states. In the sixth and seventh column we present the sum of the percentages in the second and third, and fourth and fifth column, respectively.

I_n	1QP	1QP+ph	3QP	3QP+ph	1QP(tot)	3QP(tot)
$(1/2)_1$	13	31	15	41	44	56
$(1/2)_2$	29	30	9	32	59	41
$(3/2)_1$	38	6	9	47	44	56
$(3/2)_2$	2	33	23	42	35	65
$(3/2)_3$	7	39	19	35	46	54
$(5/2)_1$	37	18	10	9	55	45
$(5/2)_2$	0	32	21	46	32	68
$(5/2)_3$	6	39	17	38	45	55
$(7/2)_1$	-	33	23	44	33	67
$(7/2)_2$	-	40	18	42	40	60
$(9/2)_1$	-	47	20	34	47	53
$(9/2)_2$	-	13	26	61	13	87
$(11/2)_1$	-	10	24	66	10	90

Table 6.7 The quasicluster-type composition of the states in ^{63}Zn . The description is analogous to the caption of table 6.6.

I_n	1QP	1QP+ph	3QP	3QP+ph	1QP(tot)	3QP(tot)
$(1/2)_1$	33	37	6	24	70	30
$(1/2)_2$	16	42	14	28	58	42
$(3/2)_1$	47	17	3	33	64	36
$(3/2)_2$	5	48	16	31	53	47
$(3/2)_3$	3	57	15	26	59	41
$(5/2)_1$	50	14	3	33	64	36
$(5/2)_2$	0	60	14	26	60	40
$(5/2)_3$	2	59	14	25	61	39
$(7/2)_1$	-	59	10	31	59	41
$(7/2)_2$	-	65	10	25	65	35
$(9/2)_1$	-	65	9	26	65	35
$(9/2)_2$	-	35	15	50	35	65
$(11/2)_1$	-	37	14	49	37	63

Table 6.8 The quasicluster-type composition of the states in ^{65}Zn .
The description is analogous to the caption of table 6.6.

I_n	1QP	1QP+ph	3QP	3QP+ph	1QP(tot)	3QP(tot)
$(1/2)_1$	40	28	4	28	68	32
$(1/2)_2$	19	42	12	27	61	39
$(3/2)_1$	44	22	2	31	67	33
$(3/2)_2$	1	59	17	22	60	40
$(3/2)_3$	4	59	13	24	63	37
$(5/2)_1$	55	10	1	34	65	35
$(5/2)_2$	0	62	14	24	62	38
$(5/2)_3$	3	60	13	24	63	37
$(7/2)_1$	-	62	14	24	62	38
$(7/2)_2$	-	66	8	26	64	36
$(9/2)_1$	-	65	9	26	65	35
$(9/2)_2$	-	48	8	45	48	52
$(11/2)_1$	-	52	3	46	52	48

Table 6.9 The quasicluster-type composition of the states in ^{67}Zn .
The description is analogous to the caption of table 6.6.

I_n	1QP	1QP+ph	3QP	3QP+ph	1QP(tot)	3QP(tot)
$(1/2)_1$	31	21	8	40	52	48
$(1/2)_2$	21	25	15	39	46	54
$(3/2)_1$	4	35	23	38	39	61
$(3/2)_2$	33	22	5	40	55	45
$(3/2)_3$	1	51	19	29	52	48
$(5/2)_1$	41	14	3	42	55	45
$(5/2)_2$	1	41	22	36	42	58
$(5/2)_3$	3	44	20	33	47	53
$(7/2)_1$	-	43	22	35	43	57
$(7/2)_2$	-	43	21	36	43	57
$(9/2)_1$	-	46	19	35	46	54
$(9/2)_2$	-	21	19	60	21	79
$(11/2)_1$	-	20	16	64	20	80

isotopes is a strong mixing between 1QP (+ph) and 3QP (+ph) states, induced by the quasicluster-vibration interaction. In the QCV model are *no* almost pure 1QP and 1QP + ph states. This appears in spite of the fact, that the particle-vibration coupling strength is of an intermediate value.

6.3 ELECTROMAGNETIC PROPERTIES

By using the QCV model wave functions, we calculated the matrix elements of the E2 and M1 operators (see chapter 5, formulas (5.18)-(5.21)). The same parameters in the electromagnetic operators have been used as in the CV model calculations for ^{67}Zn of refs^{1,2)};

$$\begin{aligned} e^{\text{SP}} &= 0.5 e & g_R &= Z/A & g_\lambda &= g_\lambda^{\text{free}} = 0 \\ e^{\text{VIB}} &= 2.0 e & g_S &= 0.7 g_S^{\text{free}} & g_p &= -1.0 \end{aligned}$$

In table 6.10 we present the calculated (and experimental^{6,9)}, where available) static electric quadrupole and magnetic dipole moments for $^{61,63,65,67}\text{Zn}$. We note that the identification of states, derived from the wave functions, can also be traced in the electromagnetic

Table 6.10 Theoretical (QCV model and shell model) and available experimental values for the static electric quadrupole and magnetic dipole moments in $^{61,63,65,67}\text{Zn}$.

I_n	$\mu(\text{nm}) \times 100$				$Q(\text{eb}) \times 100$			
	^{61}Zn	^{63}Zn	^{65}Zn	^{67}Zn	^{61}Zn	^{63}Zn	^{65}Zn	^{67}Zn
QCVM (1/2) ₁	40	42	51	53				
SM				66				
exp				58±3				
QCVM (1/2) ₂	68	69	61	53				
QCVM (3/2) ₁	-105	-90	-87	42	-9	16	16	-17
SM		-71	-106	-26		23	22	-1
exp		-28	-78±20	50±6				
QCVM (3/2) ₂	64	44	48	-79	8	1	5	18
SM			52				12	
exp			73±25					
QCVM (5/2) ₁	116	113	100	103	-24	-16	4	18
SM		149	143	147		-10	-1	10
exp			77	88			-2	15±2
QCVM (5/2) ₂	-32	-17	113	121	-5	-4	2	6
QCVM (7/2) ₁	113	117	134	117	-13	-6	-1	12

The experimental values are taken from ref¹⁴⁾. The shell model results (SM) are from ref¹¹⁾ with $e_p(\text{eff})=1.6e$, $e_n(\text{eff})=1.0e$ and bare g factors.

properties. Specifically, $|Q(5/2)_1^-(^{67}\text{Zn})| = 0.18 \text{ eb} \gg |Q(5/2)_1^-(^{65}\text{Zn})| = 0.04 \text{ eb}$. This decrease in magnitude is already a zeroth-order effect; the electric quadrupole moment for a one-quasiparticle state is proportional to $u^2 - v^2$. In ^{67}Zn and ^{65}Zn $u_5^2 - v_5^2 = -0.44$ and -0.02 , respectively (see table 6.1). Obviously $Q(5/2)_1^-(^{65}\text{Zn})$ is small and very sensitive to slight changes in the BCS solutions. In ^{63}Zn it becomes larger in magnitude and is negative.

The magnetic moment of the $(5/2)_1^-$ states in all the Zn isotopes hardly changes with particle number (and with occupation probabilities v_5^2); it is proportional to $u_5^2 + v_5^2 = 1$. The experimental values are in agreement with these simple predictions of the QCV model. A similar situation appears for the $(1/2)_1^-$ states in $^{65}, ^{67}\text{Zn}$ in the QCV model: $\mu(1/2)_1^-(^{67}\text{Zn}) = 0.53 \text{ nm} = \mu(1/2)_1^-(^{65}\text{Zn}) = 0.51 \text{ nm}$.

For the $(3/2)_1^-$ and $(3/2)_2^-$ states we noticed, looking at the wavefunctions, a crossing between ^{65}Zn and ^{67}Zn . Indeed in the QCV model $\mu(3/2)_1^-(^{65}\text{Zn}) = -0.87 \text{ nm} = \mu(3/2)_2^-(^{67}\text{Zn}) = -0.79 \text{ nm}$; both states arise from the 1QP state $|3\rangle$ in the zeroth-order approximation. On the other hand $\mu(3/2)_2^-(^{65}\text{Zn}) = 0.48 \text{ nm}$ has the same sign as $\mu(3/2)_1^-(^{67}\text{Zn}) = 0.24 \text{ nm}$; both states arise from the configuration $|5, 12\rangle$. The available experimental data corroborate this $(3/2)_1^- - (3/2)_2^-$ crossing. It would be interesting to measure the missing magnetic moment $\mu(3/2)_2^-(^{67}\text{Zn})$.

We point out here that for some effects the 3QP states, although they mix strongly in the wave functions of the low-lying states, do not change the qualitative (or even semi-quantitative) predictions of the simple one-quasiparticle case. This can be understood as a systematic feature due to a Ward-like identity for the coupled particle-vibration system^{3, 4, 5}. In fact, what

is lost due to the decrease of the main components, is approximately recovered by the additional components. Therefore, strong 3QP admixtures do not influence strongly some 1QP features. In the diagram language, the vertex corrections (of the same sign as the zeroth-order component) and the self-energy corrections (of the opposite sign to the zeroth-order component) approximately cancel. On the other hand, for properties, for which a Ward-like identity does not hold, a completely new pattern arises; for example, the particle-vibration coupling brings in $^{65,67}\text{Zn}$ one $(3/2)^-$ state with zeroth-order component $|\overset{v}{S}, 12\rangle$ to low energy. This is caused by the strong coupling to the 3QP state $|(\overset{v}{S}^3)3/2\rangle$. This pushing down of the state $|\overset{v}{j}, 12; j-1\rangle$ by the configuration $|(\overset{v}{j}^3)j-1\rangle$ is a well known feature in the CV model and cannot be reproduced in a one-quasiparticle-phonon model.

In tables 6.11-6.13 we present the calculated (and, where available, experimental) $B(E2)$ and $B(M1)$ values for ^{61}Zn - ^{67}Zn . Also some shell model¹¹⁾ results are given; we compare the QCV model and the shell model in section 4. Experimental $B(E2)$ and $B(M1)$ values are scarcely available for ^{61}Zn and ^{63}Zn . For ^{65}Zn and ^{67}Zn there occur experimental data, which are derived from mixing ratios and branching ratios with large errors; so, these values are very uncertain (the errors may be as large as 50 to 100 per cent). In the table these values are preceded by the symbol \approx . The agreement of the QCV model results with the experimental $B(E2)$ and $B(M1)$ values is rather good. Note, that the single-particle $B(M1)$ transitions of the $(3/2)_1^-$ and $(3/2)_2^-$ states in ^{67}Zn and the $(3/2)_1^-$ state in ^{65}Zn to the ground state are ℓ -forbidden, if the term $|Y_2 \otimes \overset{v}{S}|_1$ is neglected in the effective M1 ope-

Table 6.11 Theoretical (QCV model) B(E2) and B(M1) values for ^{61}Zn and ^{63}Zn .

$I_n \rightarrow I'_n$	B(E2) ($e^2\text{fm}^4$)		B(M1) ($\text{nm})^2 \times 10^4$	
	^{61}Zn	^{63}Zn	^{61}Zn	^{63}Zn
$(1/2)_1 \rightarrow (3/2)_1$	66	12	1097	5771
$(5/2)_1 \rightarrow (3/2)_1$	4	8	80	60
$\quad \rightarrow (1/2)_1$	76			
$(1/2)_1 \rightarrow (5/2)_1$		157		
$(3/2)_2 \rightarrow (3/2)_1$	111	14	46	1095
$\quad \rightarrow (1/2)_1$	84	7	1124	4
$\quad \rightarrow (5/2)_1$	84	173	1	7
$(5/2)_2 \rightarrow (3/2)_1$	180	212	277	970
$\quad \rightarrow (1/2)_1$	49	2		
$\quad \rightarrow (5/2)_1$	9	17	3	94
$(1/2)_2 \rightarrow (3/2)_1$	86	116	6589	460
$\quad \rightarrow (1/2)_1$			0.5	11
$\quad \rightarrow (5/2)_1$	0.4	20		
$(7/2)_1 \rightarrow (3/2)_1$	10	23		
$\quad \rightarrow (5/2)_1$	135	168	61	25
$(7/2)_2 \rightarrow (3/2)_1$	153	153		
$\quad \rightarrow (5/2)_1$	6	29	571	223
$(9/2)_1 \rightarrow (5/2)_1$	168	195		
$(11/2)_1 \rightarrow (7/2)_1$	181	173		

rator. If this term is omitted in the QCV model, our results would be about the shell model results, which were calculated without $|Y_2^0 \bar{S}|_1$.

In figures 6.2 - 6.4 the calculated and experimental (if available) branching ratios are presented, together with the half-lives for ^{63}Zn - ^{67}Zn , respectively.

In ^{63}Zn only three half-lives are known experimentally. Two of these values are reproduced reasonably well.

In ^{65}Zn the half-lives are reproduced quite well. The most branching ratios agree well with experiment; only the branching ratios of the $(1/2)_2^-$ and the $(3/2)_1^-$ states are not good.

The calculated branching ratios for ^{67}Zn agree very well with the experimental ones. The half-lives are reproduced reasonably well, except for the $(1/2)_1^-$ state, the half-life of which is a factor 8 too low.

Table 6.12 Theoretical and available experimental B(E2) and B(M1) values for ^{65}Zn .

I_n	+	I'_n	B(E2) ($e^2\text{fm}^4$)			B(M1) ($\text{nm}^2 \times 10^6$)		
			QCVM	SM	exp	QCVM	SM	exp
$(1/2)_1$	+	$(5/2)_1$	87	98	103 ± 6			
$(3/2)_1$	+	$(5/2)_1$	60	0.4	≈ 240	398	130	450 ± 50
	+	$(1/2)_1$	73	41		1290	370	> 680
$(3/2)_2$	+	$(5/2)_1$	220	410	≈ 160	24	20	50
	+	$(1/2)_1$	25	6.6	≈ 450	594	1300	540
	+	$(3/2)_1$	20			342		
$(5/2)_2$	+	$(5/2)_1$	125	13		78	210	
	+	$(1/2)_1$	55					
	+	$(3/2)_1$	57			75		
	+	$(3/2)_2$	0.1			11		
$(7/2)_1$	+	$(5/2)_1$	213	260		1	80	
	+	$(3/2)_1$	27					
	+	$(3/2)_2$	0.6					
	+	$(5/2)_2$	10			900		
$(1/2)_2$	+	$(5/2)_1$	17					
$(7/2)_2$	+	$(5/2)_1$	12			14		
$(9/2)_1$	+	$(5/2)_1$	201					
$(9/2)_2$	+	$(5/2)_1$	0.6					
$11/2)_1$	+	$(7/2)_1$	195					
	+	$(9/2)_1$	75			5		

The experimental values are taken from ref^[1].
See also the caption of table 6.13.

Summarizing: we have shown, that especially for a good reproduction of the spectra it is not enough to couple 1QP states to phonons. The QCV model (a three-quasiparticle cluster coupled to phonons) produces spectra, which agree with experiment for $^{61,63,65}\text{Zn}$ equally well as for ^{67}Zn . For all these nuclei the same parametrization was used. The electromagnetic properties, calculated with the QCV model wave functions, are described rather well. The QCV model wave functions are rather simple and give therefore an easy insight into the structure of the odd Zn isotopes.

Table 6.13 Theoretical and available experimental B(E2) and B(M1) values for ^{67}Zn .

$I_n \rightarrow I_n'$	B(E2) ($e^2\text{fm}^4$)			B(M1) ($\text{nm})^2 \times 10^4$		
	QCVM	SM	exp	QCVM	SM	exp
$(1/2)_1 \rightarrow (5/2)_1$	36	10	4.5 ± 1.5			
$(3/2)_1 \rightarrow (5/2)_1$	262	75	285 ± 21	38	8	55 ± 2
$\rightarrow (1/2)_1$	13	120	≈ 200	30	5600	34 ± 1
$(3/2)_2 \rightarrow (5/2)_1$	0	130	7.5 ± 1.5	305	2	≈ 100
$\rightarrow (1/2)_1$	103	0.1	≈ 300	3487	3700	≈ 700
$\rightarrow (3/2)_1$	9			556		M1
$(7/2)_1 \rightarrow (5/2)_1$	232	220	220 ± 20	9	40	≈ 7
$\rightarrow (3/2)_1$	63		≈ 40			
$\rightarrow (3/2)_2$	37		≈ 40			
$(5/2)_2 \rightarrow (5/2)_1$	65	98	86 ± 6	68	50	≈ 210
$\rightarrow (1/2)_1$	127		≈ 160			
$\rightarrow (3/2)_1$	65			11		
$\rightarrow (3/2)_2$	41			108		
$\rightarrow (7/2)_1$	3			845		
$(1/2)_2 \rightarrow (5/2)_1$	42					
$(9/2)_1 \rightarrow (5/2)_1$	175	170				
$(7/2)_2 \rightarrow (5/2)_1$	2			249		
$(9/2)_2 \rightarrow (5/2)_1$	4					
$11/2)_1 \rightarrow (7/2)_1$	204					
$\rightarrow (9/2)_1$	91			124		

The experimental values are taken from refs^{13,16,17,111}. The values, preceded by \approx , are very uncertain. The shell model results (presented in column "SM") are obtained with $e_p(\text{eff})=1.6e$ and $e_n(\text{eff})=1.0e$ and bare g factors.

6.4 COMPARISON OF THE QCV MODEL WITH OTHER MODELS

The Zn isotopes were described earlier with two types of models:

- 1) the one-quasiparticle-vibration model (the QV model)
- 2) the shell model.

In this section we compare the QCV model with these models.

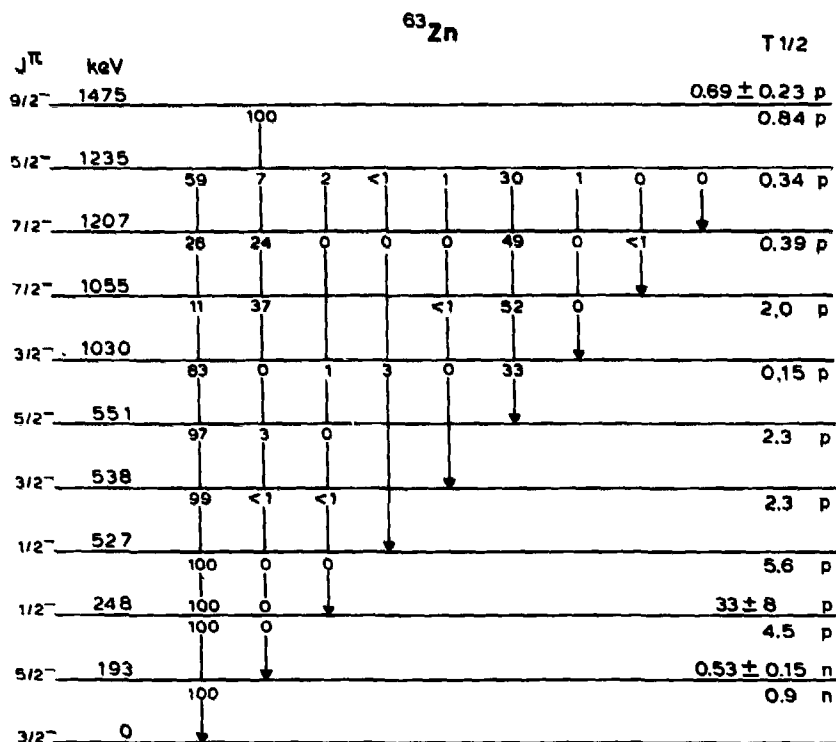


Figure 6.2 QCV model and experimental branching ratios for ^{63}Zn . The experimental values^{1,2)} are presented above the levels and the calculated ones below.

6.4.1 Comparison of the QCV model to the QV model

The QV model space is included in the QCV model space, so it can at best produce similar results. The wave functions of the QCV model (see tables 6.2 - 6.9) contain 1QP components and 3QP components in equal strength. This means, that a description of only one quasiparticle coupled to phonons is expected to be poor. In the spectra, calculated with the QV model, some states are missing already at low energy. For example the $(3/2)_1^-$ state in ^{67}Zn and the $(3/2)_2^-$ state in ^{65}Zn , for which the configuration $|(5^3)3/2^->$ is

^{65}Zn

J^{π}	keV						T 1/2	
$9/2^{-}$	1263	100					0.88 p	
$7/2^{-}$	1253	11		20	51	29	0	3.1 p
$5/2^{-}$	1047	34	0	66	2	58	<1	0.24 p
$3/2^{-}$	910	50	15	24	9			0.27 p
$1/2^{-}$	867	0		100	0			<0.2 n
$7/2^{-}$	864	100		0				5.2 p
$5/2^{-}$	769	58	7	34				4.2 p
$3/2^{-}$	207	16	76	8				0.15 n
$3/2^{-}$	115	81	19					0.44 n
$1/2^{-}$	54	100						1.6 μ
$5/2^{-}$	0							1.9 μ

Figure 6.3 QCV model and experimental branching ratios for ^{65}Zn . See also the caption of figure 6.2.

^{67}Zn

J^{π}	keV						T 1/2	
$7/2^{-}$	1657	44	<1	<1	<1	56		2.3 p
$9/2^{-}$	1516	100						0.4 p
$5/2^{-}$	887	48	13	4	30	<1		1.2 p
$7/2^{-}$	815	95		5	<1			6.3 p
$3/2^{-}$	394	19	70	11				14 p
$3/2^{-}$	185	93	7					1.04 n
$1/2^{-}$	93	100						9.1 μ
$5/2^{-}$	0							1.2 μ

Figure 6.4 QCV model and experimental branching ratios for ^{67}Zn . See also the caption of figure 6.2.

important cannot be described in this model. In refs^{10,15)} it is assumed, that these states are a pure configuration $|(5^3)3/2\rangle$ and it is hoped, that the other $(3/2)^-$ states are described well. The QCV model wave functions show, that this assumption is not valid. The same arguments apply to other spins also. The QCV model shows, that one may not expect good results of the QV model.

6.4.2 Comparison of the QCV model with the shell model

Van Hienen et al.¹¹⁾ performed shell model calculations for the Zn isotopes, in which ^{56}Ni was assumed to be an inert core. The two protons and the remaining neutrons could occupy the $2p_{1/2}$, $1f_{5/2}$ and $2p_{3/2}$ orbits. No truncation was made, which means, that matrices had to be diagonalized with a dimension up to 2000. The maximum dimension in the QCV model is 124; in practice one needs an amount of computertime in the shell model calculations, which is about a factor of hundred times as big as the time, needed in the QCV model.

The effective one- plus two-body Hamiltonian was derived in ref¹³⁾ for the Ni and Ca isotopes. In the calculation of the spectra all the parameters were taken to be constant, just as in the QCV model!

The calculated spectra are shown in figure 6.5. The spectra below 1.5 MeV excitation energy are very similar to ours (see figure 6.1). The ordering of the lowest six states is reproduced a little better in the QCV model: the spin of the ground states are all correct and the triplet $(1/2)_2^-$, $(3/2)_2^-$, $(5/2)_2^-$ in ^{63}Zn is reproduced roughly.

Above 1.5 MeV the shell model produces more states than the QCV model. This can (partly) be explained by the fact that the maximum number of phonons in these

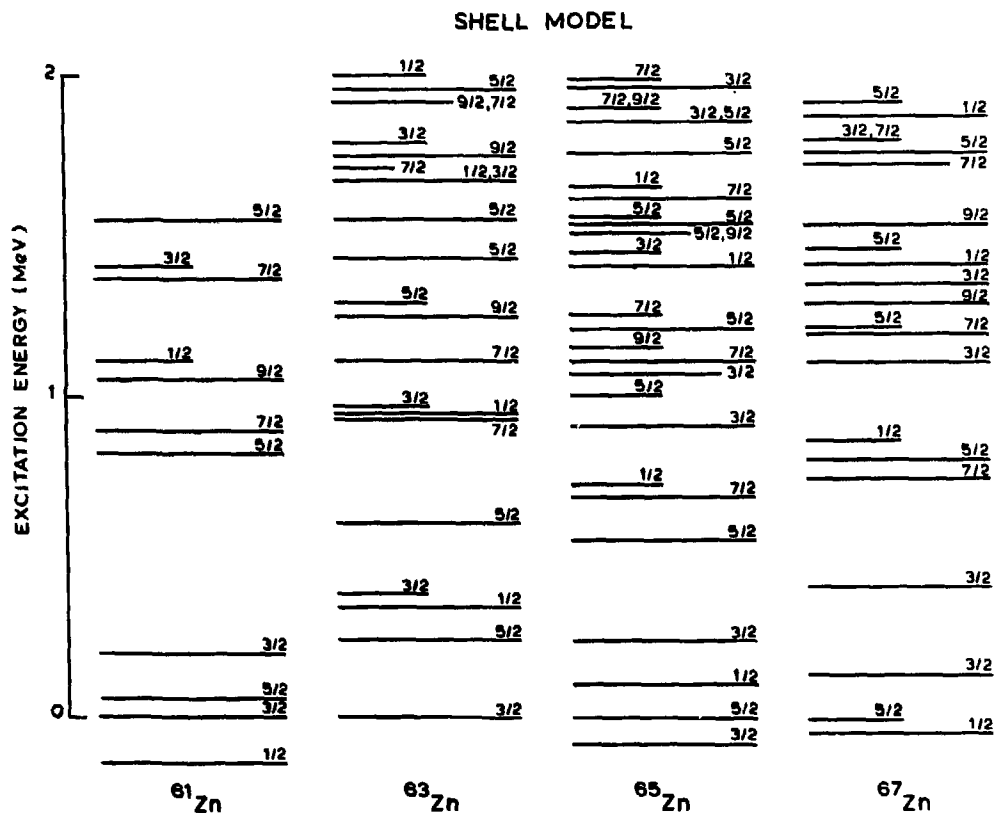


Figure 6.5 The negative-parity spectra of $^{61,63,65,67}\text{Zn}$, calculated with the shell model¹¹⁾. No free parameters are contained in the calculation.

calculations was only two. Paar²⁾ used in his CV model calculation for ^{67}Zn also three-phonon states and produced above 1.5 MeV more states than the QCV model calculation does.

The calculated shell model $B(E2)$ and $B(M1)$ values for ^{65}Zn and ^{67}Zn are shown in tables 6.12 and 6.13. The effective charges for the proton and the neutron were found by fitting to the experimental $B(E2)$ values. In the QCV model no such fit was done. Nevertheless, the QCV model $B(E2)$ values are a little better, especially for the $(3/2)^-$ states.

For the M1 transitions bare values for the g factors were used; the results were not very sensitive to the values of these g factors. In the QCV model the core polarization effects were simulated by

- a) a renormalization of g_s ($=0.7 g_s^{\text{free}}$)
- b) the addition of the term proportional to $|Y_2^0 \hat{S}|_1$ to the effective magnetic operator.

The B(M1) values are reproduced clearly better in the QCV model than in the shell model. For the $(3/2)^-$ states this is largely explained by the additional term in the M1 operator, which is present in the QCV model, but not in the shell model calculations of ref¹¹⁾.

The calculated shell model electric quadrupole and magnetic dipole moments are shown in table 6.10 together with the QCV model results. The parameters for the effective M1 and E2 operators in the shell model are the same as used for the calculated B(M1) and B(E2) values. In almost all cases the results of the two models have the equal sign and about the same magnitude. The magnetic dipole moment of the $(3/2)^-$ state in ^{67}Zn is badly reproduced in the shell model; also the transitions of this state to the $(5/2)^-$ state is not correct. The wave function of this state is clearly not as good as the one of the QCV model. Probably, the one- plus two-body Hamiltonian, which was derived for the Ni and Cu isotopes is not correct any more for ^{67}Zn .

Let us summarize the comparison of the QCV model results and the shell model results. The spectra of the QCV model are slightly better than the ones of the shell model. Also the electromagnetic properties of the QCV model are slightly more in agreement with the available experimental data.

The conclusion of this comparison is, that the degrees of freedom of the QCV model (*viz.* a few quasi-

particles and quadrupole vibrations) are well chosen for the odd Zn nuclei. The QCV model results are at least as good as the shell model results. Since the computational efforts are much less for the QCV model than for the very large shell model calculations, we think, that the QCV model is to be preferred as a predictive tool in nuclear spectroscopy for nuclei away from closed shells.

References

- 1) G. Vanden Berghe, Nucl. Phys. A 265 (1976) 479
- 2) V. Paar, E. Coffou, U. Eberth and J. Eberth, J. Phys. G 2 (1976) 917
- 3) V. Paar, Phys. Lett. 60 B (1976) 129
- 4) V. Paar and S. Brant, Nucl. Phys. A 303 (1978) 96
- 5) V. Paar and S. Brant, Phys. Lett. 74 B (1978) 297
- 6) P.J. Twin, private communication
- 7) O.M. Mustafa et al., J. Phys. G 4 (1978) 99; private communication
- 8) A. Kogan et al., J. Phys. G 5 (1978) 755
- 9) R.R. Lornie et al., J. Phys. G 6 (1978) 923
- 10) A. Weidinger, E. Finckh, U. Jahnke and B. Schreiber, Nucl. Phys. A 149 (1970) 241
A. Charvet, J. Sau, R. Duffait and R. Chery, Phys. Rev. C 15 (1977) 1679
J.J. Dikshit and B.P. Singh, J. Phys. G 2 (1976) 219
- 11) J.F.A. Van Hienen, W. Chung and B.H. Wildenthal, Nucl. Phys. A 269 (1976) 159
- 12) M. Sakakura, Y. Shikata, A. Arima and T. Sebe, Z. Phys. A 289 (1979) 163
- 13) J.E. Kooops and P.W.M. Glaudemans, Z. Phys. A 280 (1977) 181
- 14) Table of Isotopes, Ed. C.M. Lederer and V.S. Shirley (seventh edition), 1978, J. Wiley and sons
- 15) M.J. Throop, Y.T. Cheng and D.K. McDaniels, Nucl. Phys. A 239 (1975) 333
- 16) A. Nilsson and Z.P. Sawa, Phys. Scripta 9 (1974) 83
- 17) C. Bargholtz, L. Eriksson and L. Gidefelt, Z. Phys. A 263 (1973) 89
- 18) A. Bohr and B. R. Mottelson, Nuclear Structure, vol.2, Benjamin, New York (1975) page 418 vv

Curriculum vitae

De schrijver van dit proefschrift werd in 1950 in Amsterdam geboren. Na het behalen van het diploma Gymnasium 6 in 1968 aan het Christelijk Lyceum te Alkmaar, begon hij zijn studie aan de Vrije Universiteit te Amsterdam. In 1971 legde hij het kandidaats-examen wis- en natuurkunde af met sterrenkunde als bijvak. In 1975 volgde het doctoraal examen met als hoofdvak theoretische natuurkunde en als bijvak wis-kunde. Daarna was hij vier jaar als medewerker van de Stichting voor Fundamenteel Onderzoek der Materie bij de werkgroep theoretische Kernfysica van de Vrije Universiteit te Amsterdam werkzaam. Naast zijn onderzoek verleende hij assistentie bij diverse colleges aan voor- en nakandidaatsstudenten.

VRIJE UNIVERSITEIT TE AMSTERDAM

**THE BROKEN-PAIR MODEL FOR NUCLEI
AND ITS EXTENSION WITH
QUADRUPOLE VIBRATIONS**

**a description of odd
N=50 isotones and Z=30 isotopes**

ACADEMISCH PROEFSCHRIFT

**ter verkrijging van de graad van
doctor in de wiskunde en natuurwetenschappen
aan de Vrije Universiteit te Amsterdam,
op gezag van de rector magnificus
dr. H. Verheul,**

**hoogleraar in de faculteit der wiskunde en natuurwetenschappen,
in het openbaar te verdedigen
op donderdag 8 november 1979 te 13.30 uur
in het hoofgebouw der universiteit,
De Boelelaan 1105**

door

PAULUS HOFSTRA

geboren te Amsterdam



AMSTERDAM 1979

Promotor: Prof. dr. E. Boeker

Copromotor: Dr. K. Allaart

